3-22-2020

Enhancement of 5G Network Performance Using Non-Orthogonal Multiple Access (NOMA)

Faeik Tayseer Al Rabee
University of South Florida

Enhancement of 5G Network Performance Using Non-Orthogonal Multiple Access (NOMA)

by

Faeik Tayseer Al Rabee

A dissertation submitted in partial fulfillment
of the requirements for the degree of
Doctor of Philosophy
Department of Electrical Engineering
College of Engineering
University of South Florida

Co-Major Professor: Richard D. Gitlin, Sc.D.
Co-Major Professor: Nasir Ghani, Ph.D.
Ismail Uysal, Ph.D.
Srinivas Katkoori, Ph.D.
Gabriel Arrobo, Ph.D.

Date of Approval:
February 26, 2020

Keywords: SIC Receiver, MAC, M2M, ALOHA-NOMA Protocol, Channel Capacity

Dedication

To my parents, Tayseer and Na'ayem, who are my motivation to give and be amongst the best and their love and guidance are with me in whatever I pursue; my siblings, Fayez, Suha, Fadi, and Sahar, who have helped me whenever I needed them and supported me each step of the way.

Acknowledgments

First and foremost, I extend my thanks to Allah, praised and exalted is He, for everything that He granted me in this life and for giving me the opportunity to keep growing and improving myself, with the ultimate goal of better serve society.

I would like to express my deepest appreciation to my major advisor, Prof. Richard D. Gitlin, for his invaluable guidance, support, patience, encouragement, and life teachings throughout my study. He has always amazed me with his high degree of professionality, expertise, humbleness, management skills, morality, and great kindness. I have learned a great deal from him both technically and philosophically. I will internalize all he has taught me in my future life and the rest of my career, because it is something that will help me to achieve even greater objectives.

I would thank Prof. Nasir Ghani, a co-major advisor, for his assistance, support, and advice in addition to many stimulating and enlightening discussions. I am also grateful to my committee members, Dr. Ismail Uysal, Dr. Srinivas Katkoori, and Dr. Gabriel Arrobo for being part of my doctoral committee and for the knowledge that I acquired from their feedback during the candidacy presentation and dissertation defense. I also thank all the staff at the Department of Electrical Engineering at USF, specifically Ms. Hamilton and Ms. Brandt, for their kindness and sincere assistance whenever I need.

I am also thankful to my sponsoring university, Al-Balqa' Applied University (BAU), for their support to complete my doctoral degree and faith in me.

I would like to thank my dear colleagues at the Innovations in Wireless Information Networking Laboratory (*i*WINLAB) who have challenged me constantly with their brilliance and

inspired me to reach beyond myself during my time as a Ph.D. student at the University of South Florida (USF).

I have always grateful to my parents Tayseer Al Rabee and Na'ayem Alsawaleha, my lovely sisters, Suha and Sahar, and my dear brothers Fayez and Fadi, who always support and encourage me during my studies and prayed for me. I could never thank them enough, but I want them to know that I am always grateful to Allah, praised and exalted is He, for having such a great family like them.

A special thanks to Prof. Mansour I. Abbadi and Prof. Nihad I. Dib for their always support and trust of me during my Master and Ph.D. journey.

Last, but by no means least, it is an understatement to say that I am simply thankful to the United States for giving me the chance to get my Ph.D. The level of respect and diversity to be found here is absolutely breathtaking. My time in the US has been an incredible part of my journey through life with priceless memories. I find myself getting choked up when trying to find the words to finally say goodbye. It will not be a permanent goodbye; I have made too many lifelong friends and met too many kind people to never visit again. My feet will leave this country but my heart, absolutely not. So in lieu of goodbye, I would rather say thank you, America, for everything.

Table of Contents

List of Figures

Abstract

This dissertation is composed of two parts. The first presents several approaches to enhance the performance of 5G wireless systems by using NOMA (Non-Orthogonal Multiple Access) as the multiple access technique under different scenarios and performance metrics. The second investigates the performance of a wireless system network using a mobility model to evaluate the channel capacity taking into account motion. Both studies are directed towards improving the system performance in wireless communication systems.

In the first part, the optimum received power level for uplink power-domain NOMA with ideal Successive Interference Cancellation (SIC) reception is derived for any number of transmitters. The results show that the optimum received power level increases linearly (in dB) as the number of transmitters N are increased and the maximum required received signal-to-interference-plus-noise ratio (SINR) increases exponentially (or equivalently, linearly in dB) with the number of users N. An interesting observation is that the optimum power levels are very similar to that of the μ-law encoding used in the pulse code modulation (PCM) speech companders.

Next, a scalable, energy efficient, and high throughput medium access control (MAC) protocol, which is called the ALOHA-NOMA protocol, is proposed for Internet of Things (IoT) wireless 5G applications incorporating pure ALOHA with power domain NOMA. The simplicity of ALOHA and the superior throughput of NOMA and its ability to resolve collisions via use of a SIC receiver, makes ALOHA-NOMA an excellent candidate for a MAC protocol that can be utilized for a network of low complexity, low traffic IoT devices. The results show that the ALOHA-NOMA protocol significantly improves the throughput performance with respect to pure

ALOHA, e.g., a SIC receiver that separates 5 signals can boost the throughput of classical ALOHA from 0.18 to 1.27 and with 100 active IoT devices the throughput is increased (at a greater than linear rate) to 40.

Following this, the bit error rate (BER) performance of a system with uplink power-domain NOMA and SIC reception using BPSK, QPSK, and 16-QAM modulations schemes in the presence of channel estimation errors is investigated. For each modulation level, two scenarios are considered: perfect channel estimation and a channel with estimation errors. The simulation results show that, for the two scenarios, the amount by which the BER of the SIC receiver increases as the modulation order is increased for a given noise level and the degree to which performance is degraded at high estimation error values. In addition to the BER performance study, for the same system model, a SIC detector degradation study in the presence of channel estimation errors, for the three modulations schemes, is presented. The study shows how the SIC degradation increases as a result of increasing the estimation errors and/or the modulation level. Somewhat surprisingly, for the three modulation schemes and for a small estimation error values, a linear relation is shown between the SIC degradation and the estimation error.

Finally, a channel capacity analysis for a random waypoint (RWP) mobility model in a wireless system network is introduced. The channel capacity for this model is derived for a Rayleigh fading channel with a maximum ratio combining (MRC) diversity receiver. The effect of the number of receiver branches on the channel capacity is analyzed and then the derived channel capacity is compared with the classic Additive White Gaussian Noise (AWGN) Shannon capacity and the static model Rayleigh fading channel capacity. The results show the level that the derived channel capacity increases as the number of MRC branches is increased. Also, the comparison shows that the AWGN channel capacity is greater than the RWP model channel

capacity as it is not affected as severely by fading as the RWP mobility model. On the other hand, the RWP channel capacity is slightly larger than the static model Rayleigh fading channel capacity since severe fading will not affect the RWP model for as long a time duration as it affects the static Rayleigh model.

Chapter 1: Introduction

The Fifth Generation (5G) mobile system have the potential to revolutionize societies and economics by providing anywhere and anytime connectivity for anyone and anything [1]- [2]. Therefore, intensive research on optimizing 5G wireless communication networks is progressing in different areas [3]-[5]. As a technology, 5G is considered as the successor to the current 4G Long Term Evolution (LTE) standard [6] and is expected to be released commercially in 2019-2020. To address current subscriber demands, 5G will require new network and radio access technologies. Three application domains for 5G mobile network services and applications have been identified by the International Telecommunication Union (ITU) [7]: Enhanced Mobile Broadband (eMBB) [8], Massive Machine Type Communications (mMTC) [9], and Ultra-reliable and Low-latency Communications (URLLC) [10]. To support these services and applications requirements, 5G not only aims to support the need for higher data rates, broader coverage, and higher capacity, but also it is more encompassing than these tradional wireless metrics [11]. For example, eMBB networking must meet the demanding requirements for bandwidth services required by today's evolving digital lifestyle, such as virtual reality (VR) and high definition (HD) video [12]. In addition, mMTC, which is also referred to as the Internet of Things (IoT) [13], must satisfy the requirements of high connection density, such as in smart buildings and cities. Furthermore, URLLC aims to meet the digital industry requirements of latency sensitive services, such as remote management, e-health, and automated driving [12]. These categories and applications are illustrated in Figure 1.1. The communication demands of machine-to-human and

machine-to-machine type applications will also be supported by the 5G mobile communication system with the goal of making our life more convenient and safer [11].

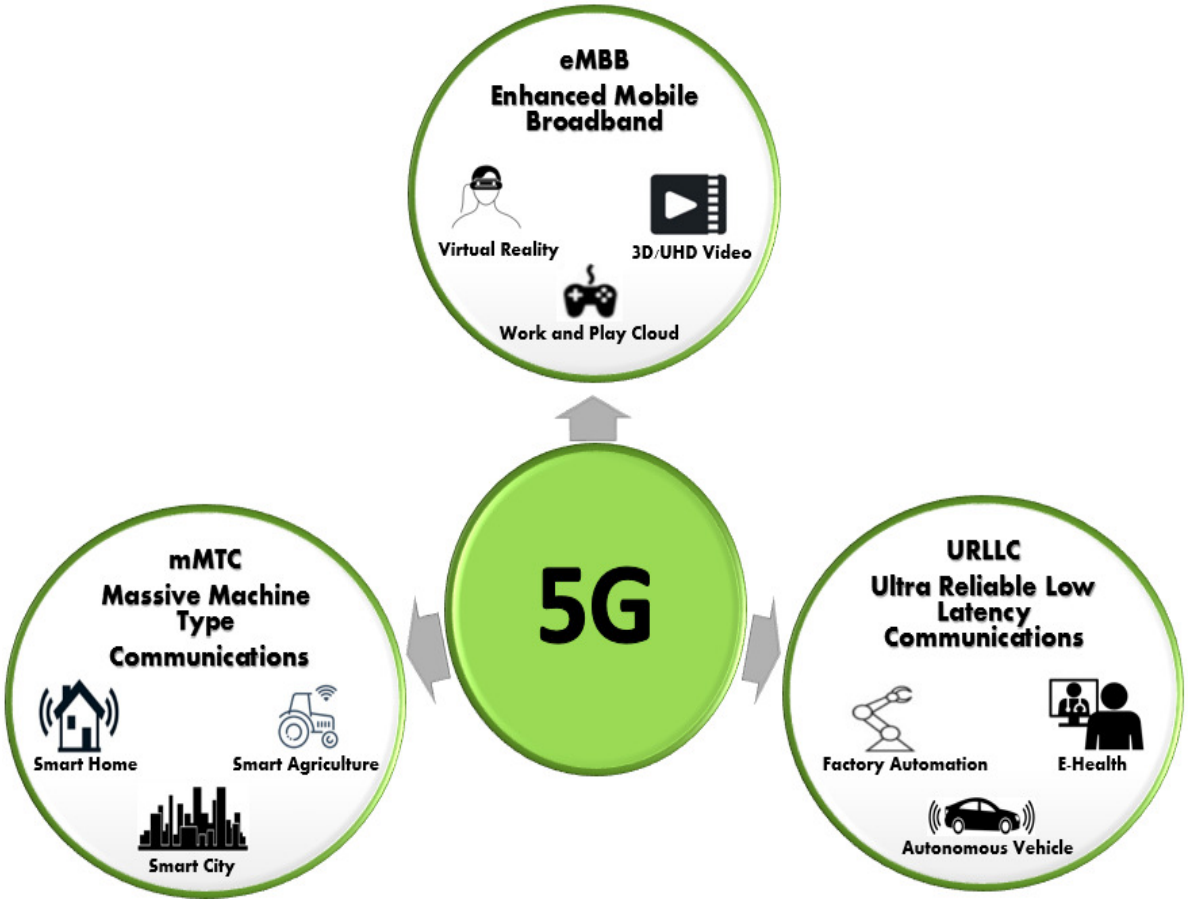

Figure 1.1 Categories and applications of 5G system.

1.1 Fifth Generation (5G) and IoT Requirements and Challenges

Here, we provide more detail to supplement the high-level 5G requirements and target applications that have been introduced in the previous section re high data speeds, low latency, high capacity, and massive connectivity [14].

- High data speed

  Practically, the high speed requirements of 5G technology will allow the data to transfer instantly. While 4G provides a maximum speed of 100 Mbps, 5G is expected to provide 1 Gbps – 10 Gbps, which means that 5G is as much as a hundred times faster than the

current 4G [12]. For example, the downloading of a high-definition movie, which might take 10 minutes to download in current 4G LTE, could take a matter of seconds using the 5G technology [15].

- Low Latency

  The latency is defined as the response time between the user request and the action being taken by a machine, application, etc. As a result, the 5G lower latency requirement of 1 ms and less will reduce the delay and improve the applications of streaming as video calling, online gaming, and live broadcasting events [16]. Additionally, lower latency will play a major factor in sensing and controlling applications as remote healthcare and autonomous vehicles [17].

- High capacity

  As a comparison to the current mobile technologies, the frequency bands of 5G will add more capacity which means that a greater capacity and additional spectrum will enable more data, more users, and faster connections [18].

- Massive connectivity

  One difference between 5G and 4G LTE is that the 5G will be designed for multiple traffic types rather than one traffic type [19]. At the same time, each traffic type will have different requirements. It is expected that, using 5G, billions of machines and sensors will be connected to the network [20]. Basically, connecting billions of devices without human intervention is at a scale not seen before. These objectives are illustrated in Figure 1.2.

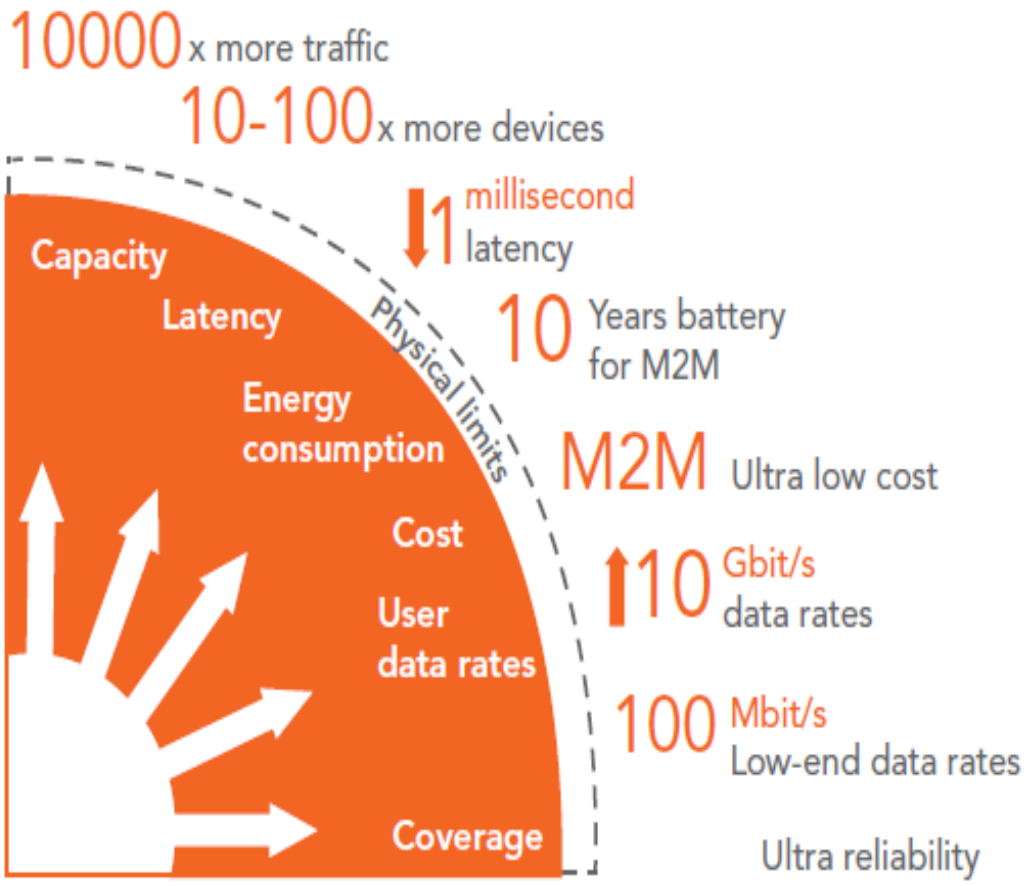

Figure 1.2 Objectives for 5G wireless system [21]. Adapted with permission.

The mobile activities that require buffering in 4G mobile networks will occur near-instantaneously in 5G mobile networks which means that the IoT is predicted to create a massive increase in the connections/number of devices across the wireless networks (Massive IoT) [22]. Massive IoT refers to the enormous number of IoT devices and sensors that are communicating with one another and typically transmitting data that is not delay sensitive. To support the devices that have long battery life with sending data of low data rates, Massive IoT should have deep coverage and density [21]. Typical applications include sensors that support smart cities, smart logistics, etc. Some of these applications of Massive IoT in 5G mobile networks are shown in Figure 1.3.

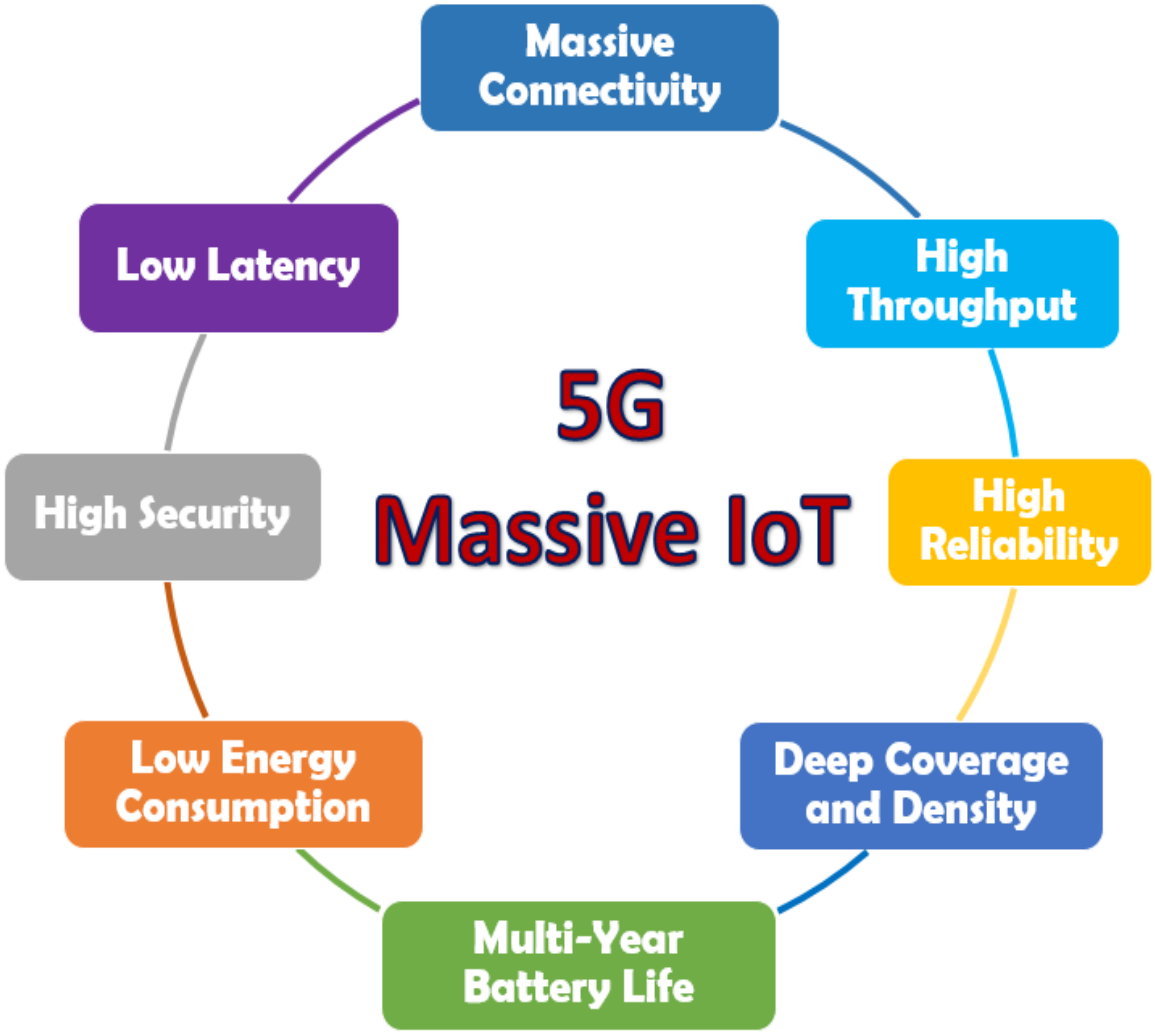

Figure 1.3 Massive IoT applications in 5G mobile networks.

Many companies and research labs are focusing on the connectivity of future services using IoT, and there substantial challenges that must be addressed in the IoT as a result of the increasing number of connected devices [23]. Some of these challenges include:

- Security: This represents one of the biggest challenges to protect personal data since the probability of a security breach increases as the number of devices is increased [24]. Because the Internet represents the backbone for IoT networks, there will be vulnerability to hacking and cyber attacking [25]. Private data and important information can be exposed by an IoT product with a poor design [19]. As a result, with

the many types of IoT devices and the different data they transmit, security is considered as a top concern [23].

- Connectivity: Reliable, secure, and managed connectivity is essential to connect large numbers of devices [25]. A centralized paradigm to connect and authorize different devices/nodes in a network [20], is sufficient when ten, hundreds, or thousands of devices are involved. But, such a model will be a bottleneck when billions of devices join a network [19]. Consequently, future IoT networks will likely depend on decentralized networks to overcome network damage in case of a network server or other failures [24].
- Hardware and device compatibility: Since IoT will utilize a plurality of technologies, this will impose the requirement for novel software and hardware to connect the devices [25].

1.2 Fifth Generation (5G) Radio Access Technologies

To address 5G challenges, the integration of existing technologies with new radio access technologies, such as the recently introduced 5G New Radio (NR) standard is anticipated [26]. In addition, new frequency bands are expected to be used. Several important physical layer technologies, which will be crucial for 5G wireless system, are Massive Multiple-Input and Multiple-Output (MIMO) [27], millimeter wave (mmWave) [28], and non-orthogonal multiple access (NOMA) [29].

- Massive MIMO: This represents an extension of the MIMO technology [30] and it groups antennas arrays together at the transmitter and receiver to provide better throughput and spectrum efficiency [31]. Conventional MIMO uses a small numbers of antennas, say 20 or less, to transmit data. On the other hand, massive MIMO uses a

few hundred antennas at base station (BS) to simultaneously serve many tens of devices and terminals. Massive MIMO aims provide greater spectral efficiency by spatial multiplexing several terminals in the same time-frequency resource. Two major innovations to improve capacity are offered by massive MIMO for 5G networks: beamforming and multi-user MIMO (MU-MIMO) [33]-[34], both of which will play a major rule in increasing the total network capacity and the single-user throughput [35].

- Millimeter Wave (mmWave): Today, more data is consumed by more people and devices than ever before on existing radio spectrum bands of the mobile providers [36]. As a result, less bandwidth is assigned for everyone which causes more dropped connections and slower services [37]. To address this problem, providers started experimenting with mmWave transmission by using higher frequencies than those that have traditionally been used [38]. Compared to the current used bands of sub-6 GHz, mmWave cellular systems operates in the 30-300 GHz band which gives it the ability to support data rates of multiple Gb/s owing to the large bandwidth [39]. In addition, very small components and antennas are used for the higher millimeter wavelengths compared to those for lower frequencies which offers a simpler design process for equipment [40]. Furthermore, the narrow beam and short range of these waves can lead to low interference from nearby radios and at the same time increase the security since the signals is restricted in small area [41]. As a result, mmWave is considered as another key enabling technology for 5G wireless networks. On the other hand, there are some challenges and constraints, related to the propagation in the mmWave frequency bands. For example, mmWave systems introduce a higher path loss due to the use of high

frequencies and in contrast to the microwave signals since they have less diffraction, mmWave signals are more vulnerable to blockages.

- Non-Orthogonal Multiple Access (NOMA): NOMA has been proposed as a promising multiple access (MA) technique in order to meet the requirements for 5G wireless communications and enhance the performance in IoT networks to enable massive connectivity, high throughput, low latency, and high reliability [42]. In contrast to conventional orthogonal multiple access (OMA) [43], a key feature of NOMA is to support a higher number of users than the number of available orthogonal time, frequency, or code dimensions [44]. Basically, NOMA is divided in two main categories, namely, power-domain NOMA and code-domain NOMA [45]-[46]. NOMA utilizes successive interference cancellation (SIC) [47] at the receiver side to detect the desired signals and enhance the spectral efficiency [48]. A detailed discussion about NOMA features and a comparison between it and OMA will be introduced in the next chapter.

1.3 Research Motivation

Over the past few decades, the wireless communication systems of 1G, 2G, 3G, and 4G have witnessed a revolution in their radio access technologies which are typically characterized by frequency division multiple access (FDMA), time division multiple access (TDMA), code division multiple access (CDMA), and orthogonal frequency division multiple access (OFDMA) as the key multiple access technologies [49]- [52]. These technologies belong to the category of orthogonal multiple access (OMA) where the resources are orthogonally allocated to multiple users in frequency, time, or code. As a result, the number of users that can be supported is limited by the available orthogonal dimensions [53]. Up till now good system performance can be achieved by

these technologies, but they still do not have the ability of addressing the 5G network challenges described above. To adequately serve the application classes of 5G, eMBB, mMTC, and URLLC, several challenges must be addressed, higher capacity, high spectral efficiency, massive connectivity, low latency [54]. As a result, NOMA has recently received significant attention for 5G wireless networks and is considered as a strong candidate to overcome these challenges [55]. For example, with large numbers of connected IoT devices, NOMA is expected to meet the requirement that mMTC that can connect around one million devices per square kilometer [56].

The objectives of this dissertation are to evaluate a novel approach for enhancing 5G system performance by utilizing NOMA as the multiple access technique for different application scenarios and performance metrics. Evaluating the optimum power levels of an uplink NOMA system and proposing a new NOMA-based medium access protocol to enhance the system throughput are some of the motivations of this dissertation that will be presented in the next section where the research areas of this dissertation are described.

1.4 Contributions and Organization of This Dissertation

This dissertation is focused on enhancing the performance of 5G network using NOMA. The contributions presented in this dissertation are the following:

- *Optimum power levels for uplink NOMA for 5G wireless communication systems* [57]
  Although massive MTC devices are usually power limited, they have applications with diverse quality of service (QoS) requirements such as, industrial automation and real-time localization [58]. Therefore, energy efficient transmission is a crucial requirement in most cases and it is important to design an energy-efficient power control scheme for uplink NOMA systems with QoS constraints [59]. However, extensive research, in the literature, has been done on power control and power allocation to analyze the

performance of a NOMA system [60] – [63]. For example, in [60], a power allocation scheme under minimum rate constraints has been proposed for NOMA system. Our research is directed toward determining the optimum received uplink NOMA power levels using a SIC detector for any number of transmitters and then comparing the derived results of the optimum power levels [57].

- *Medium access control (MAC) protocol for massive M2M IoT networks* [64]

  In M2M, tens of thousands of low complexity IoT devices can transmit to a gateway. Accordingly, a novel MAC protocol that is scalable, energy efficient and has high throughput is highly desirable. There are many studies that address MAC layer issues in M2M IoT communication [65]. Our research is directed toward proposing a scalable, energy efficient and high throughput MAC protocol for M2M IoT communication incorporating pure ALOHA [66] with power domain NOMA, which is called the ALOHA-NOMA protocol [64]. The simplicity of ALOHA, and the superior throughput of non-orthogonal multiple access (NOMA), along with the ability to resolve collisions via use of SIC receiver, makes ALOHA-NOMA a good candidate for a MAC protocol that can be utilized for low complexity IoT devices.

- *Uplink NOMA system bit error rate (BER) and SIC receiver degradation performance with channel estimation errors* [67]-[68]

  Our research is directed toward investigating the BER performance of a system with power-domain NOMA and SIC reception using BPSK, QPSK, and 16- QAM modulations schemes in the presence of channel estimation errors. A simulation study of the SIC receiver degradation of uplink NOMA due to channel estimation errors is

presented for BPSK, QPSK, and 16QAM modulation, where the degradation performance is analyzed for different channel estimation error values.

- *Channel capacity of a random waypoint (RWP) mobility model for 5G wireless networks system* [69]

  The performance behavior of the 5G wireless communications system is a key parameter in improving the system networks behavior [70]. The performance of 5G can be characterized using several parameters such as capacity, outage probability, and spectral efficiency, etc. Channel capacity represents a fundamental measure of performance in information theory, as it defines the upper bound of the maximum transmission rate of data at a vanishingly small bit error rate (BER) [71]. Moreover, channel capacity is used to study the effect of multipath fading statistical models where the received signal power is characterized [72]. As discussed in the literature, static wireless networks have mostly been analyzed using these models [73]. In static models, the average received power is constant since the transmitter-receiver distance is constant. On the other hand, in mobile communication systems, the distance between the transmitter and receiver is not constant and it follows a somewhat random behavior. Several mobility models have been discussed in the literature, for example random waypoint (RWP) and random walk (RWM) models [74]- [75]. So far, a lot of research has been devoted to the study of wireless communication networks capacity in terms of static model only [76]- [77]. To our knowledge, it is notable that these studies have not been considered the dynamic case to find the channel capacity of the wireless system network. Our research is directed toward deriving the channel capacity for a RWP mobility model of a Rayleigh fading channel [78] using a maximum ratio

combining (MRC) diversity receiver [79] and determining the effect of the number of receiver branches on the channel capacity. In addition, the derived channel capacity result is compared with the classic Additive White Gaussian Noise (AWGN) Shannon capacity [80] and with the static model Rayleigh fading channel capacity.

The dissertation is organized as follows. Chapter 2 presents a literature review for the different research areas in this dissertation. Determining the optimum received power levels for uplink NOMA using a SIC receiver for any number of transmitter and comparing the result with the μ-law PCM voice coder output levels are introduced in Chapter 3. A new scalable, energy efficient, and high throughput MAC protocol for M2M IoT communication, ALOHA-NOMA, is presented in Chapter 4. In Chapter 5, the BER performance and SIC receiver degradation of uplink NOMA using different modulation schemes is analyzed in the presence of channel estimation errors and then the simulation results are introduced. The channel capacity of the RWP dynamic model of a Rayleigh fading channel using MRC receiver is derived in Chapter 6. Chapter 7 summarizes the research contributions in this dissertation and provides future research directions.

Chapter 2: Literature Review

In this chapter, a literature review of the prior art of the three main topics of this dissertation is provided. First, a review of the NOMA technology proposed for 5G wireless systems and the associated IoT networks are reviewed. In addition, some prior art NOMA performance studies are presented. Second, a brief review and prior art of the MAC protocols proposed as candidates for M2M communication are introduced. Finally, an overview of the channel capacity in 5G wireless networks using a dynamic mobility model is presented.

2.1 NOMA in 5G Wireless Systems

In the past few decades, cellular communication systems have grown rapidly moving towards a paradigm shift where the users will be provided connectivity through heterogeneous networks [81]. For cellular communications, radio access technologies are often characterized by their multiple access (MA) techniques [82]. Designing a suitable MA technique is an important aspect for improving the system capacity. The 1G cellular system is an analog voice system and uses FDMA to provide voices services and supports a 10 kbps data rate. 2G provides digital voice and text messages services, using TDMA/FDMA, with a date rate of 300 kbps. With 3G, mobile internet and integrated voice services are provided using CDMA with a 50 Mbps data rate. OFDM and SC-FDMA are used in 4G to support high capacity mobile multimedia with a 100 Mbps data rate [83]. Using these MA techniques, different orthogonal resources either in time, frequency, or code are allocated to different users and these techniques are categorized as Orthogonal Multiple Access (OMA) technologies [84]. Specifically, OFDMA (for the downlink) and SC-FDMA (for the uplink) were adopted as OMA technologies for 4G, which were standardized by the 3rd

Generation Partnership Project (3GPP) [85] as LTE and LTE-Advanced, to support the user's quality of services (QoS) requirements. Using OFDMA, with multi-carrier transmission, the spectrum is divided into narrow-band 15 kHz subcarriers [86]. The interference between the adjacent subcarriers is eliminated by selecting the center frequency of each subcarrier in a way that ensures that all the subcarriers are mathematically orthogonal to each other and this eliminates interference between the adjacent subcarriers. So, the need of separating the subcarriers by means of a frequency guard-band is avoided by the orthogonality [87]. This represents one advantage of OFDMA.

Although OFDMA offers some advantages, one of the disadvantages of OFDMA is its high peak-to-average power ratio (PAPR), which requires highly linear power amplifier [88]. The effect of a high PAPR reduces the power efficiency and increases the power consumption of mobile user equipment (UE) that shortens the battery life. In downlink transmission because of the availability of power at the base station (BS), this issue is not serious. But since a mobile user is limited by the battery capacity, it represents a major concern in uplink transmission [89]. In order to overcome this disadvantage of OFDMA, SC-FDMA, a modified version of OFDMA, has been adopted as the standard for LTE uplink multiple access transmission. Although the orthogonal subcarriers are used to transmit data symbols in SC-FDMA, they are transmitted sequentially rather than in parallel as in OFDMA with a lower PAPR. So, SC-FDMA was attractive for uplink transmission in LTE [90].

The diversity of applications and requirements, high speed mobile internet, IoT applications, and smart applications that 5G networks will need to support is one of the biggest differences between 5G and the previous generations. 5G wireless systems are expected to provide high spectral efficiency, increased data rate, lower latency, and massive connectivity. Further, a

large number of wireless connections supporting IoT applications will represent a revolution of 5G [91]. Consequently, it remains a challenge for OMA to satisfy these requirements of 5G. For example, the number of available orthogonal resources provides a limitation for the number of supported users in OMA, which means that it cannot support the 5G requirements of a huge number of connected IoT devices [92]. As a result, NOMA has been proposed as a promising MA candidate, for more efficient spectrum reuse. In contrast to OMA, the innovative principle of NOMA is to allow multiple users to share the same resources, either in time, frequency, or code [93]. In other words, one frequency channel is allocating to multiple users at the same time within the same cell [94] and Successive Interference Cancellation (SIC) is generally used at the receiver to recover the data. To support IoT applications, a downlink version of NOMA, which is called multiuser superposition transmission (MUST) [95], has been proposed for 3GPP-LTE-Advanced networks which gives NOMA the ability to be compatible with the current and future communication systems.

Comparisons between NOMA and OMA shows that NOMA provide a spectral efficiency and throughput substantially better than OMA [29], under certain conditions. For example, in OFDMA, the overall system suffers from low throughput and spectral efficiency by assigning a specific frequency to each user whether or not the user has a good or bad channel. On the other hand, using NOMA, the same frequency resource may be assigned to multiple simultaneous users with good (strong received signal) and bad (weaker received signal) channel conditions [29]. And, ideally, a SIC detector eliminates the interference at the receiver. So, under certain circumstances enhanced spectral efficiency and throughput may be achieved by using NOMA rather than OMA. Furthermore, scheduling in OFDMA leads to high latency when a higher access priority is given to a user with good channel condition and a lower access priority may be assigned to a user with

bad channel conditions that creates high latency and unfairness problems. In contrast, by serving multiple users simultaneously with different channel conditions, NOMA can provide low latency and improved fairness in addition to high massive connectivity, where the number of supported users in OMA is restricted by the number of available orthogonal resources. Using 5G, the data rate is expected to be 10 times of the 4G data rate (1 Gb/s – 10 Gb/s). And the latency is 1 ms or less which is one-fifth of the 4G latency [29]. These requirements are expected to be met by using as a MA technique. Basically, NOMA is divided in two main categories, power-domain NOMA and code-domain NOMA. The key feature of power-domain NOMA is to allow different users to share the same time, frequency, and code, but with different, specified power levels. In code-domain NOMA, different spread-spectrum codes are assigned to different users and are then multiplexed over the same time-frequency resources [45]. Different variations of these schemes have been proposed in the literature, e.g., sparse code multiple access (SCMA) [96] and multi-user shared access (MUSA) [97] have been proposed as code-domain NOMA schemes. In SCMA, according to a time-frequency domain codebook set, the coded bits of multiple data layer are directly mapped to a multi-dimensional sparse codeword, and the data of multiple users are transmitted on the same resources [98]. At the receiver side, for multiuser detection target, the message passing algorithm (MPA) is used [99]. The complexity of MPA is rather than high. On the other hand, in MUSA, non-orthogonal short sequences are used to spread the modulated symbols of multiple users among them and then these symbols are transmitted over the same time-frequency resources [98]. The SIC detector is realized at the receiver side for multi-user detection (MUD) process which has a complexity lower than MPA. The main objective of this dissertation focuses on power-domain NOMA instead of the code-domain NOMA, and further discussion of different code-domain NOMA schemes can be found in [100]- [105].

The key concept of power-domain NOMA is that different power levels are assigned to different users according to their channel quality, while sharing the same resources of time, frequency, and code among multiple users. At the receiver side, a SIC detector is applied, in the uplink and downlink, to separate and decode the superimposed signal of multi-user signals by exploiting the power difference between them [106]-[107]. Using SIC each user's signal is successively decoded. For example, after the user's signal with the highest power is decoded, then it is subtracted from the combined signal before decoding the next user's signal. In other words, as one of the user signals is decoded, the residual user signal is considered as noise. The process is repeated until the last signal is decoded, with each decoding having the benefit of the former signals having been removed [108]. Practically, users are ordered depending on their signal strengths. So, the SIC receiver first decodes the strongest signal, then it subtracts this signal from the combined signal, and finally the weakest is detected in the presence of only noise. The basic concept of using power-domain NOMA in the downlink and uplink is presented next.

2.1.1 Uplink and Downlink NOMA

For uplink NOMA system, SIC is applied at the base station (BS). Different users signals are transmitted to the BS and different channel coefficients are associated with the received signal at the SIC. For simplicity, an uplink NOMA model of two users that have different channel coefficients is considered. Assuming that the two users transmits their signal at the same time and frequency and are synchronized with each other. The BS receives the superimposed signal of the two users and then SIC is applied to decode each signal. The received signal at the BS is the superimposed signal of the two users but with different channel coefficients. Assuming user 1 has a signal of x_1 with channel coefficient h_1 and user 2 has a signal of x_2 with channel coefficient h_2,

respectively. Additionally, user 1 and user 2 have corresponding power coefficients as P_1 and P_2, respectively. This model is illustrated in Figure 2.1 as shown below.

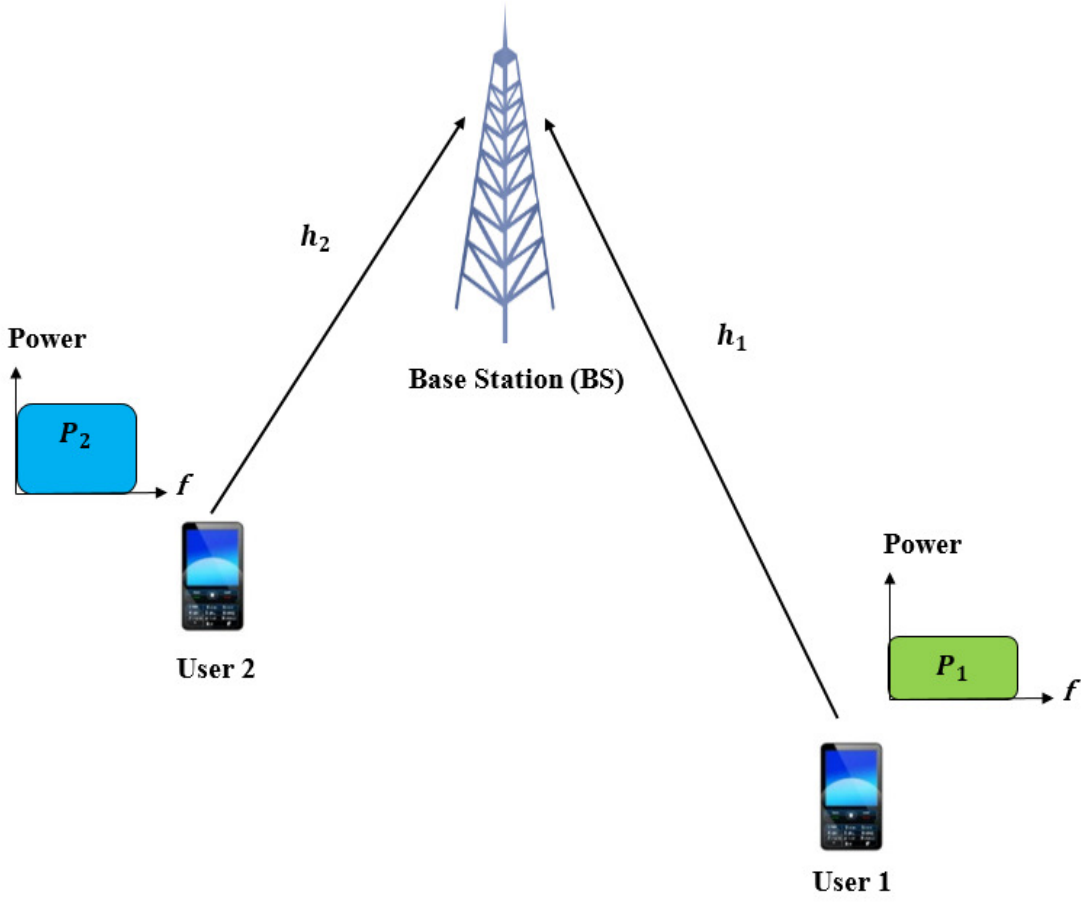

Figure 2.1 Uplink power-domain NOMA system of two users.

Assuming that x_2 represents the strongest signal, then the analysis of this model is explained as follows. The signal of the first user x_1, which has power P_1, is transmitted to the BS through a channel with known coefficient h_1. In the same way, the second user signal x_2, with power P_2, is sent to the BS with a known channel coefficient h_2. As the power coefficients P_i are included in the users signals x_i, the received signal, at the base station (BS), y, is given as:

$$y = h_1 x_1 + h_2 x_2 + n, \qquad (2-1)$$

where n is the AWGN with zero mean and variance σ^2.

The SIC receiver is used at the BS to decode the two received signals in two stages. In the first stage, the SIC receiver detects the strongest signal of user 2 from the superimposed signal and noise as given in (2-1), and the other signal is considered as a noise (or interference). Then, the decoded signal of user 2 is subtracted from the superimposed signal and the signal of user 1 is decoded.

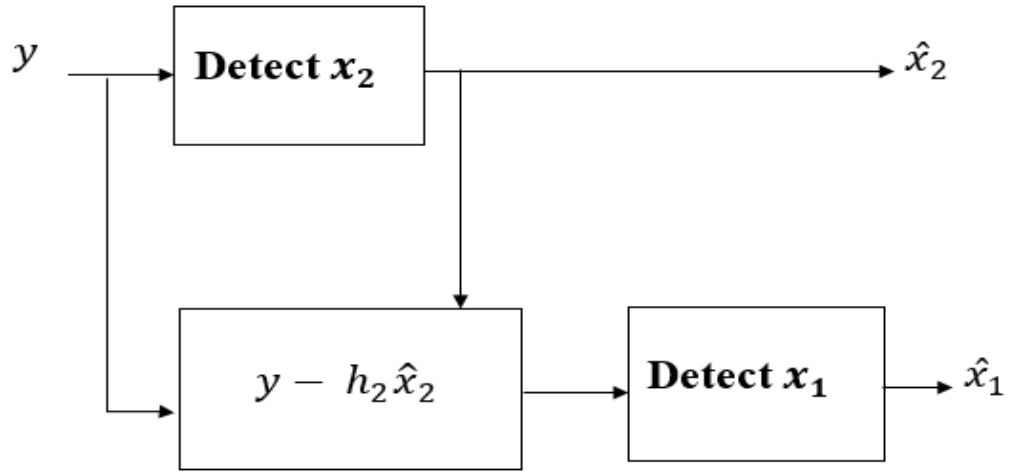

Figure 2.2 Illustration of SIC detection at the BS.

In downlink NOMA system, the same analysis of uplink NOMA can be followed but the SIC detector is applied at the receiver side of users instead of the BS. As a comparison, there are some differences between the two systems. The implementation of multi-user detection and interference cancellation is of greater complexity in the downlink than in uplink because the lack of a centralized processing unit and the limited mobile users processing capabilities [109]. However, it is likely that downlink NOMA does not scale in capacity, especially, when the number of users is large as envisioned in IoT networks. In addition, the SIC receiver in downlink NOMA needs to successfully decode the user signals and for the same issue of large number of users any error propagation in the detection process may remarkably reduce the NOMA performance [110].

Therefore, the research studies in this dissertation focus on using uplink NOMA instead of downlink NOMA.

Several research studies of the performance of uplink NOMA system are in [111] – [115]. For example, in [111], a power allocation scheme has been proposed and then the throughput maximization for uplink NOMA under the total transmission power constraints with minimum rate requirements of users has been investigated. The results show that the throughput uplink NOMA performance with the proposed scheme is much better than OMA for different users date rate. In [112], the authors have introduced an algorithm to investigate the optimal power allocation for uplink NOMA and derive an expression for the optimal closed-form power allocation. The proposed scheme and the simulation results demonstrate a performance enhancement of the proposed algorithm compared to OMA system. The resource allocation problem for uplink multi-carrier NOMA in a device-to-device (D2D) underlaid cellular network has been investigated in [113]. The existence of D2D pairs, where adjacent users/terminals use a direct link to communicate rather than sending their signals to the BS or central node, leads the NOMA users to have different degree of interference. An algorithm has been proposed to model the user clustering and solve the power allocation problem [113]. The results show the convergence of proposed algorithm which achieve near optimal performance in addition to higher fairness than in OMA. In [114], the authors have examined the uplink NOMA performance by proposing an uplink NOMA system with cooperative full-duplex relaying (CFR-NOMA) in which the near user acts as a full-duplex relay for the far user. The investigation of the outage probability and average sum rate has been introduced by deriving closed-form analytical expressions on the outage probability and average sum rate [115]. In addition, optimal power allocation scheme to maximize the average sum rate

has been studied. The simulations result show that a significant improvement in the outage probability and average sum rate has been observed over the conventional uplink OMA.

In this dissertation, an analysis for the optimum received power levels of uplink power-domain NOMA, using a SIC detector, is presented in Chapter 3. The optimum received power level is determined for any number of transmitter. Then, the results are compared with μ-law PCM levels to give some intuitive insight as to the significance of the optimum power levels. To address the requirements of M2M IoT communication, a new MAC protocol, which is called ALOHA-NOMA is proposed and discussed in Chapter 4. The performance of uplink power-domain NOMA is studied in this dissertation where the BER performance is investigated in the presence of channel estimation errors for uplink NOMA and SIC reception using BPSK, QPSK, and 16- QAM modulations schemes. Furthermore, for the same uplink NOMA system, the SIC degradation is analyzed for different channel estimation error values in terms of the bit error rate (BER). These studies are presented in Chapter 5 of this dissertation.

2.2 MAC Protocols for M2M Communication

In Wireless Sensor Networks (WSN) [116], which is a rapidly growing application area, randomly distributed sensors are used by a set of nodes to monitor environmental or physical conditions such as, motion, pressure, temperature, etc., which are widely used in different applications of life as health, military, traffic control, and manufacturing applications [117]. WSNs generally experience performance degradation due to, insufficient coverage, scalability, congestion, and lack of robustness. Similarly, the sensors nodes are distributed in large numbers of places and they have limitations of coverage area and power consumption [118]. To understand WSN behavior, it is important to analyze the network performance. In addition to the above mentioned issues, some parameters like throughput and delay are important in characterizing WSN

performance. However, energy efficiency represents an important metric to measure WSN performance, since energy consumption represents a main problem for WSNs that often leads to a node failure [119]. MAC protocols play a major role in WSNs due to their ability of establishing a communication link to transfer data and save energy that results in enhancing the WSN performance [120].

In the open systems interconnection (OSI) model [121], the MAC is a sublayer in the data link layer (DLL) [122] which is the second layer of the OSI model. Many MAC protocols have been standardized by the Institute of Electrical and Electronics Engineers (IEEE), as Ethernet (IEEE 802) standards [123], for local area networks (LAN) and metropolitan area networks (MAN) [124]-[125]. Actually, the IEEE divided the DLL in two sublayers: logical link control (LLC) [126] which is the above sublayer that represents the control sub-layer, and the MAC layer which is the lower sub-layer. This is illustrated in Figure 2.3. Mainly, the MAC function is to provide channel access and an addressing mechanism that allow each available node on the network to communicate with other nodes on the same or other network [120].

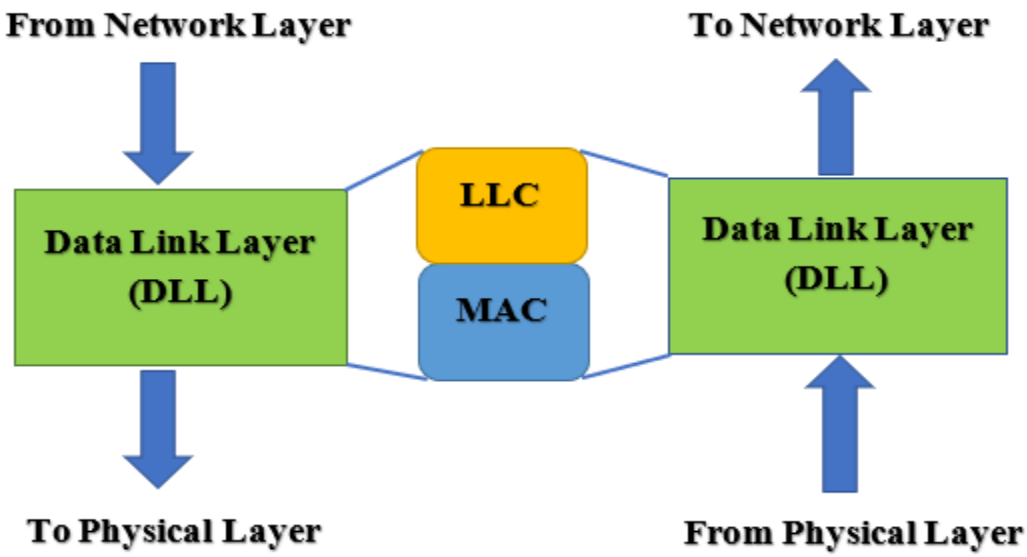

Figure 2.3 Illustration of DLL in OSI model.

MAC protocols, can be classified into three main categories, contention-based [127], scheduled-based (contention-free) [128], and hybrid protocols [129]. The MAC categories and their assigned protocols are show in Figure 2.4 and explained next.

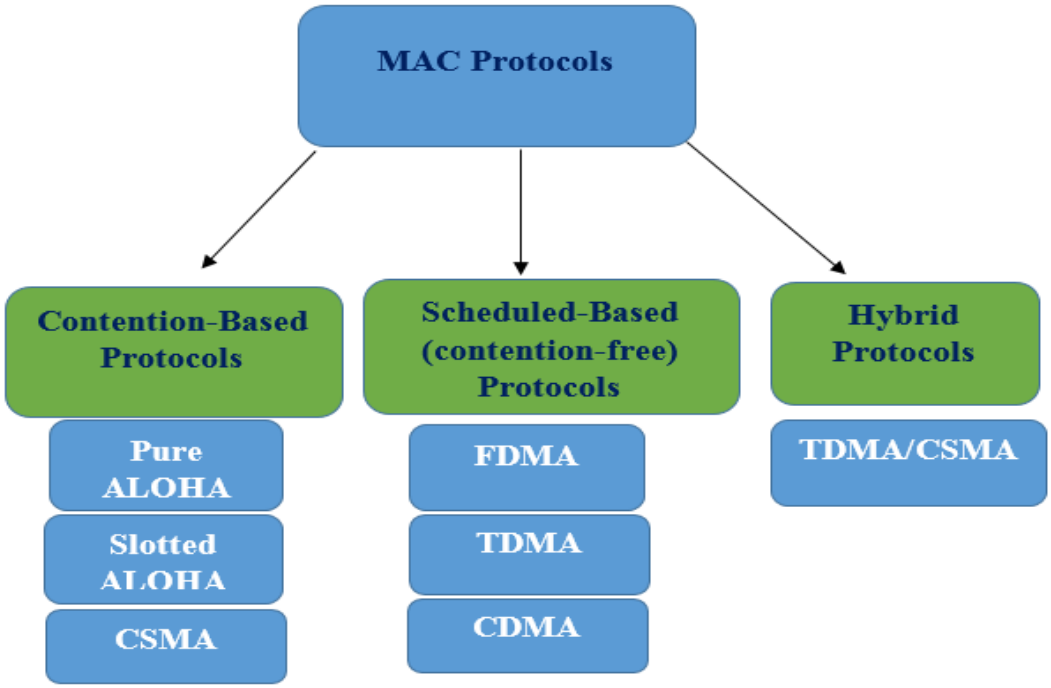

Figure 2.4 Examples of MAC protocols in WSNs.

- *Contention-based protocols*

  In these protocols, which are referred as random access protocols, the nodes are allowed to access the shared wireless medium independently. Although these protocols can provide good adaptive and scalable features, the nodes cannot know when the channel is available to send their packets. Therefore, many nodes send their packets and access the channel at the same time. This results in a collision which represents a major performance limitation for these protocols [127]. ALOHA, also called pure ALOHA [66], slotted-ALOHA [130], and Carrier Sense Multiple Access (CSMA) [131] represent well known contention-based protocols.

In ALOHA, which was developed at the University of Hawaii, each user generates packets and all of them have the same fixed length time period. When a user has a packet to transmit, the packet is immediately transmitted. The sender waits for an acknowledgement that the transmission has been correctly received. When a transmission of a packet does not interfere with any other packet transmission, the transmitted packet is received correctly. But if two or more packet transmissions overlap in time, a collision occurs and neither of the colliding packets is received correctly and they have to be retransmitted. The throughput, which is defined as the average number of successfully transmitted packets per unit of time, is the major ALOHA performance metric. The maximum throughput that can be supported by ALOHA is 18%, which is considered a low throughput, as a result of collisions.

In slotted ALOHA, which is an improved version of the original ALOHA, the channel time is divided into discrete intervals (slots) and a packet can be sent only at the beginning of the time slot and only one packet can be sent by each time slot. Slotted ALOHA doubles the throughput of ALOHA, to 36%, [130].

Although ALOHA and slotted ALOHA are simple, their efficiency is low. As a result, if the users listen to the channel before transmitting their packets, a lot of collisions can be avoided and this is the concept of CSMA [131]. In CSMA, only one user can transmit, otherwise a collision occurs and leads to data packet loss. CSMA initiates transmission when the user needs sending the data over the channel. In this case, each CSMA listens to the channel to check for any other in-progress transmissions. If a transmission is detected, then the user waits for it to end before transmitting their data. CSMA is commonly used in Ethernet (IEEE 802.3) networks [123]. CSMA with

Collision Detection (CSMA/CD) and CSMA with Collision Avoidance (CSMA/CA) represent two types of CSMA [132]-[133]. Simply, in CSMA/CD, the channel is monitored after a packet is sent to check if the transmission is successful or not. A successful transmission means that the transmission process is completed; otherwise, the packet is sent again [132]. In contrast, the idea of CSMA/CA is that each user should have the ability to receive while transmitting, in order to detect a collision from other users [133].

- *Scheduled-based (contention-free) protocols*

  In contention-free protocols only one sensor node is allowed to access the channel at any given time, which avoids collisions [134]. Actually, at any given time, resources are allocated to individual nodes to guarantee that each resource is accessed by only one node [128]. Based on these resources, frequency, time, or code, one of three scheduled protocol are used. These protocols are, FDMA, TDMA, and CDMA.

- *Hybrid Protocols*

  In these protocols, the advantages of the TDMA scheduled based protocol and the CSMA contention-based protocol are combined where the data packets are transmitted using TDMA [129]. As compared to the contention and scheduled categories protocols, hybrid protocol can support better flexibility in addition to that they are considered as energy efficient protocols.

For massive number of devices in IoT, M2M enables connectivity between them [135]. M2M has some network challenges related the large number of connected devices such as quality of service (QoS), scalability, enhanced throughput, and network resources management. In addition, power consumption and changing of the service requirements based on the existing

applications are also considered as challenges for M2M [136]. As a result, MAC protocols play a major role in the performance of M2M communication [137]. For example, ZigBee (IEEE 802.15.4) [138], which is one of the most used technologies for IoT, is considered as a potential candidate for M2M communication [139]. In ZigBee, the contention-based CSMA/CA is used to reduce the collisions.

The incorporation and development of MAC protocols for M2M communications is a very current research area [140]- [142]. In [140], an access control algorithm, which is called adaptive traffic load slotted ALOHA, has been proposed to avoid the access M2M network congestion under high traffic loads and improves the resources utilization. The results show that the proposed algorithm is robust against different traffic loads and the access successful rate is increased dramatically. In [141], a hybrid MAC protocol for M2M protocols has been proposed. In this protocol, orthogonal codes for channel contention are used and a logical queue is used to schedule the nodes. The results show that the proposed protocol is more efficient and provides better packet delivery ratio than the well-known distributed queuing collision avoidance (DQCA) in addition to it is simplicity of implementation. A scalable hybrid MAC protocol, based on CSMA and TDMA, has been designed in [142] for heterogeneous M2M networks. The protocol organizes the contention and the reservation process of different devices two parts: transmission only period (TOP) and contention only period (COP) to enhance the M2M network energy consumption which is investigated by the resulting results and showed the effectiveness of the proposed protocol.

However, the increasing number of node density in M2M may add a limitation on using the contention-based protocol according to the resulting collisions which results in poor performance [143]. Although IEEE 802.11 [144] represents the most widely used protocols and uses CSMA/CA, it cannot be widely used for M2M according to its inability to be capable of

increasing the network size (not scalable) and large amount of wasted energy as a result of the collision, and the control packets overhead [145]. Contention-free protocols offer dynamic adaptation in their operation but this needs additional overhead which limit the overall improvement. For example, CDMA protocol is not suitable for low-cost M2M applications according to its complexity as a result of the near-far problem which needs a power control technique to address it.

In this dissertation, the simplicity of ALOHA and the superior throughput of NOMA [by resolving the collisions using SIC detector] has been utilized to propose a novel MAC protocol to address the requirements of M2M IoT communication. The proposed protocol is called ALOHA-NOMA [64]. The analysis show that the proposed protocol is scalable, energy efficient, and has high throughput which makes it a good candidate for a MAC protocol to be utilized for low complexity IoT devices [64]. More details about the proposed ALOHA-NOMA protocol and its performance are introduced in Chapter 4.

2.3 Channel Capacity of 5G Wireless Networks Using Dynamic Random Waypoint (RWP) Mobility Model

Channel capacity, which was defined by Claude Shannon as the upper bound on the maximum rate at which information can be reliably transmitted over a communication channel [80], represents one several parameters that are used to characterized the performance of 5G wireless network systems, in addition to outage probability and spectral efficiency [146]. As a result, these parameters can measure the network quality and capacity, respectively. As is well known, the channel capacity in an AWGN environment was derived by Shannon in 1948 [80]. Several decades later, the channel capacity for fading environments was introduced [147]-[148]

and the effect of multipath fading statistical models, which to date have primarily considered the static wireless network model, has been studied and measured by calculating the channel capacity.

Average received power represents a primary parameter that characterize the system behavior. In addition to its use as a received signal strength indicator to help in designing of power control and handover algorithms, it is central to determining wireless networks capacity [149]. In static models, it is given as given as a function of the transmitted power, transmitter-receiver distance, and path loss exponent. Since the transmitter-receiver distance is constant, in static models, the average received power is constant [150]. In contrast, in mobile systems, the transmitter-receiver distance is not fixed and it follows a random pattern. The variation of received signal power occurs due to node mobility, distance dependent path loss, and multipath fading which results in time varying received power, which, in general, that does not exhibit the same behavior as static wireless networks. Several mobility models have been discussed in the literature and a popular used one is called the random waypoint (RWP) model [74]. This model, which was proposed by Johnson and Maltz [151], describes how the mobile users (nodes) change their velocity and location over time in addition to their movement pattern. The concept of RWP will be introduced in Chapter 6.

The channel capacity of wireless communication networks has been studied in the literature in static models as introduced in [152]-[154]. In [152], the authors have been presented an architecture for analyzing the capacity when Device-to-Device (D2D) communications share the channel resources with cellular links. The authors in [153] have been studied the achievable transmission capacity of secondary users in heterogeneous networks. In [154], the optimal D2D transmission capacity and density in different bands have been studied. It is notable that, the dynamic case, in these studies, have not determined the channel capacity of the wireless system

network. Recent research [155] and [156], has studied the outage probability in a dynamic model. In [155], an expression of the outage probability in dynamic mobility model over a Rayleigh fading channel has been derived. In [156], the distribution probability density (PDF) function and the outage probability of dynamic mobility model has been derived over a (η-μ) fading channel. This research discussed the outage probability not the channel capacity.

In Chapter 6 of this dissertation, the RWP mobility model channel capacity of a Rayleigh fading channel, using a maximum ratio combining MRC diversity receiver, is derived. Then, the derived result is compared with the AWGN Shannon capacity and the capacity of a static model Rayleigh fading channel.

2.4 Concluding Remarks

In this chapter, an overview of NOMA techniques in 5G wireless systems and related performance research studies were presented. Then, the MAC protocols that are used in M2M and IoT applications and the corresponding challenges were introduced. Finally, an overview of 5G wireless network channel capacity using dynamic RWP mobility was presented.

Chapter 3: Uplink Non-Orthogonal Multiple Access (NOMA) Optimum Received Power Levels[1]

3.1 Introduction

As it is mentioned earlier in Chapter 1 and Chapter 2, the multiple access technique plays a major role in 5G mobile system performance. NOMA has been proposed as promising multiple access technique in order to meet the stringent requirements for 5G wireless communications and enhance the performance in IoT networks such as, high throughput, low latency, high reliability, and massive connectivity. As a result, NOMA is considered as a strong candidate for 5G applications and consequently it is important to investigate the performance of the 5G wireless communications system using this technology for different scenarios and performance metrics.

In this chapter, an analysis of uplink power-domain NOMA is presented to evaluate the optimum received power levels. The relation is determined for any number of transmitters, using an optimized SIC detector that can decode the transmitted signals by cancelling the interference. The optimum received power levels are derived, and compared with the result of the well-known μ-law pulse code modulation (PCM) levels [157] to point an unexpected and striking similarity between the two systems.

The system model of the proposed scenario is presented in the next section. Then, the derived result and the comparison study is introduced and analyzed. Finally, the conclusions of this chapter is presented in the last section.

1 The content of this chapter has been published in [57], and it is included in this dissertation with a permission. Permission is included in Appendix A.

3.2 System Model

Without loss of generality, the system model first considers an uplink NOMA system of three mobile users and a BS receiver and the result is then generalized for N users. The corresponding system diagram is illustrated in Figure 3.1. Using NOMA, a frequency channel is allocated to multiple simultaneous users within the same cell with good (strong received signal) and bad (weaker received signal) channel conditions[2]. And, ideally, the SIC detector is applied at the receiver side to recover the data and eliminate the interference by using successive interference cancellation [47].

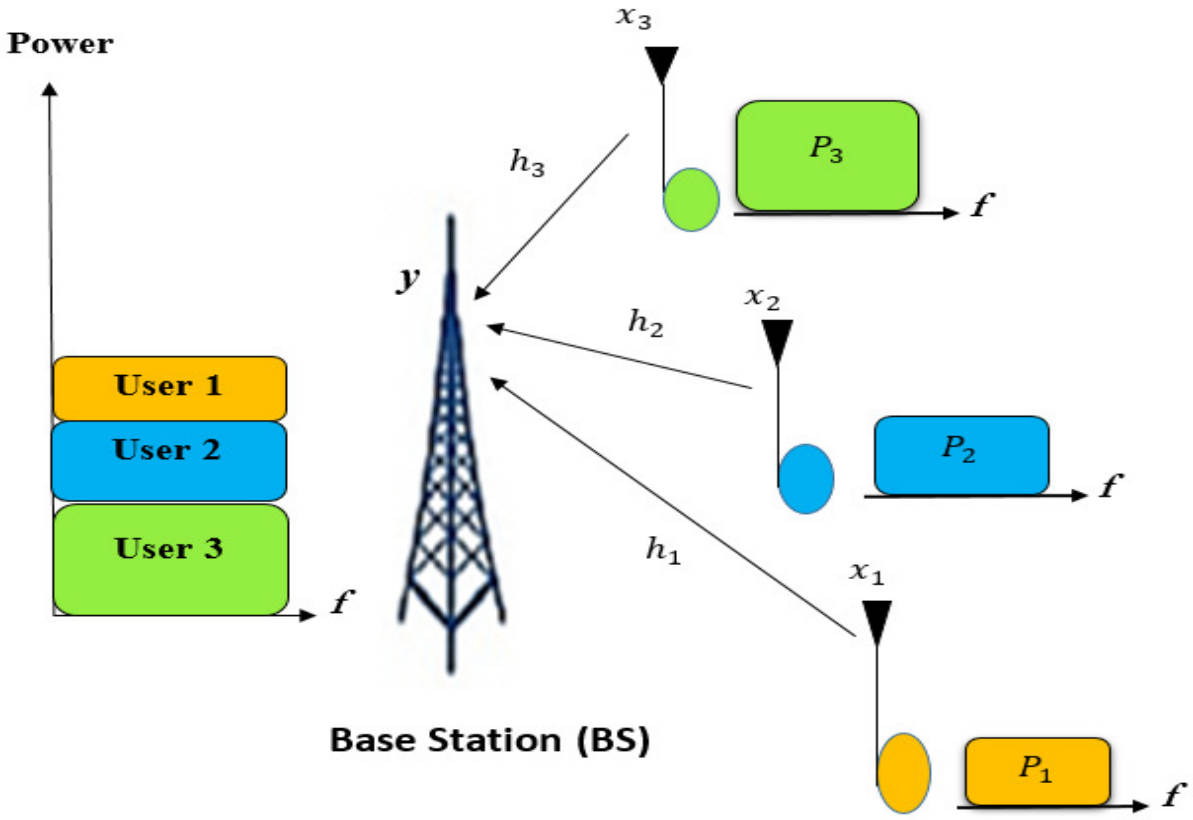

Figure 3.1 Uplink power-domain NOMA with ideal SIC reception.

2 Once the channel attenuation has been determined, the power of the received signals can be adjusted by varying the transmitter powers. We will assume that this has been accomplished and we refer to "strong" and "weak" signals received at the base station.

NOMA with SIC exploits the signal-to-interference-plus-noise ratio (SINR) difference among users because of the non-uniform power allocation at the user transmitters. It will be assumed that the three users transmit their signal at the same time and frequency and are synchronized with each other. The superimposed signal of the three users, with different channel coefficients, is received by the BS and then SIC is applied to decode each signal. By assuming that the third user signal x_3 is the strongest signal and the first user signal x_1 as the weakest signal, the model analysis is explained as follows. The first user signal x_1, which is scaled by a power coefficient P_1, is transmitted to the BS through a channel with known coefficient h_1. Similarly, the signal of the second user x_2, which is scaled by a power coefficient P_2, is transmitted to the BS through a channel with known coefficient h_2. Furthermore, the signal of the third user x_2, which is scaled by a power coefficient P_3, is transmitted to the BS through a channel with known coefficient h_3. As the power coefficients P_i are included in the users signals x_i, the superimposed signal at the base station (BS), which is defined as y, is given as:

$$y = h_1 x_1 + h_2 x_2 + h_3 x_3 + n, \qquad (3-1)$$

where the parameter n is the well-known Additive White Gaussian Noise (AWGN) with zero mean and variance σ^2.

The SIC receiver, at the BS, decodes the three received signals in three successive stages. In the first stage, the strongest signal of the third user is first decoded from the superimposed signal and the other users signals are considered as noise (or interference). After that, the decoded signal of the third user is subtracted from the delayed and stored combined received signal. Then, the second user signal is decoded in the second stage and the first user signal is considered as interference. Finally, in the third stage, the weakest signal of the first user is decoded, only in the presence of AWGN, after the decoded signal of the second user is subtracted from the combined

signal. The concept of using a SIC receiver for successive decoding the three signals is illustrated in Figure 3.2.

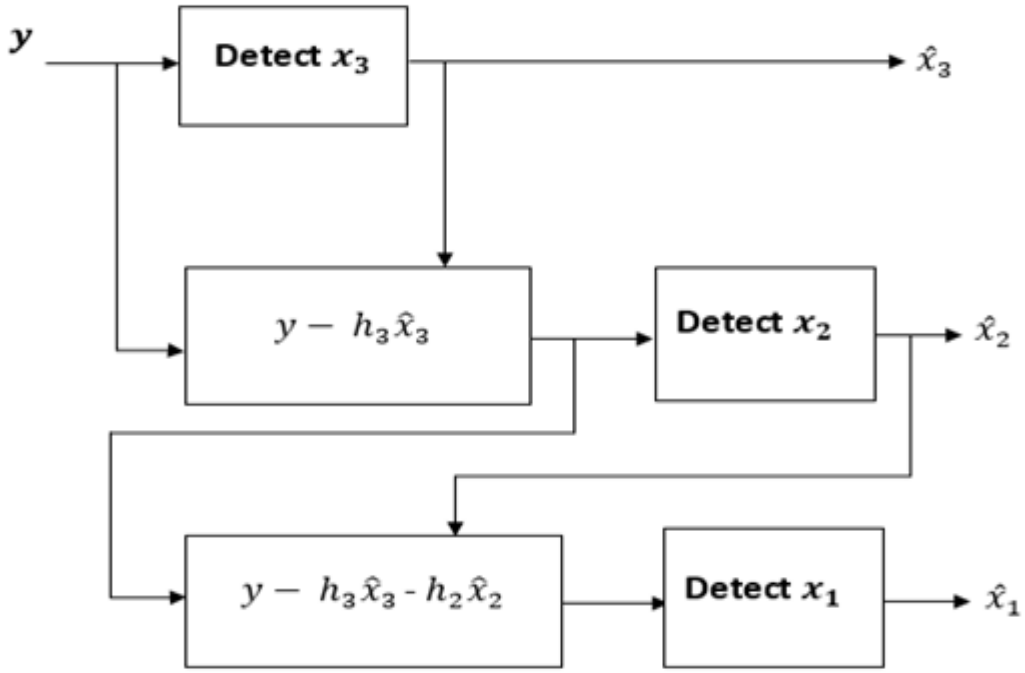

Figure 3.2 The SIC detector at the BS for three users.

In this research, the optimum received power levels of uplink power-domain NOMA, using a SIC detector, is determined for any number of transmitters [57]. Then, a comparison between the obtained results of the optimum power levels with μ-law PCM levels is introduced to demonstrate a surprising connection between the two systems The optimum received power level is determined for each signal so as to achieve the same bit error rate (BER) for each received signal. The optimum received power level for each transmitter is computed and then compared with a specified value (threshold value) of SINR to achieve the same BER for each signal. The optimum received power level is derived for the case of three transmitters and then it is generalized for *N* transmitters.

To derive the general formula for the optimum received power levels, the signal power of the first transmitter P_1 is determined and then it is compared with the required threshold SINR.

The required SINR is assumed to be the same for each signal. The value P_1 such that x_1 can be accurately received is

$$\frac{P_1 {h_1}^2}{{\sigma_n}^2} = SINR, \qquad (3-2)$$

which is rewritten as

$$P_1 = \frac{{\sigma_n}^2}{{h_1}^2} SINR. \qquad (3-3)$$

Similarly, the second transmitter power, P_2, is computed via the iterative equation

$$P_2 \, {h_2}^2 = \; SINR \left(P_1 {h_1}^2 + \; {\sigma_n}^2 \right) \qquad (3-4)$$

Substituting (3-3) in (3-4) gives that

$$P_2 = \frac{{\sigma_n}^2}{{h_2}^2} \; SINR \; (SINR + 1). \qquad (3-5)$$

As observed in (3-5), the power value P_2 depends on the power value of the first transmitter P_1. The same rule is iteratively applied to determine P_3, which depends on the previous values of P_1 and P_2 and is determined to be

$$P_3 \, {h_3}^2 = \; SINR \left(P_1 {h_1}^2 + \; P_2 {h_2}^2 + \; {\sigma_n}^2 \right)$$

$$P_3 = \frac{{\sigma_n}^2}{{h_3}^2} \; SINR \; (SINR^2 + 2 \, SINR + 1). \qquad (3-6)$$

This iteration is extended for *N* transmitters and the optimum received power levels are determined as a function of the noise power value, ${\sigma_n}^2$, channel coefficient h_i, and the required SINR as

$$P_i \, {h_i}^2 = \; SINR \left(P_1 {h_1}^2 + \; P_2 {h_2}^2 + \cdots + \; P_{i-1} {h_{i-1}}^2 + {\sigma_n}^2 \right)$$

$$P_i = \frac{\sigma_n^2}{{h_i}^2} \; SINR \; (1 + SINR \;)^{i-1}, i = 1,2, \ldots, N. \qquad (3-7)$$

In next section, the optimum received power level for different *N* and SINR are described and compared to the optimum receive power level results with the μ-law PCM levels results.

3.3 Optimum Received Power Levels

In this section, the derived optimum received power levels relation, (3-7), is evaluated using MATLAB for different values of *N* and different values of SINR (in dB). In Figure 3.3, the optimum received power levels for different values of *N*, where SINR= 2 dB is fixed for each user, is presented.

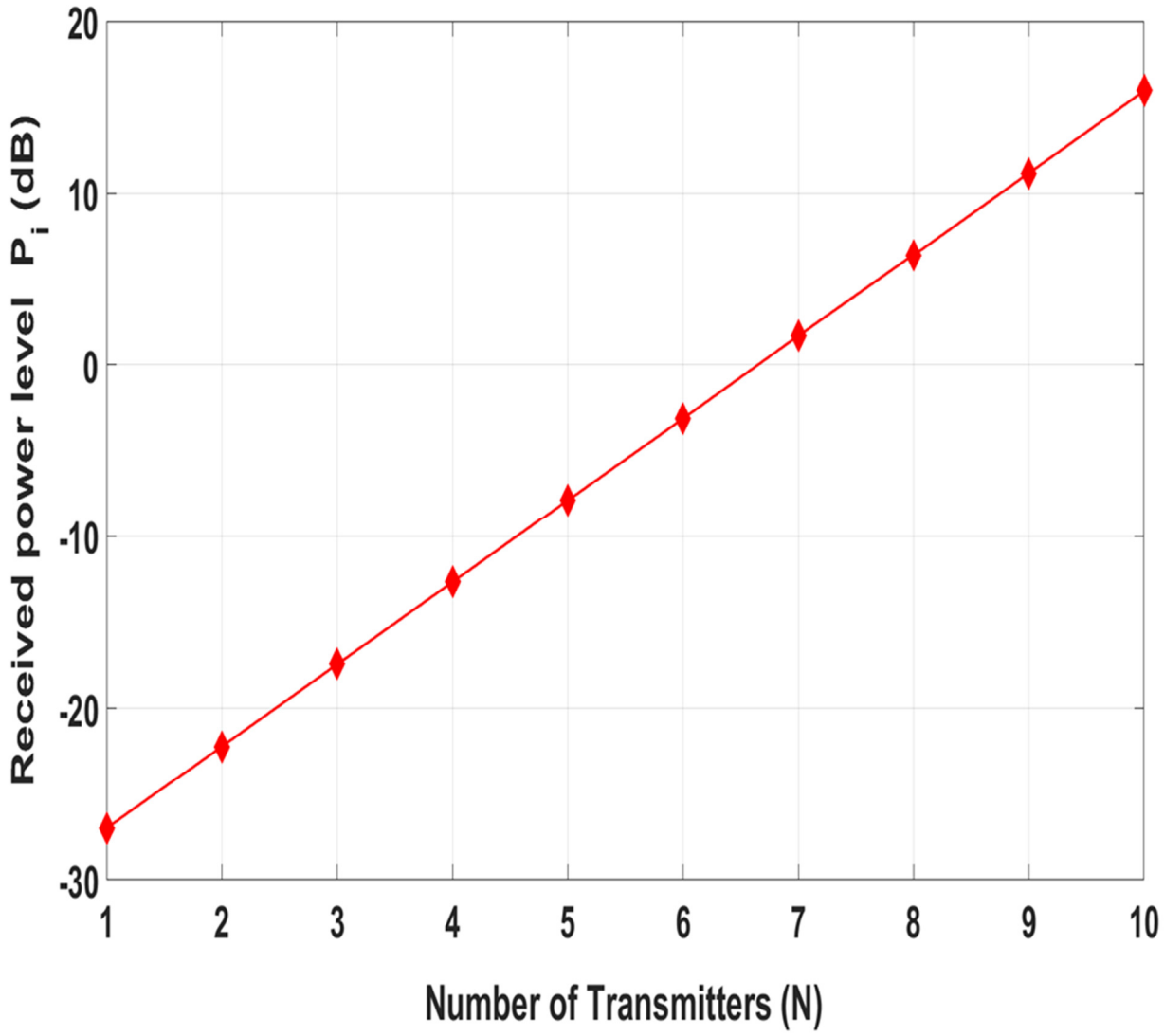

Figure 3.3 Received power levels for different number of transmitters *N* and SINR = 2 dB.

The optimal received power levels for several values of SINR are depicted in Figure 3.4.

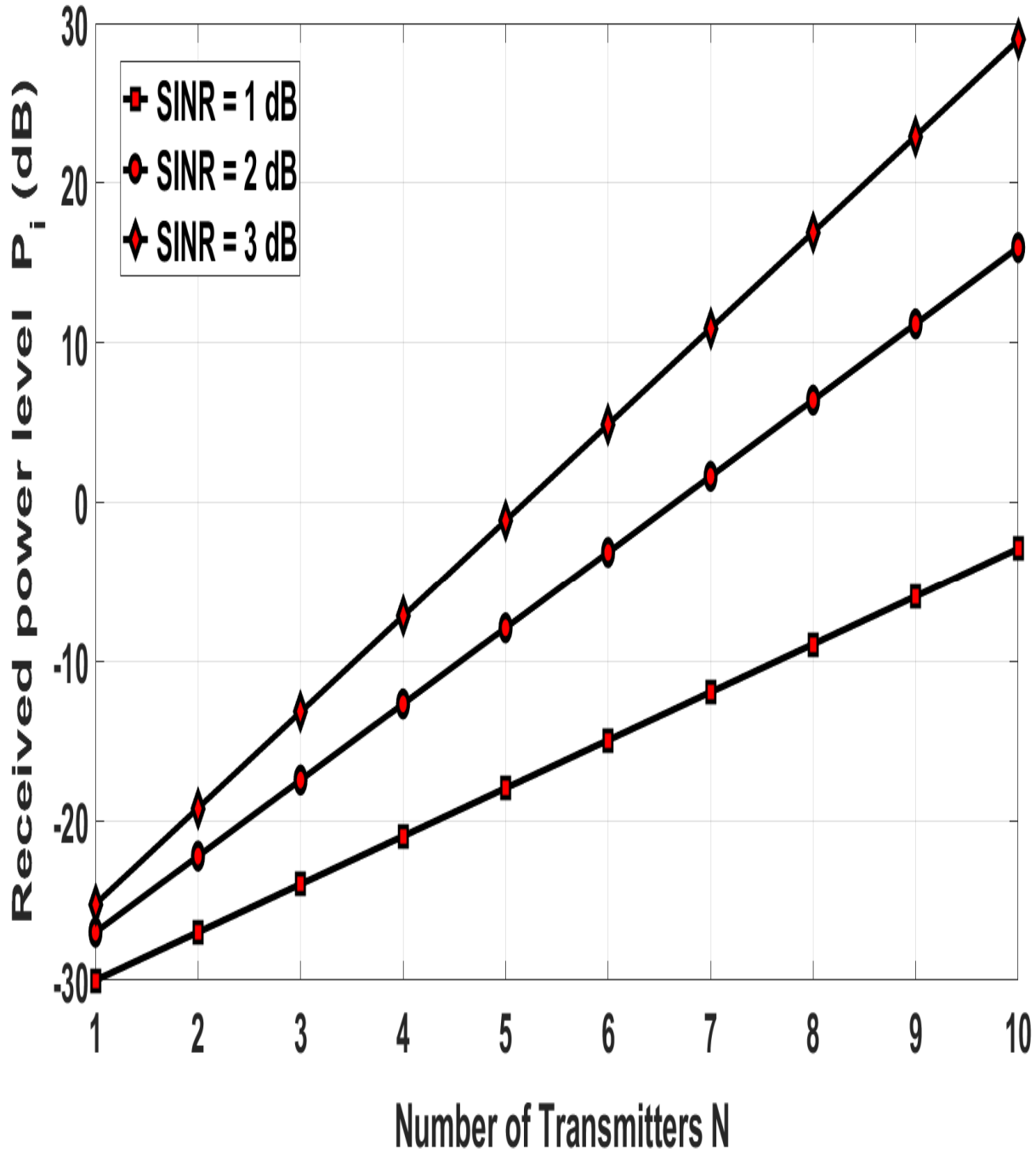

Figure 3.4 Received power levels for $N = 10$ and different SINR values.

As given in (3-7) and shown in Figure 3.3 and Figure 3.4, for an AWGN channel and constant SINR, the optimum received power level increases as the number of transmitters increases and the channel gain of one user does not affect the power level of another user (when it is perfectly canceled by the SIC receiver).

A comparison between the optimum power levels derived above and the μ-law compander power levels was investigated. The motivation being similar criteria (constant SINR for each signal) for the SIC receiver and constant Signal/(Quantizing Noise) for each PCM (μ-law compander sample level). The μ-law compander used in classic telephony PCM is given as [157]

$$F(x) = sgn(x)\ \frac{ln\ (1 +\ \mu\ |x|\ )}{ln\ (1 +\ \mu)}, \qquad (3-7)$$

where x is the signal input amplitude and the companding parameter μ is equal to 255 in the standard PCM system in North-America and Japan.

Assuming an AWGN channel, the optimum power levels are very similar to the μ-law encoding used in PCM speech companders, where the ratio of signal power to quantization noise is kept constant. As shown in Figure 3.5, a μ-law compander has a linearly increasing relation in the companded signal and is remarkably similar to the optimum received NOMA power levels shown in Figure 3.3 and Figure 3.4. As noted above, this similarity is because the design criteria for μ-law coding, keeping the ratio of the signal power to quantization noise constant for all signal levels, is very similar to the NOMA requirement of constant received SINR for each received signal.

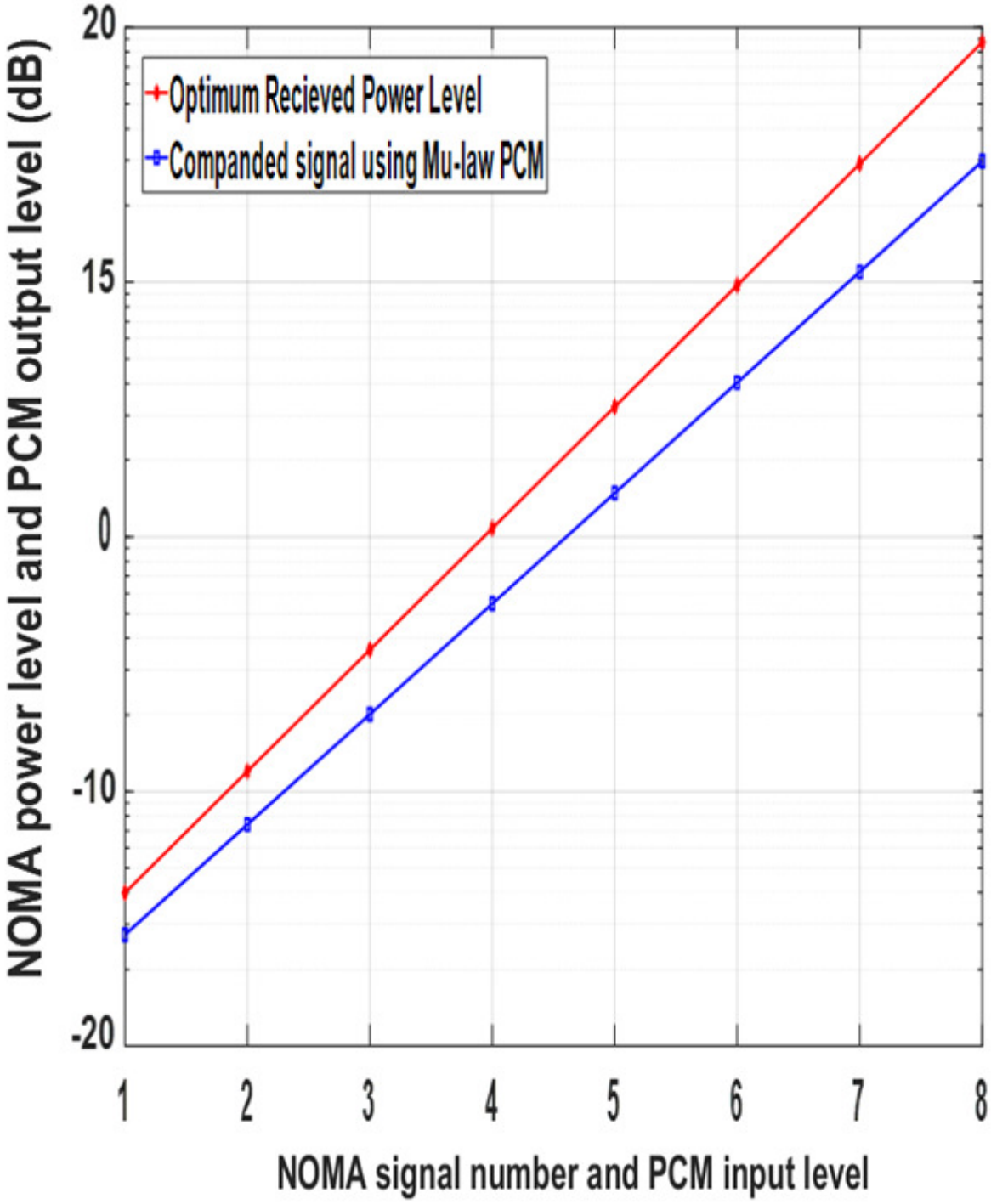

Figure 3.5 NOMA optimum power levels versus μ-law levels.

3.4 Concluding Remarks

In this chapter, a formula for the optimum received power levels for uplink power-domain NOMA with ideal SIC reception was derived. The derived results show that the optimum received power level increases linearly (in dB) as the number of transmitters N is increased and the maximum required received SINR increases exponentially (or equivalently, linearly in dB) with the number of users N. An interesting observation is that the optimum power levels are very similar to that of the μ-law encoding used in the PCM speech companders.

Chapter 4: ALOHA-NOMA Protocol for Massive Machine-to-Machine (M2M) of IoT Communication[3]

4.1 Introduction

The anticipated rapid growth of both the number of connected devices and the data volume that is expected to be associated with the IoT applications, has substantially increased the likelihood of massive M2M type communication within 5G wireless communication systems. M2M communication without human intervention, which is expected to constitute a significant portion of the IoT, leads to a rethinking of the medium access control (MAC) layer. In M2M, it is possible that tens of thousands of low complexity IoT devices will transmit to a gateway. Accordingly, a novel MAC protocol that is scalable, energy efficient and has high throughput is highly desirable. This MAC protocol must be compatible with the low complexity requirements of IoT devices, which have limited battery and memory, as well.

As discussed in Chapter 2, contention-free MAC protocols such as TDMA, FDMA or CDMA cannot provide high throughput to meet the demands of large number of IoT devices due to control overhead and unused empty slots, and furthermore they are not scalable. On the other hand, contention-based protocols such as CSMA/CA performs well only for small networks and they do not have sufficient throughput for large scale networks due to collisions. The same issues are valid for the familiar ALOHA and slotted ALOHA protocols. Moreover, CSMA/CA is energy

3 The content of this chapter has been published in [57], and it is included in this dissertation with a permission. Permission is included in Appendix A.

inefficient, since it requires continuous channel monitoring and there is a significant overhead due to control packets that are not compatible with the limited battery requirements of IoT devices.

The main aim of this research is to propose a scalable, energy efficient and high throughput MAC protocol for M2M communication. The simplicity of ALOHA and the superior throughput of non-orthogonal multiple access (NOMA) and its ability to resolve collisions via use of a SIC receiver, makes ALOHA-NOMA [64] an excellent candidate for a MAC protocol that can be utilized for low complexity IoT devices. It is worth noting that the main impediments of ALOHA, which are the low throughput and high collision rate, can be overcome with NOMA. The proposed ALOHA-NOMA protocol is a promising method that does not require any scheduling, where the IoT devices may transmit to the gateway at the same time on the same frequency band. The protocol is also energy efficient such that the devices are not obliged to listen to the channel, and has high throughput as will be demonstrated in this chapter.

There are many studies that address MAC layer issues in M2M communication, e.g., see [65] and references therein. Among those, the combination of slotted ALOHA with an interference cancellation (SIC) [47] receiver proposed in [158]-[160] are the closest protocols to the proposed ALOHA-NOMA in this paper. However, there are salient differences in the proposed ALOHA-NOMA protocol with the prior art. First, ALOHA-NOMA uses pure ALOHA instead of slotted ALOHA, because slotted ALOHA requires synchronization of hundreds or thousands of IoT devices in time domain conflicts with the simplicity requirement of IoT devices. Second, the power levels of IoT devices in ALOHA-NOMA are quite important to resolve the collisions in the gateway by the SIC receiver and they are adjusted by cooperating with the gateway.

The contributions of this research work are 3-fold. First, a novel scalable, energy efficient, high throughput MAC protocol is proposed to be utilized for IoT applications that have low

complexity devices. Following that, a dynamic frame structure that provides great flexibility to accommodate the changing number of IoT devices is defined and is compatible with the proposed protocol. Finally, the superiority of the proposed ALOHA-NOMA is demonstrated in terms of throughput.

This chapter is organized as follows. In the next section, Section 4.2, the proposed ALOHA-NOMA protocol is introduced, and then a frame structure for ALOHA-NOMA is presented in Section 4.3. After that, the superiority of the proposed method regarding throughput with respect to pure ALOHA is discussed in Section 4.4 with its numerical results are presented in Section 4.5. Finally, the chapter ends with the concluding remarks in Section 4.6.

4.2 ALOHA-NOMA Protocol for IoT Applications

There is a research challenge in meeting both the low complexity requirements of IoT devices with the high throughput needs of a large IoT network. The synergistic combination of the low complexity ALOHA protocol with the promising high throughput feature of NOMA can be an appealing MAC protocol for IoT applications, dubbed ALOHA-NOMA. Note that the requirement of increased throughput makes orthogonal multiple access (OMA) protocols insufficient in providing network throughput. NOMA has emerged as a promising solution in 5G networks.

The ALOHA protocol, which was proposed nearly 50 years ago, has appealing features for IoT applications owing to its simplicity in implementation and compatibility with distributed systems. The main bottleneck of ALOHA systems is the low throughput caused by the high number of collisions, which can be improved by using NOMA. Furthermore, one of the major impediments to M2M communication, signaling overhead, can be minimized by the combination of ALOHA and NOMA. Signaling overhead is reduced in the estimation phase of the proposed

protocol in which the number of active devices are estimated by the gateway, which is discussed in the next section, by the unique feature of ALOHA and NOMA where each user is able to transmits whenever it wants. Accordingly, the overhead to establish a connection between the IoT device and the gateway can be drastically reduced before communication begins. This issue is further explained in Section 4.3.

Many IoT devices that are transmitting simultaneously on the same frequency with different power levels to the IoT gateway can be separated via use of a SIC receiver employed at the IoT gateway. A sample illustration of this scenario is depicted in Figure 4.1.

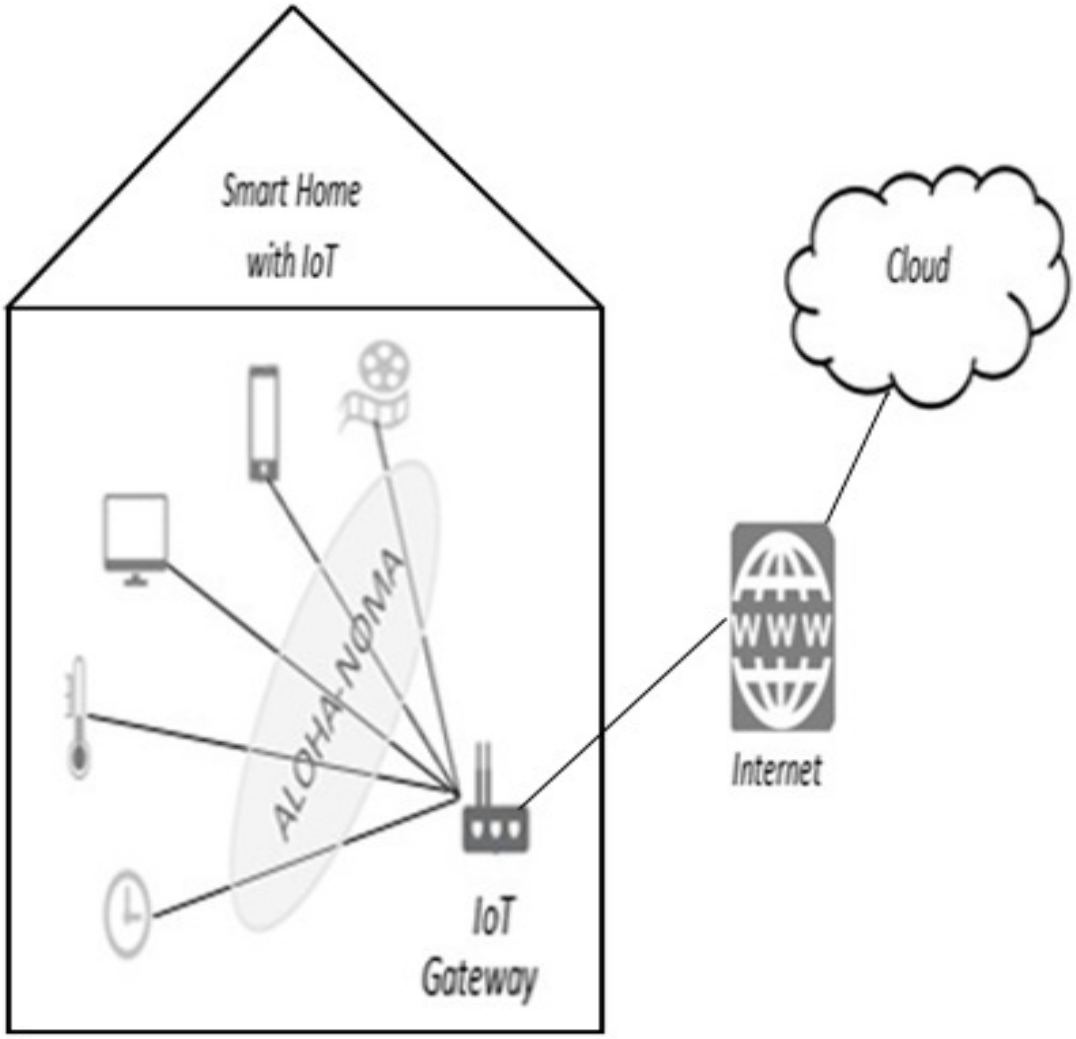

Figure 4.1 A use case for ALOHA-NOMA in the smart home with IoT.

In this model, IoT devices send their data to the IoT gateway on demand using the ALOHA-NOMA protocol and the IoT gateway distinguishes the signals using a SIC receiver. One of the biggest advantage of ALOHA-NOMA in this topology is that ability to support different heterogeneous devices that belong to different providers without the need for a specific network configuration.

The proposed ALOHA-NOMA protocol is scalable in terms of throughput versus the number of nodes. With this protocol, any node can transmit whenever it wants so that any number of nodes can join or leave the network without any network management involvement before communicating. It is an energy efficient protocol that resolves collisions, within limit on the number of simultaneous transmissions, and thus minimizes retransmission. As mentioned previously, ALOHA-NOMA increases the conventional ALOHA throughput significantly. That is, the normalized throughput increases more than linearly with the total number of users as discussed in Section 4.4. The main drawback of the proposed protocol is the increased computational complexity of SIC receiver due to the high number of nodes. However, this can be easily managed, because gateways are much more powerful devices than the low power IoT devices.

4.3 Dynamic Frame Structure for ALOHA-NOMA Protocol

One of the main practical challenges in the proposed ALOHA-NOMA protocol is the determination of the proper power levels of IoT devices; this is critical for the SIC receiver to be able to successfully distinguish the signals. Indeed, the adjustments of power levels is the only control that must be done for IoT applications before ALOHA-NOMA-based information transfer begins. To address this challenge, a dynamic frame structure with great flexibility in accommodating the changing number of devices is designed, i.e., when a group of IoT devices

joins or leaves the network the same frame structure is employed. Such a scheme provides great flexibility in adapting to changing network environments. This structure is fundamentally different than that of a OMA system, where a new user arrival can completely change the overall frame structure such that the additional user must be assigned at a resource (e.g., time slot, frequency, or code) within the frame.

The proposed frame structure is periodic and basically composed of five phases. An illustration of the proposed periodic frame structure is given in Figure 4.2.

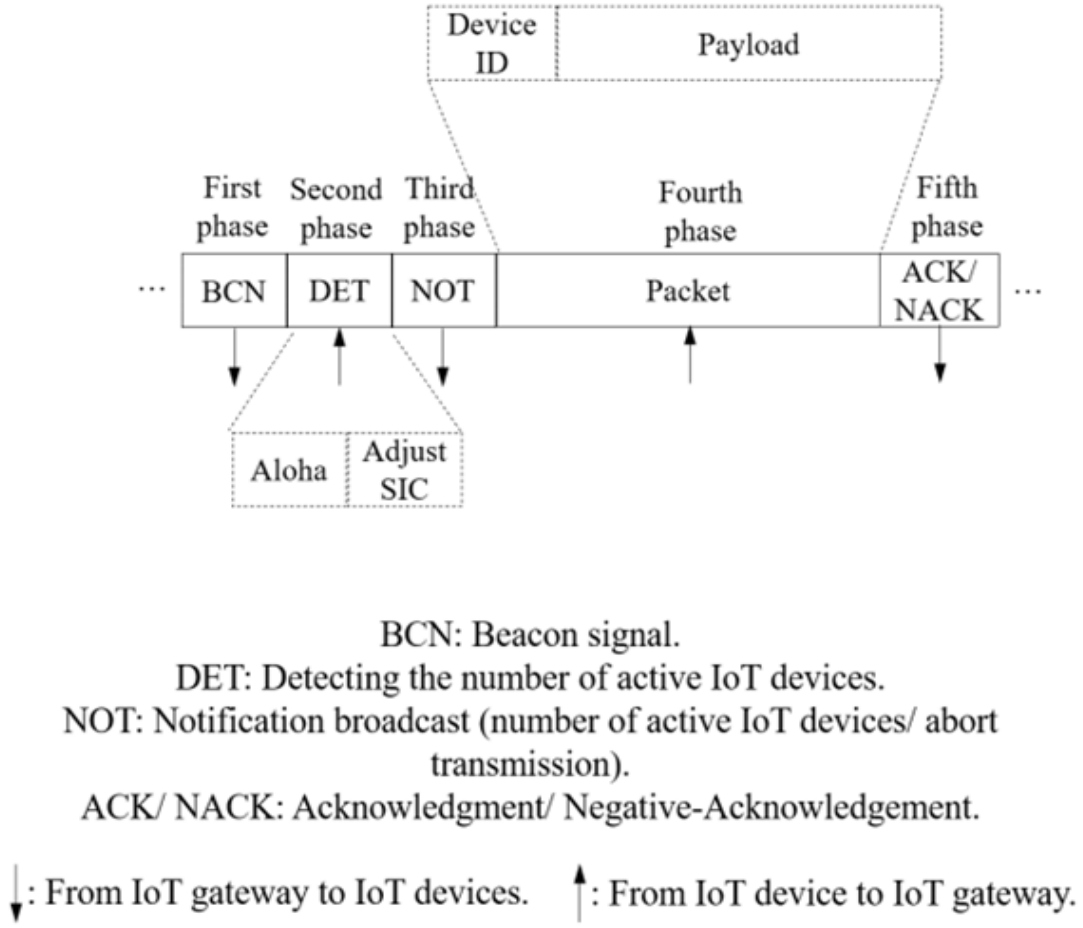

Figure 4.2 The proposed frame structure.

Accordingly, the gateway first transmits a beacon signal. Next, the IoT devices with packets to transmit send "dummy" (without data content) packets to help the gateway estimate the total number of active devices in the medium. The number of IoT devices are estimated at each period via multi-hypothesis testing [161], and the SIC receiver is implemented to decode a fixed number of different packets. A SIC receiver that can process m signals is denoted as SIC(m) and m is referred as the SIC degree. Detecting the number of signals using multiple hypothesis testing was previously addressed in [162]. If the total number of devices detected is less than or equal to m, the number of signals is broadcast to the transmitters. If the total number of devices that are detected exceeds m, a back-off command is issued. Each device randomly picks a number/identity that maps to the appropriate power level and all the devices transmit their packets to the gateway, and provided that each of the devices has (randomly) picked a different identity (i.e., power level) the messages are detected and acknowledged. The fifth phase, an acknowledged (ACK) packet, can contain the unique IoT device numbers corresponding to successfully decoded packets so that each device can understand whether its packet is successfully received. Note that this frame structure is preserved when the number of IoT devices changes, which provides great flexibility, because the length of first three phases is fixed independently of the number of IoT devices. Although one can consider that the first three phases and the ACK phase decrease throughput efficiency, they are considerably shorter than the fourth phase or payload.

To give more detail on the protocol, the gateway initially transmits a beacon signal and in the second phase, all IoT devices that send packets in this frame transmit simultaneously on the same frequency to the IoT gateway using an ALOHA protocol. Then, the IoT gateway estimates the number of IoT devices by multi-hypothesis testing and the SIC receiver is set to decode this number of IoT devices using NOMA. Notice that it would lead to easier implementation if all IoT

devices are registered to the gateway instead of multi-hypothesis testing, however, this may significantly increase the length of control phase and thus decrease the payload or throughput considering the large number of IoT devices. A popular method in multi-hypothesis testing that can be used to find the number of IoT devices at the gateway is based on the Bonferroni Inequality [161] which states that, given any set of events, the probability of their union is smaller than or equal to the sum of their probabilities.

More precisely, *M* independent null hypotheses are tested such as H_1, H_2, …, H_M where H_i is the event that i^{th} user exists (i.e., transmits). Each of the hypothesis has corresponding p-values, p_1, p_2, …, p_M, respectively. The number *N* is the total number of the true null hypothesis or the total number of IoT devices in the medium such that $N \leq M$. The value of *N* is unknown at the gateway and estimated probabilistically. Accordingly, the probability of having *N* active IoT devices can be specified as

$$P\,(\,N\ number\ of\ IoT\ devices\,) = (\,1-\alpha\,)^N\,\alpha^{M-N}, \qquad (4-1)$$

where α is determined using the Bonferroni Inequality given by

$$P\left(\bigcup_{n=1}^{M}\left(P_i \leq \frac{\alpha}{M}\right)\right) \leq \alpha. \qquad (4-2)$$

Once the total number of IoT devices, *N*, is estimated, the SIC receiver at the gateway decodes the *N* strongest signals. Assuming IoT devices send their address/ID in the "dummy" packet, the gateway decodes these packets and broadcasts the number of devices with these addresses/IDs in the third phase. The devices who don't get detect their address/ID, do not transmit a payload. Those devices that detect their address/ID from the gateway message change their power according to the power back-off scheme as proposed in [162]. In particular, each device randomly selects their power levels among the set of optimal values introduced in Chapter 3. For the receiver to work

properly, the transmitters must have chosen different power levels. The active IoT devices that do not detect their address/ID from the gateway may increase their transmit powers slightly in the next round. This will affect the outcome of the multi-hypothesis testing as well. In the fourth phase, the payload information is sent to the gateway by all the IoT devices that detected their address/ID from the gateway. The fourth phase of the proposed frame structure can be considered as pure NOMA. The successfully detected packets are acknowledged in the last phase. This procedure repeats periodically.

4.4 Throughput of ALOHA-NOMA

One of the most critical parts of the proposed frame structure depends on the determination of the number of IoT devices in the second-phase. If only pure ALOHA was used in the second phase, the performance would be unsatisfactory since only 18% of the IoT devices can be detected at a time on average. To address this problem, the ALOHA protocol is replaced with ALOHA-NOMA in the second phase of the proposed frame structure. Accordingly, the number of devices are first estimated according to the superposed signal strength based on multi-hypothesis testing as was done in [162]. Note that in this phase the aim is not to detect the packets, but only to estimate the number of active devices. Once the number of active devices is estimated, the SIC receiver is set to decode this number of signals and the packets are detected. It is worth emphasizing that at each round the power level of each device randomly and independently changes, and thus SIC receiver can successfully recover the signals if the devices selected distinct power levels. These two consecutive parts inside the second phase are denoted as ALOHA and NOMA, respectively, which explains the reason of referring to this protocol as ALOHA-NOMA.

The main aim of this section is to specify the throughput increase of ALOHA-NOMA with respect to pure ALOHA. The ALOHA throughput can be considerably increased by working in

conjunction with NOMA, which will allow simultaneous users to successfully communicate with the gateway during the vulnerable period which is, in ALOHA, represents the total period of time when collision may occur for a packet.

A SIC receiver that can successfully detect *m* transmissions, where SIC(*m*) means that the receiver can detect, at most, *m* signal, so successful reception will occur when there are *m* or fewer arrivals (transmissions) which occurs with probability

$$P\ (successful\ transmission) = \ P\ (m\ or\ less\ arrivals). \qquad (4-3)$$

Assuming a large number of IoT devices, the Poisson distribution is a reasonable model for the probability of i transmissions during the vulnerable time period and is given by

$$P(i\ successful\ transmissions) = \frac{(2gT)^i\ e^{-2gT}}{i!}, \qquad (4-4)$$

where the parameter g represents the arrival rate (packets/ second), the *T* is the packet length period, and $i = 0,1,2,\dots,m$.

Since the probability of "success" is the probability of *m* or fewer arrivals (with different power levels), the throughput, which can be defined as the time fraction during which the useful information can be carried on the channel, is given as

$$S_{th} = \sum_{i=1}^{m} \frac{(2G)^i\ e^{-2G}}{2\ (i-1)!} = \frac{e^{-2G}}{2} \sum_{i=1}^{m} \frac{2^i\ G^i}{(i-1)!}, \qquad (4-5)$$

where $G = gT$ is the normalized offer load.

In order to find the relation between the maximum throughput of ALOHA-NOMA for different values of *m*, (4-5) is used to compute the maximum throughput for each value of *m*. For *m* =1, the maximum throughput is defined by differentiating (4-5) with respect to *G* and equating to zero as

$$\frac{dS_{th}}{dG} = \frac{(-2 * e^{-2G} * 2G) + (2 * e^{-2G})}{2 * 0!} = 0. \quad (4-6)$$

Solving for G in (4-6) gives the familiar result of G = 1/2. Substituting G=1/2 in (4-5) for m = 1, gives the familiar result of ALOHA throughput of 18%. The same process may be applied with m = 2. The throughput, using (4-5) with m = 2, is

$$S_{th\ at\ m=2} = \sum_{i=1}^{2} \frac{(2G)^i\, e^{-2G}}{2(i-1)!} = \frac{(2G)^1\, e^{-2G}}{2 * 0!} + \frac{(2G)^2 e^{-2G}}{2 * 1!}. \quad (4-7)$$

The maximum throughput is obtained by differentiating (4-7) with respect to G and equating the result to zero as

$$\frac{dS_{th}}{dG} = \frac{e^{-2G}}{2}\,[2 + 4G - 8G^2] = 0. \quad (4-8)$$

Solving (4-8), the roots of G are 0.809 and -0.309. Therefore, to find the maximum throughput of ALOHA using NOMA with m =2, G = 0.8090 is substituted in (4-5) and the result is given as

$$S_{th\ max\ at\ G=0.8090\ and\ m=2} = 0.42. \quad (4-9)$$

As shown in (4-9), for m =2, the maximum throughput of ALOHA-NOMA is increased from 18% to 42%. For m = 3, the maximum throughput is

$$S_{th\ max\ at\ G=\ 1.1348\ and\ m=3} = 0.686. \quad (4-10)$$

These procedures can be applied for any number of m to determine the maximum throughput for the ALOHA-NOMA system [again assuming distinct power levels so that the SIC detector can properly operate].

4.5 Numerical Results

The throughput of ALOHA-NOMA is numerically evaluated for different values of m. The performance measure is the maximum throughput, as specified in the previous section. As shown

in Figure 4.3, the maximum throughput of ALOHA-NOMA increases with a slope that is (slightly) greater than linear with m ranging from 1 to 5. Notice that the familiar result of ALOHA throughput, which is 0.18, is observed at $m = 1$ in Figure 4.3 for the ALOHA-NOMA system.

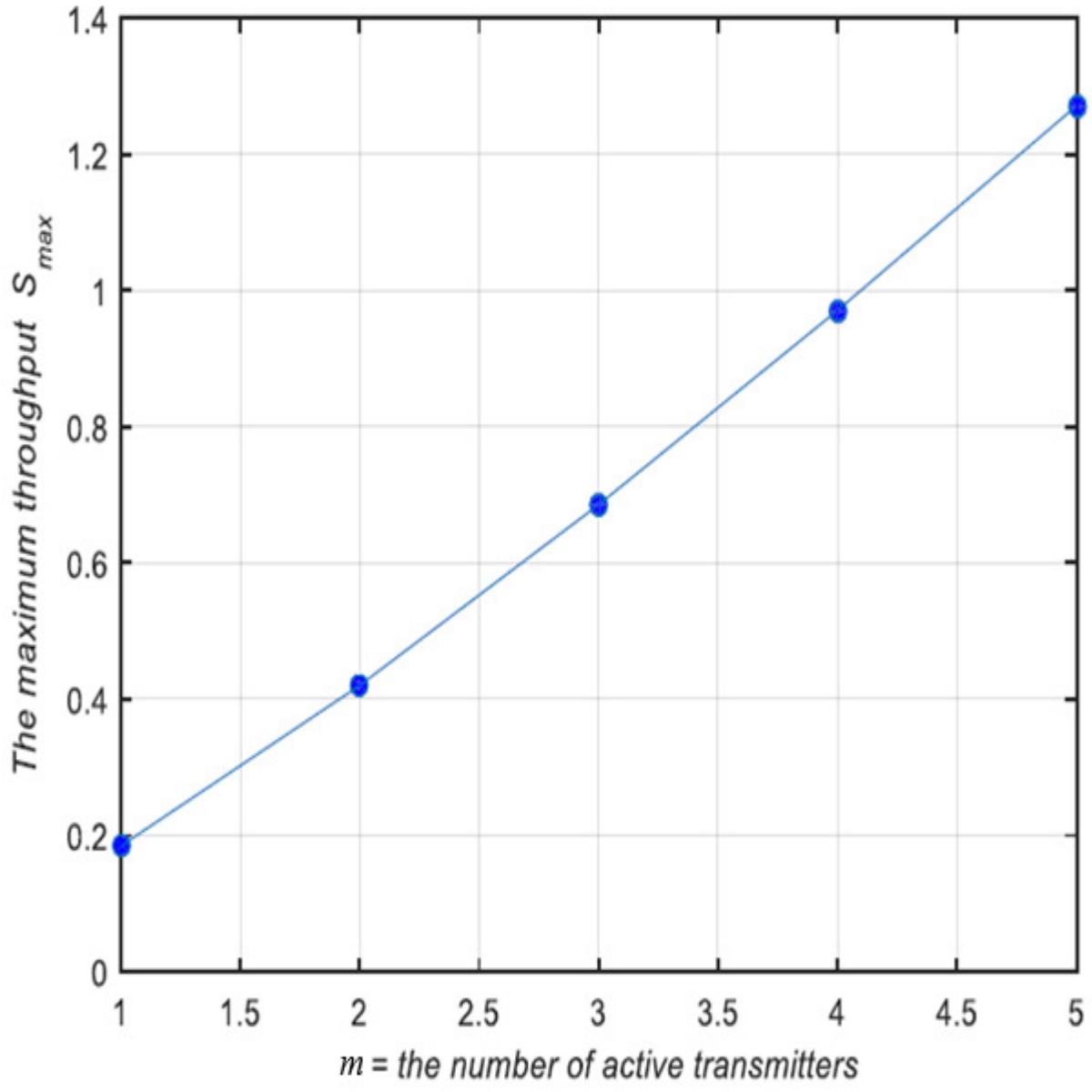

Figure 4.3 ALOHA-NOMA maximum throughput as a function of $m \leq 5$.

The maximum throughput with m is plotted for a large number of active transmitters, for $m = 20$ and $m = 100$ in Figure 4.4 and Figure 4.5, respectively. These results depict that the

maximum throughput increases with a greater than linear slope as the number of active IoT users, m, increases.

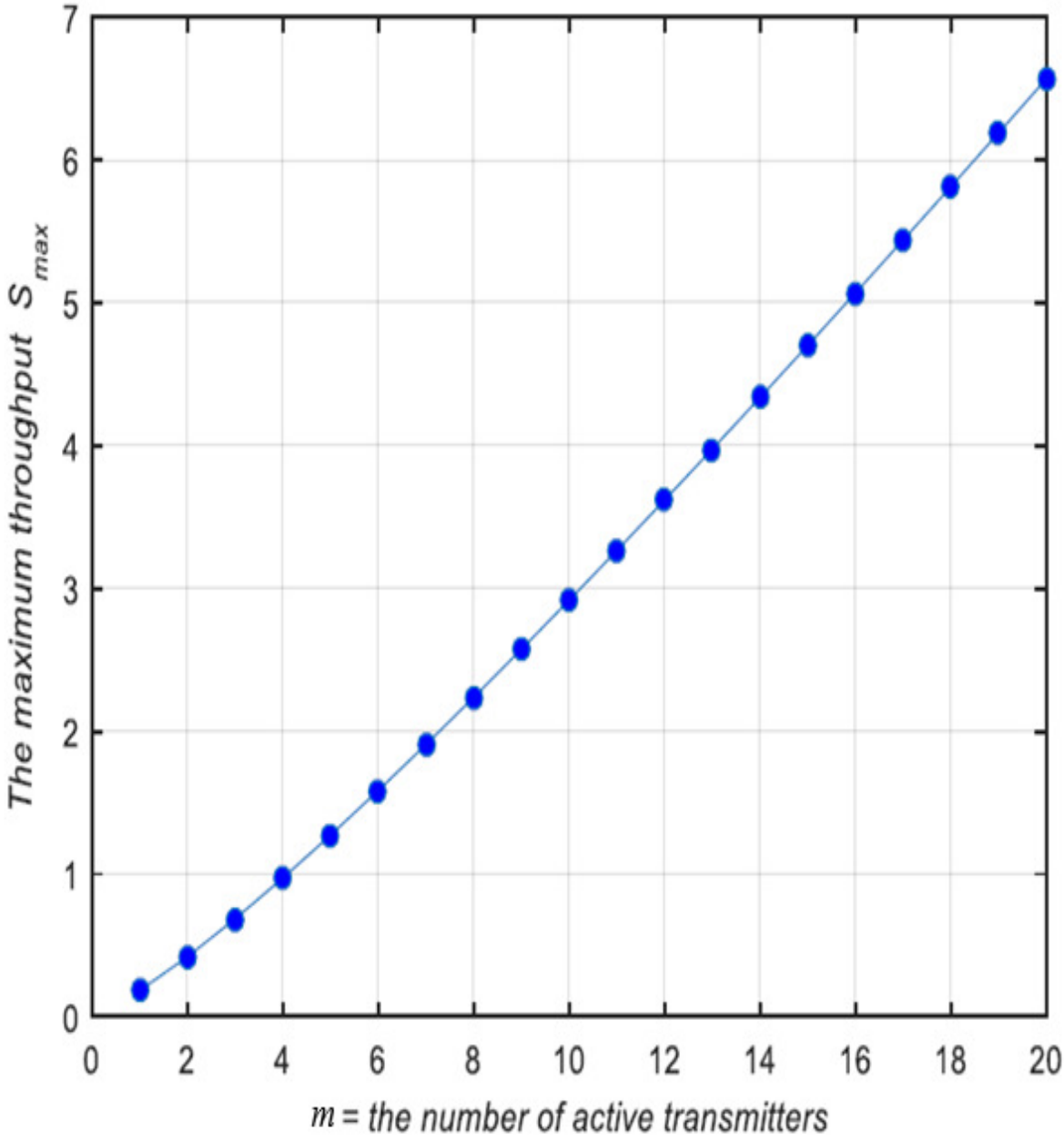

Figure 4.4 ALOHA-NOMA maximum throughput as a function of $m \leq 20$.

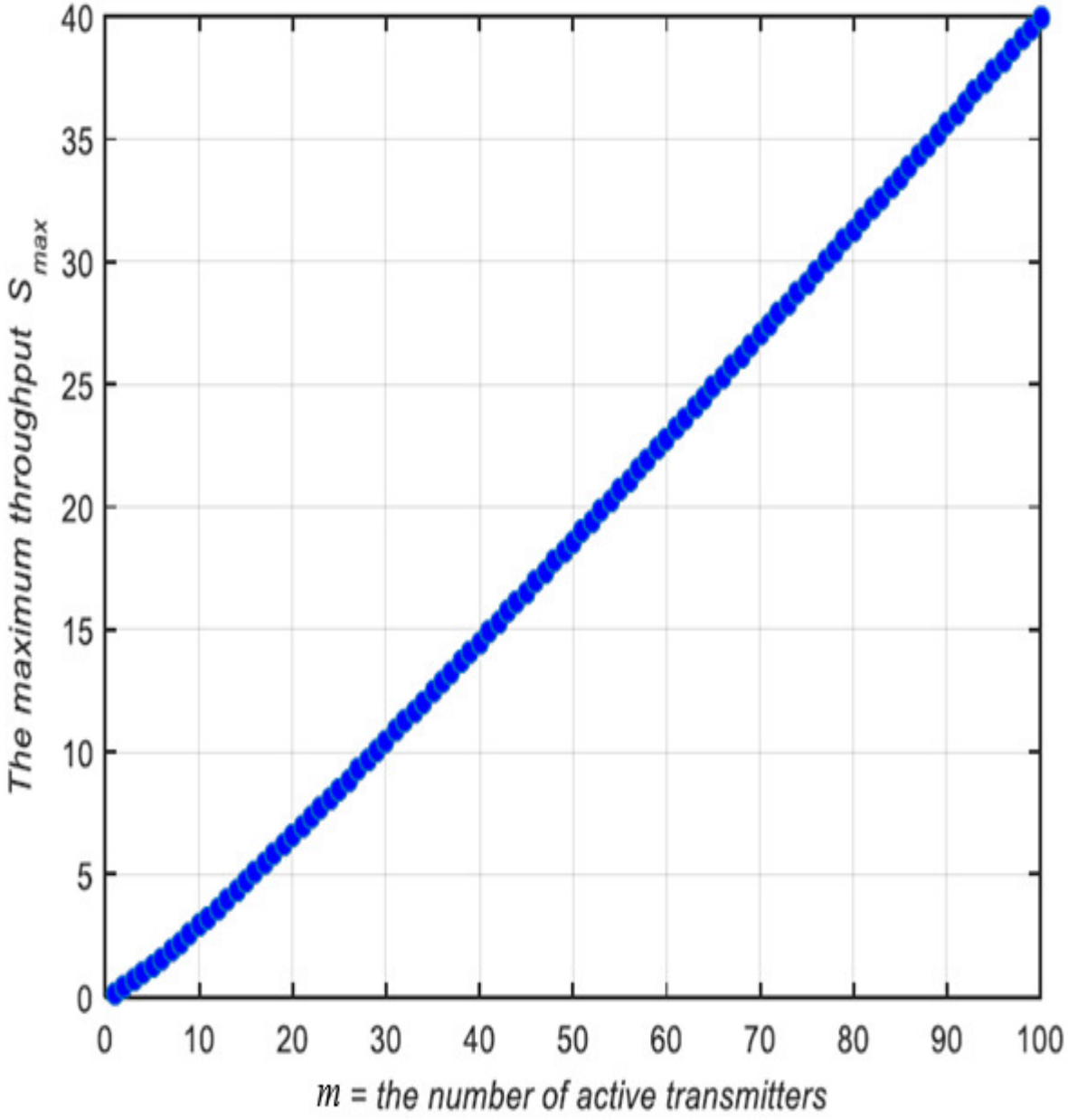

Figure 4.5 ALOHA-NOMA maximum throughput as a function of $m \leq 100$.

4.6 Concluding Remarks

This chapter presented a novel MAC layer protocol for IoT applications incorporating pure ALOHA with power domain NOMA, which is called the ALOHA-NOMA protocol. ALOHA-NOMA, a simple, easy to implement, distributed, and is a scalable protocol in terms of throughput

vs the number of IoT nodes. In addition, it is compatible with the low complexity requirements of IoT devices. The ALOHA-NOMA is energy efficient, since the SIC receiver at the gateway will minimize the retransmissions of IoT devices and does not need to listen the channel continuously. A dynamic frame structure was introduced that is robust to the changing number of devices, so that estimation of the number of active IoT devices transmitted in ALOHA is accomplished using multi-hypothesis testing that detects the packets of IoT devices using a NOMA SIC-based receiver. The ALOHA-NOMA protocol significantly improves the throughput performance with respect to pure ALOHA, e.g., a SIC receiver that separates 5 signals can boost the throughput of classical ALOHA from 0.18 to 1.27 and with 100 active IoT devices the throughput is increased (at a greater than linear rate) to 40.

Chapter 5: Performance of Uplink Non-Orthogonal Multiple Access (NOMA) in the Presence of Channel Estimation Errors[4]

5.1 Introduction

In this chapter, the BER performance of a system with power-domain NOMA and SIC [47] reception using BPSK, QPSK, and 16-QAM modulations schemes in the presence of channel estimation errors is investigated. The analysis considers two scenarios for each modulation level: perfect (ideal) channel estimation and a channel with estimation errors. The simulations results are introduced and compared for each modulation scheme/level. The ideal case investigates the effect of SNR variation on the SIC detector error rate with perfect channel estimation. In addition, a simulation study of the SIC receiver degradation of uplink NOMA due to channel estimation errors is presented for BPSK, QPSK, and 16-QAM modulation, where the degradation performance is analyzed for different channel estimation error values. Similarly, the simulation results are analyzed and compared for each modulation scheme.

This chapter is organized as follows. In Section 5.2, the system model of a two-user uplink NOMA system with SIC reception is presented. Then, the simulation results of the BER performance for different modulation schemes with and without channel estimation errors is introduced in Section 5.3. In Section 5.4, the simulation study of the SIC receiver degradation of uplink NOMA due to channel estimation errors is investigated. Finally, the chapter ends with the concluding remarks in Section 5.5.

4 The content of this chapter has been published in [67] and [68], and it is included in this dissertation with a permission. Permission is included in Appendix A.

5.2 System Model

As in the model that was presented in Chapter 3, the corresponding diagram of an uplink NOMA system, which consists of two users and a BS receiver, is illustrated in Figure 5.1.

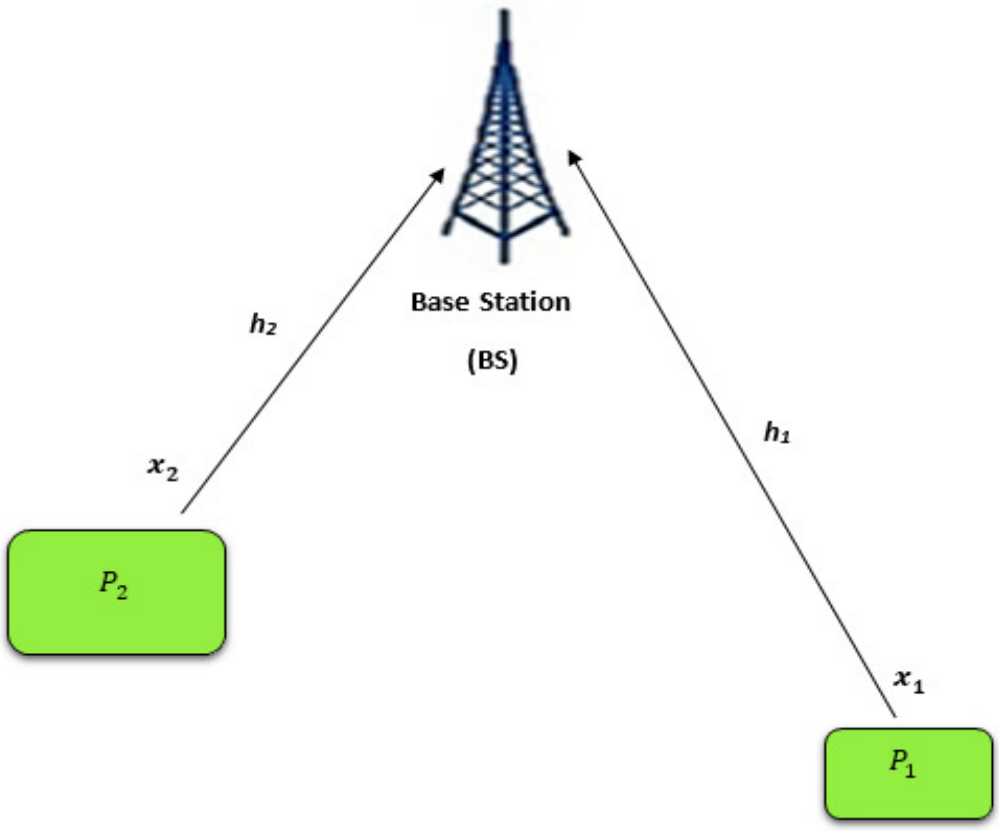

Figure 5.1 A system model for a two user uplink NOMA.

As discussed in Chapter 3 and shown in this figure, the two users transmit their signal at the same time and frequency, are synchronized with each other, the first user transmits its signal, x_1 scaled by a power coefficients P_1, to the BS over a channel with (scalar) coefficient h_1. The second user sends its signal, x_2 with its power coefficients P_2, to the BS with channel coefficient h_2. The superimposed signal of the two users, y, is received by the BS and it is represented as

$$y = h_1 x_1 + h_2 x_2 + n, \qquad (5-1)$$

where n is the additive white Gaussian noise (AWGN) with zero mean and variance σ^2.

Using the same assumptions as in Chapter 2 where the second user signal is considered as the strongest signal, then the SIC receiver is used at the BS to decode the two received signals in two stages. First, the SIC receiver detects the strongest signal of user 2 from the superimposed signal and noise that are given in (5-1), and the other signal is considered as noise. Then, the decoded signal of user 2 is subtracted from the combined received signal and the signal of the first user is decoded only in the presence of AWGN. The concept and operation of a SIC detector is explained in Chapter 2 and Chapter 3.

In Chapter 3, the optimum received uplink power levels using a SIC detector for any number of transmitters were determined. The analysis in this chapter assumed that there is a constant and known channel during the estimation and communication process. In addition, a constant channel estimation error, e, is assumed. Furthermore, the received power levels are set to the optimum levels as determined in Chapter 3.

This research focuses on studying the BER performance of a two-user uplink NOMA using a SIC detector for different modulation schemes. First, the BER performance, with various modulations schemes, is studied assuming no channel estimation error (perfect channel estimation). Second, the effect of a channel estimation error on each modulation scheme is investigated.

For the ideal scenario, the methodology assumes that the two users signals create the BPSK, PSK and 16-QAM signals. In addition, AWGN noise has been generated and then it is added to the two transmitted signals at the receiver side as shown in (5-1). Taking into account the channel attenuation, the power coefficients P_1 and P_2 have been selected so that the received signals are the optimum values as introduced in Chapter 3 and are communicated using the Slotted

Aloha-NOMA (SAN) protocol as introduced in [64] and [164]. In the present analysis, user 2 is assumed to be detected first by the SIC detector.

Similarly, for the case with channel estimation errors, the BER performance is investigated for the different modulation schemes. In addition to the same assumptions in the perfect estimation case, there are some additional assumptions. With channel estimation errors, the received signal powers are selected to be the values that would be optimal when there are no channel estimation errors. The estimation error, e, is defined as the absolute value of the difference between the channel coefficient and its estimated value normalized to the magnitude of the channel coefficient. So that, the error value is considered as a percentage value (normalized to the channel coefficient). The results have been simulated for different values of channel estimation error. For simplicity, we show the results for 0.15 and 0.25 estimation errors.

5.3 Simulation Results and Analysis

Based on the assumptions in Section 5.2, the two scenarios are simulated for the three modulation schemes and the results are analyzed. The simulation results for perfect channel estimation of BPSK uplink NOMA system with two users is shown in Figure 5.2. As expected, the figure shows that user 2 has better BER performance than user 1. In this case, the parameter that affects the performance of SIC detection is the ratio of user 2's power to the combination of user one's power plus the noise power.

As assumed, the SIC detector will detect user 2's signal first from the superimposed received signal plus noise. The noise power will have a significant effect on the detection of user 1 since the receiver first performs subtraction of the detected user 2's signal in addition to processing the noise. After detecting user 2's signal with the SIC receiver, the remaining signal, assuming correct detection of user 2, is user 1's signal in the presence of noise. So the lower power

level of user 1's signal makes detection more vulnerable to noise than user 2 and this leads to a larger BER for this user as compared to user 2.

As shown in Figure 5.2, the BER for user 2 at SNR = 0 dB is equal to 0.01 compared to 0.15 for user 1 at the same SNR of 0 dB. Furthermore, for SNR = 5 dB, user 2 has a BER of 0.001 and user 1 has a BER of 0.10. Note that decreasing the SNR makes the SIC detector experience an increased error rate, especially for user one which has a lower power level.

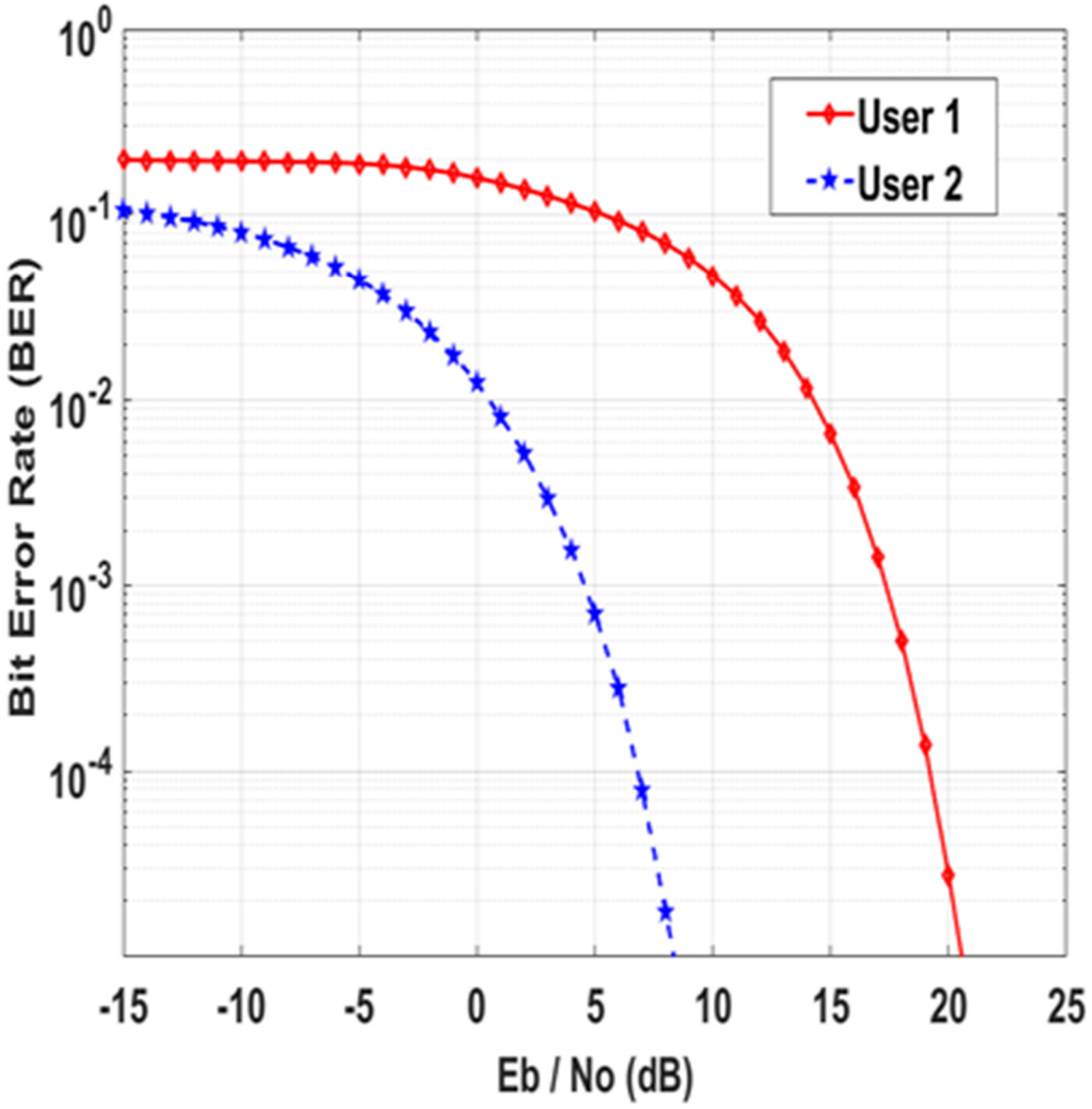

Figure 5.2 BER vs. SNR for two BPSK uplink NOMA users with perfect channel estimation.

The simulation results for BPSK modulation, but with channel estimation errors is shown in Figure 5.3. In this figure, two channel estimation errors, 0.15 and 0.25, are evaluated.

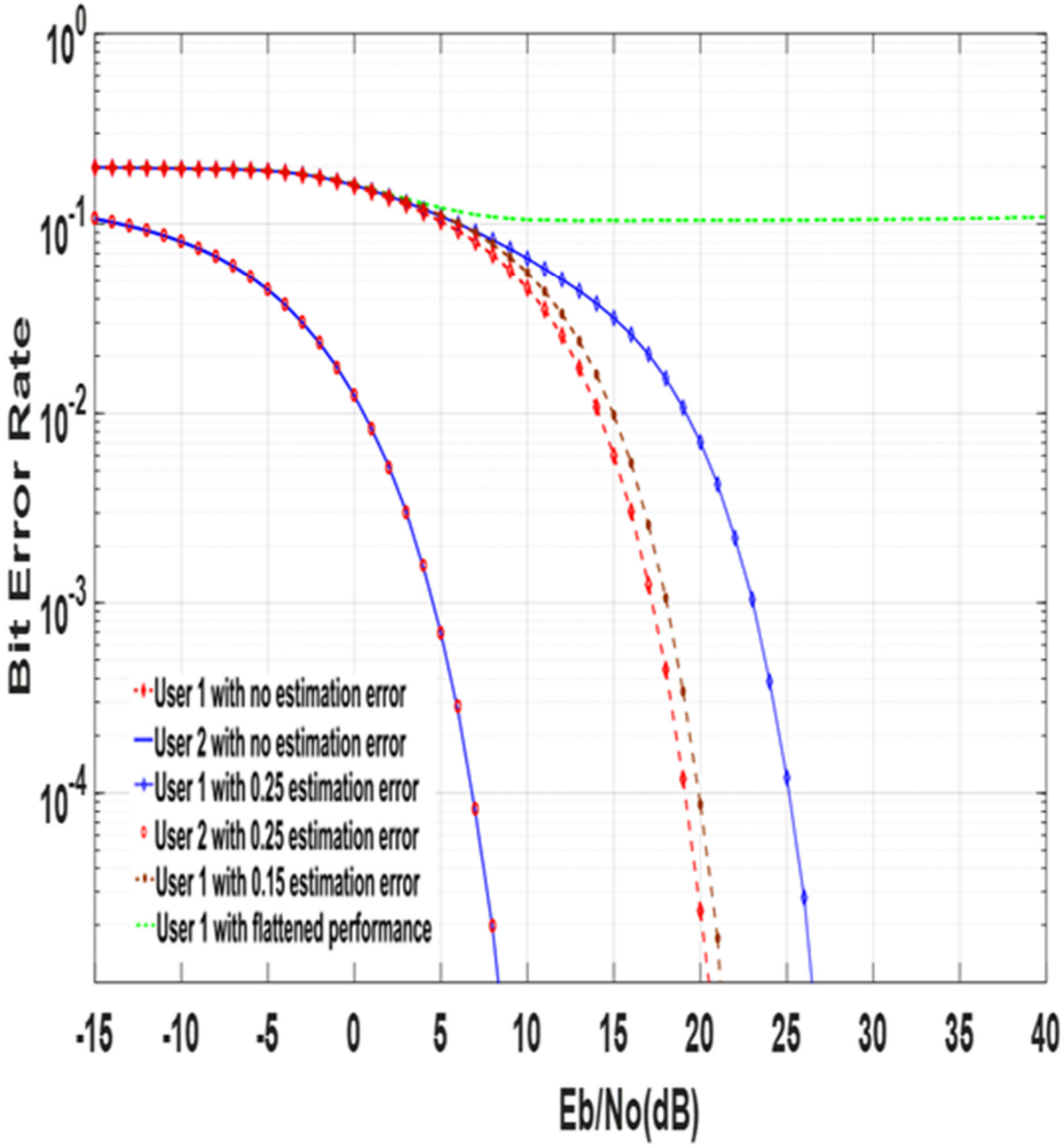

Figure 5.3 BER vs. SNR for two BPSK uplink NOMA users with different channel estimation errors.

In addition to the affecting parameters of the perfect case, adding an estimation error degrades the SIC detection process and the BER performance. Assuming detection of user 2's

signal first by the SIC detector, the remaining signal after detection user 2's signal is user 1's signal with an added estimation error in addition to the noise. This degrades signal reception and leads to a degraded BER compared to the perfect case. As expected, increasing of the estimation error, increases the BER. For example, at SNR = 15 dB, the BER for user 1 is equal to 0.01 for 0.15 channel estimation error compared to a BER of 0.007 for perfect estimation at the same SNR value. At SNR = 15 dB, the BER for user 1 is equal to 0.32 for 0.25 channel estimation error which is higher than the BER of 0.007 for perfect estimation and 0.01 for 0.15 channel estimation error at the same SNR value. As a result of the degradation in the SIC receiver, at higher estimation error values, the BPSK and the higher modulation schemes show a very high BER and a flattened performance (i.e., an error floor) in comparison to the perfect estimation and the given channel estimation errors results. The flattened performance and the SIC degradation are explained in the next section discussing SIC degradation.

The same analysis can be followed for higher modulation schemes, QPSK and 16-QAM, as shown in Figure 5.4 and Figure 5.5, respectively. In these figures, the results for various channel estimation errors are demonstrated. For the perfect channel estimation, at SNR = 5 dB, the BER of user 2 for QPSK modulation is equal to 0.005 compared to 0.14 for user 1 at the same SNR. On the other hand, for 16-QAM, the BER for user 2 at SNR = 5 dB is equal to 0.04 compared to 0.20 for user 1 at the same SNR. As a result, the BER performance of user 1 becomes worse for the same reason discussed in the perfect estimation of BPSK and at the same time increasing the modulation level increases the degradation of the BER.

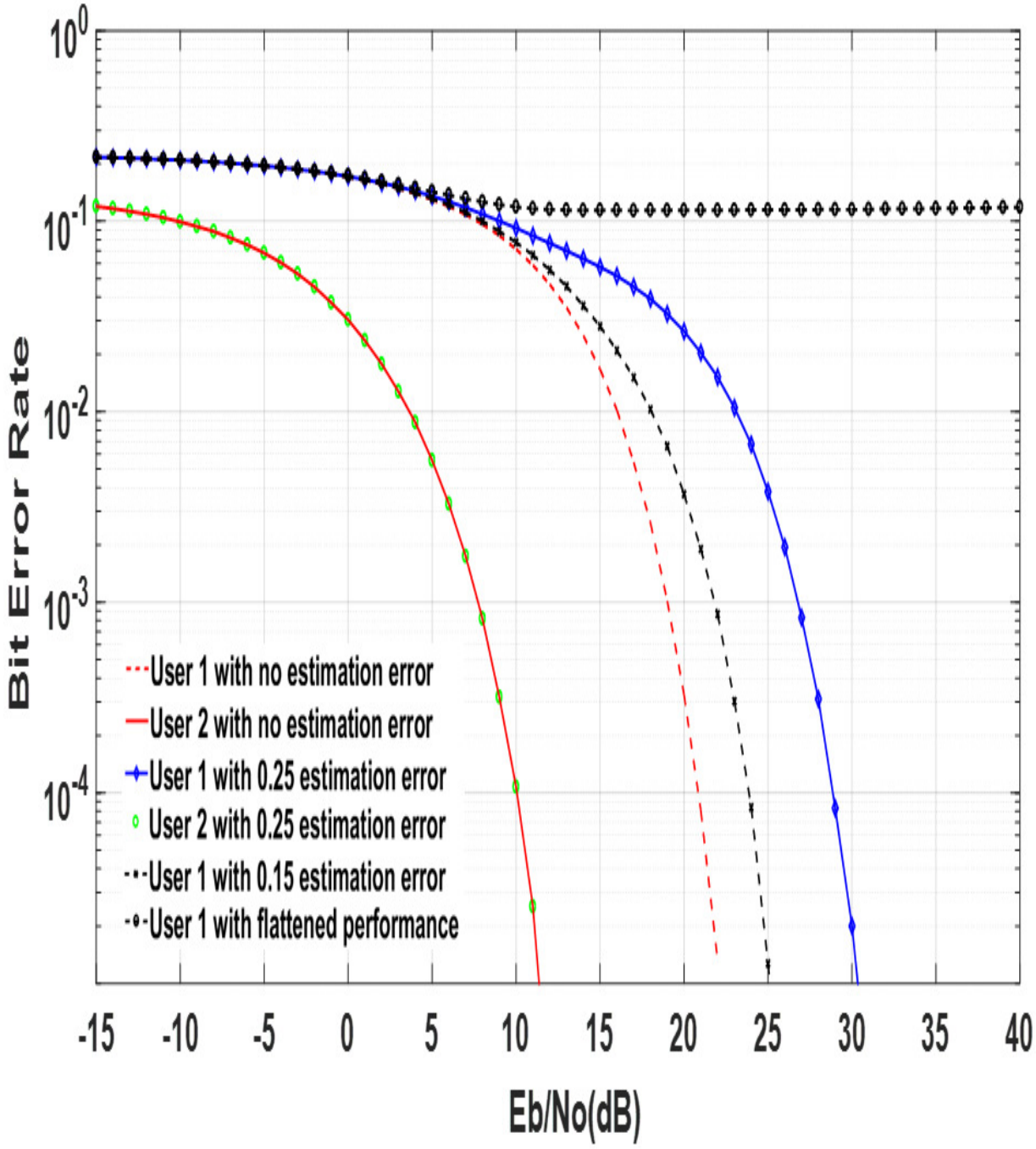

Figure 5.4 BER vs. SNR for two QPSK uplink NOMA users with different channel estimation errors.

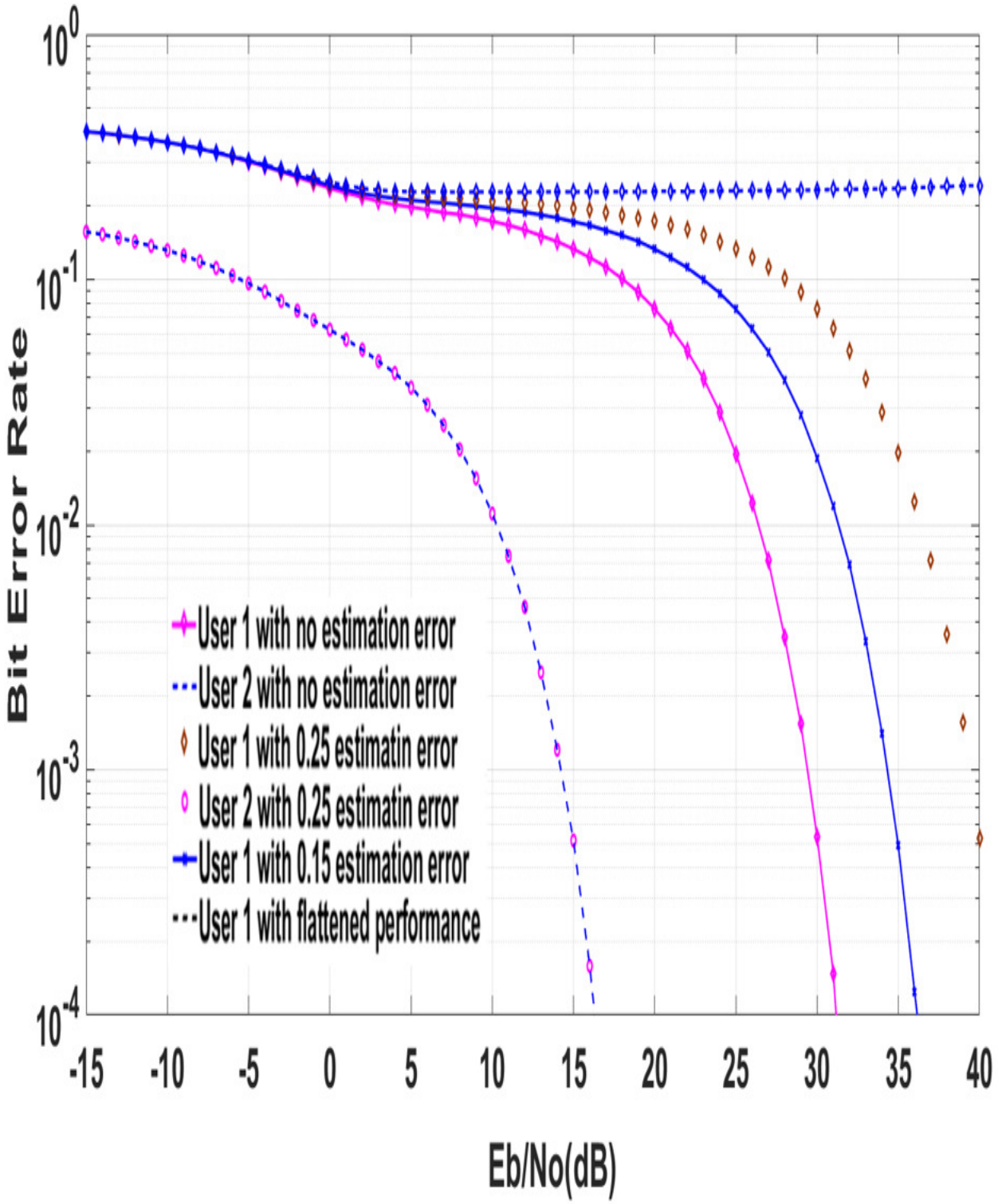

Figure 5.5 BER vs. SNR for two 16-QAM uplink NOMA users with different channel estimation errors.

For the channel estimation error scenario, 16-QAM has a higher BER than QPSK BER. For example, with a channel estimation error of 0.15, at SNR = 15 dB, the QPSK BER of user 1 is equal to 0.03 compared to 0.017 for the perfect estimation at the same SNR value. In addition, for the same channel estimation error analysis, at SNR = 15 dB and 0.15 channel estimation error, 16-QAM of user 1 has a BER of 0.17 compared to 0.07 for the perfect estimation at the same SNR value.

The BER of QPSK, assuming 0.25 channel estimation error, of user 1 is equal to 0.06 at SNR = 15 dB compared to 0.017 for perfect estimation and 0.03 for 0.15 channel estimation error at the same SNR. Furthermore, for 0.25 channel estimation error, the 16-QAM BER of user 1 at SNR = 15 dB is 0.20 compared to 0.07 for perfect estimation and 0.17 for 0.15 channel estimation error at the same SNR. As similar to the BPSK analysis, for high estimation error values, the performance of QPSK and 16-QAM has an error floor and it is flattened with a high BER.

As a result, with increased channel estimation error, the BER is also increased and further increases with increased modulation order. An interesting observation is that, at high channel estimation error, the results for the three modulation schemes indicate a very high BER and a flattened performance as compared to the perfect estimation and the given channel estimation errors results. This is due to the degradation in the SIC receiver that results in high BER which is introduced and defined next.

5.4 SIC Receiver Degradation for Uplink NOMA with Channel Estimation Errors

In this section, a simulation analysis of the SIC receiver degradation of a two user uplink NOMA due to channel estimation errors is presented. The results have been simulated using BPSK, QPSK, and 16-QAM. Furthermore, the degradation performance is analyzed for different channel estimation error values.

The study of the BER with channel estimation errors has been accomplished in Section 5.3. This study is focused on quantifying the SIC degradation in terms of the channel estimation error. For the three modulation schemes, the same procedures are followed which are:

- SIC receiver degradation is defined as when the estimation error curves start deviating from the ideal (no estimation error) curve for a given BER. This is shown as a difference in SNR (dB) between the ideal curve and the curves with different channel estimation errors values. In other words, for each modulation scheme and for a given BER, when the difference between the ideal (no channel estimation error) BER vs SNR curve and the corresponding estimation error curve begin to deviate, then this is considered as the onset of SIC degradation.
- It is assumed that a 1dB difference marks the beginning of degradation. For simplicity, for each scheme, differences of 1 dB, 4 dB, and 8 dB in SNR have been considered and then the channel estimation error values that lead to these differences have been determined. In addition, the result where the curve is flattened (i.e., an error floor occurs) has been determined for each modulation scheme. In these cases, the relation is shown as a function of BER versus the channel estimation errors.
- The results of the SIC degradation versus the channel estimation errors are introduced separately for each modulation level and then the three results are combined in the same figure to compare them.

Starting with the SIC degradation case for BPSK modulation, the three differences between user 1 channel estimation error curves and the ideal (no estimation curve) are shown in Figure 5.6. For a BER of 10^{-3}, an estimation error value of 0.10 leads to a SIC degradation of 1 dB in SNR. Similarly, an estimation error of 0.28 leads to a SIC degradation of 4 dB SNR. Furthermore, a SIC

degradation of 8 dB difference is achieved with a 0.52 estimation error. Similarly, as discussed in Section 5.3, the effect of increasing the BER by increasing the channel estimation error is observed where more BER degradation is shown as the estimation error increases. The detection of user 1 is significantly affected by the noise power because the detected signal of user 2 is already subtracted by the detector, assuming a correct detection of user 2, in addition to processing the noise. Therefore, this makes the user 1 detection process, which has a lower received power level, more vulnerable to noise than user 2. Therefore, a larger BER occurs for user 1 as compared to user 2.

An interesting observation is that, for a high channel estimation error, a flattened performance result is shown as it is compared to the ideal channel estimation case. The flattened performance is defined when a difference in SNR (dB), for a given BER, between a given estimation error curve and ideal curve reaches to infinity. The simulation results show that the performance for BPSK is flattened (i.e., an error floor is reached at an estimation error of 0.86) and the SIC becomes useless.

The analysis for QPSK is shown in Figure 5.7. As illustrated, the BER increases as the channel estimation error and the modulation level are increased. Following the same procedures for determining the SIC degradation of the BPSK, the simulation results of QPSK, for a BER of 10^{-3}, show that a SIC degradation of 1 dB SNR is achieved at an estimation error value of 0.052 compared to 0.1 for the BPSK for the same degradation level. In addition, an estimation error of 0.17 leads to a SIC degradation of 4 dB SNR compared to 0.28 for BPSK. However, the same SIC degradation level of 8 dB SNR is occurred at an estimation error of 0.34 compared to 0.52 to get the same level in the BPSK case. At high channel estimation error, a flattened performance result

for the QPSK is occurred at 0.66 channel estimation error compared to an estimation error of 0.86 for the BPSK flattened performance.

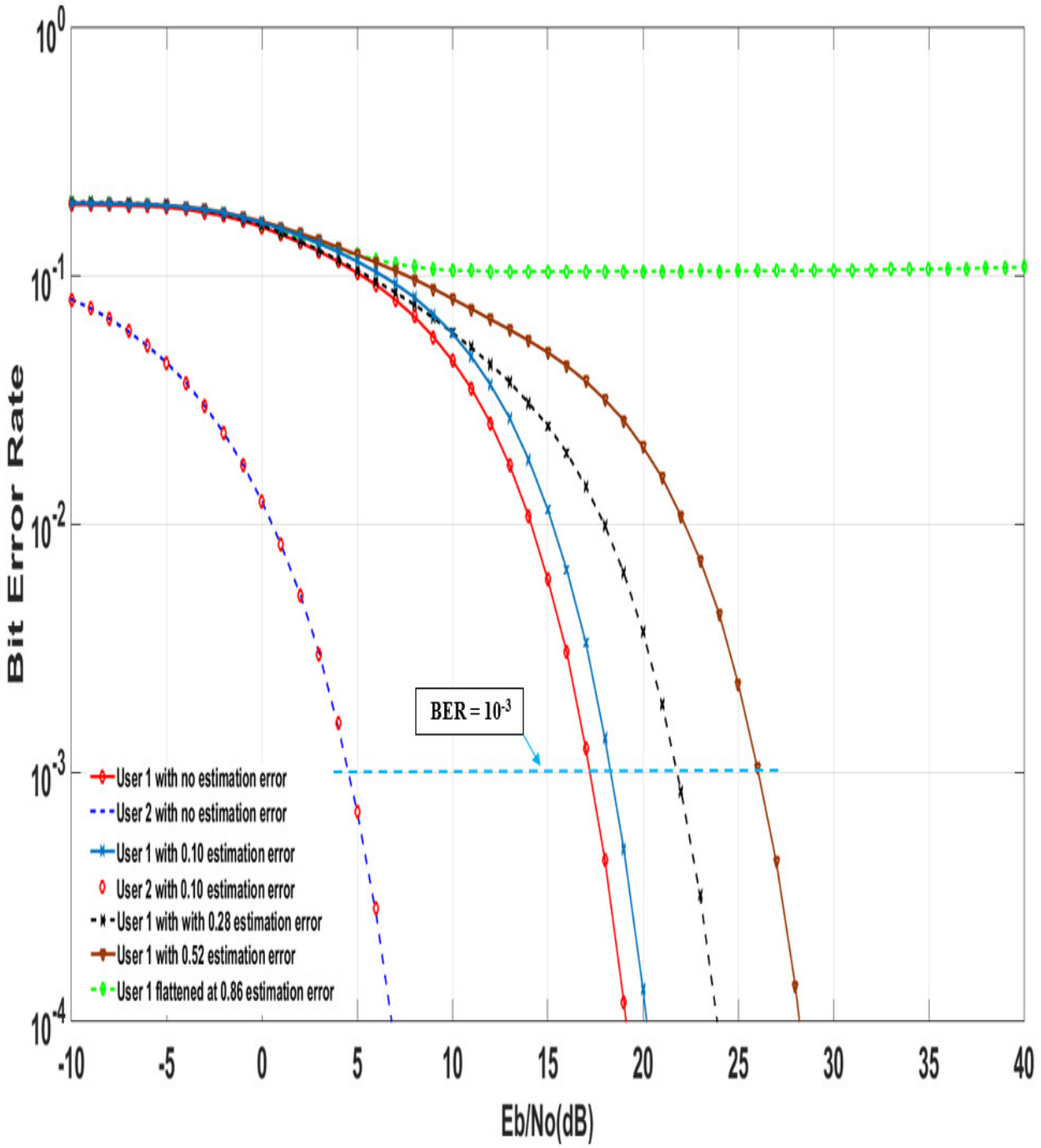

Figure 5.6 SIC degradation vs. channel estimation errors of a BPSK uplink NOMA system for BER = 10^{-3}.

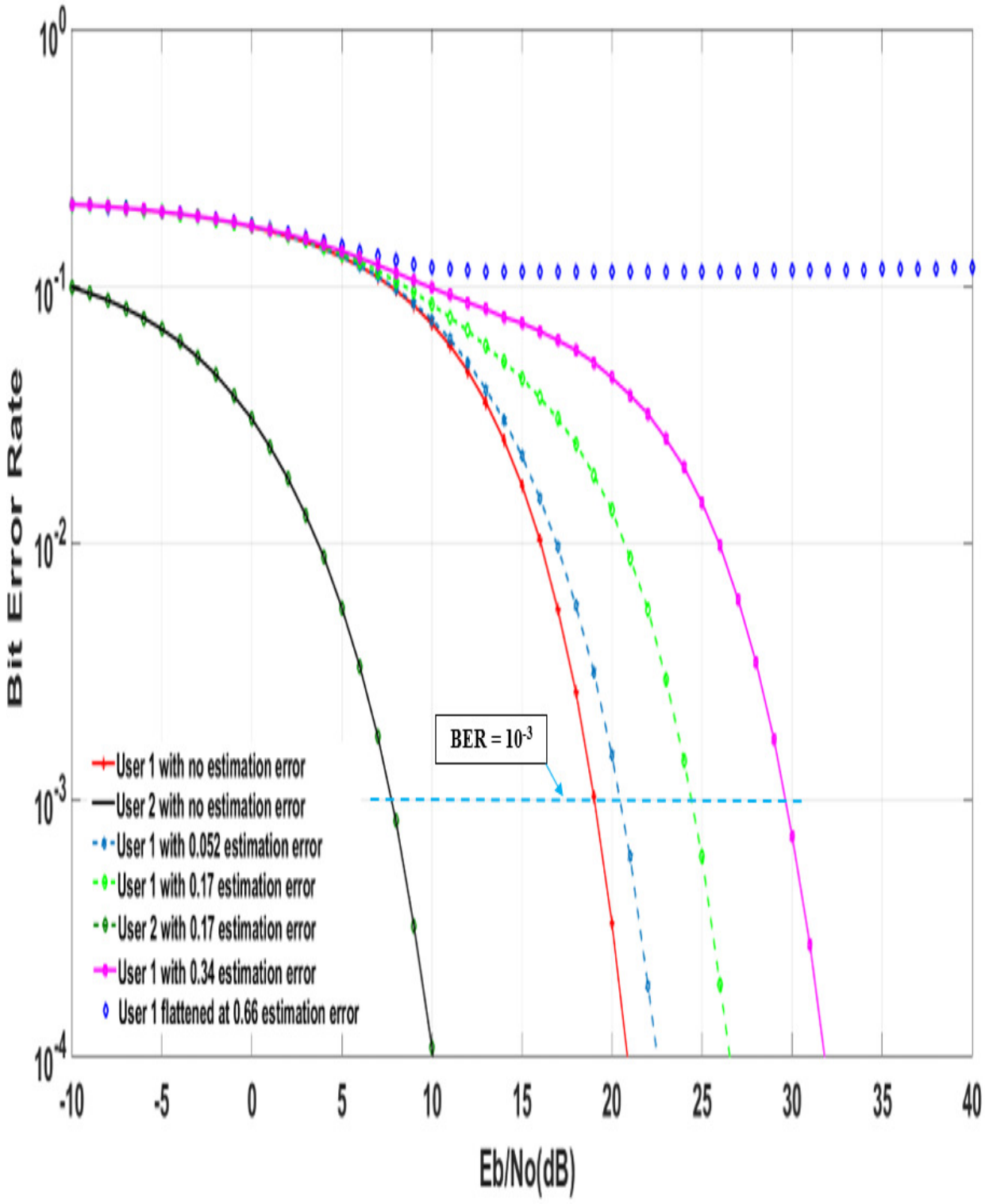

Figure 5.7 SIC degradation vs. channel estimation errors of a QPSK uplink NOMA system for BER = 10^{-3}.

Using the same analysis of the BPSK and QPSK, the results of the 16-QAM are shown in Figure 5.8.

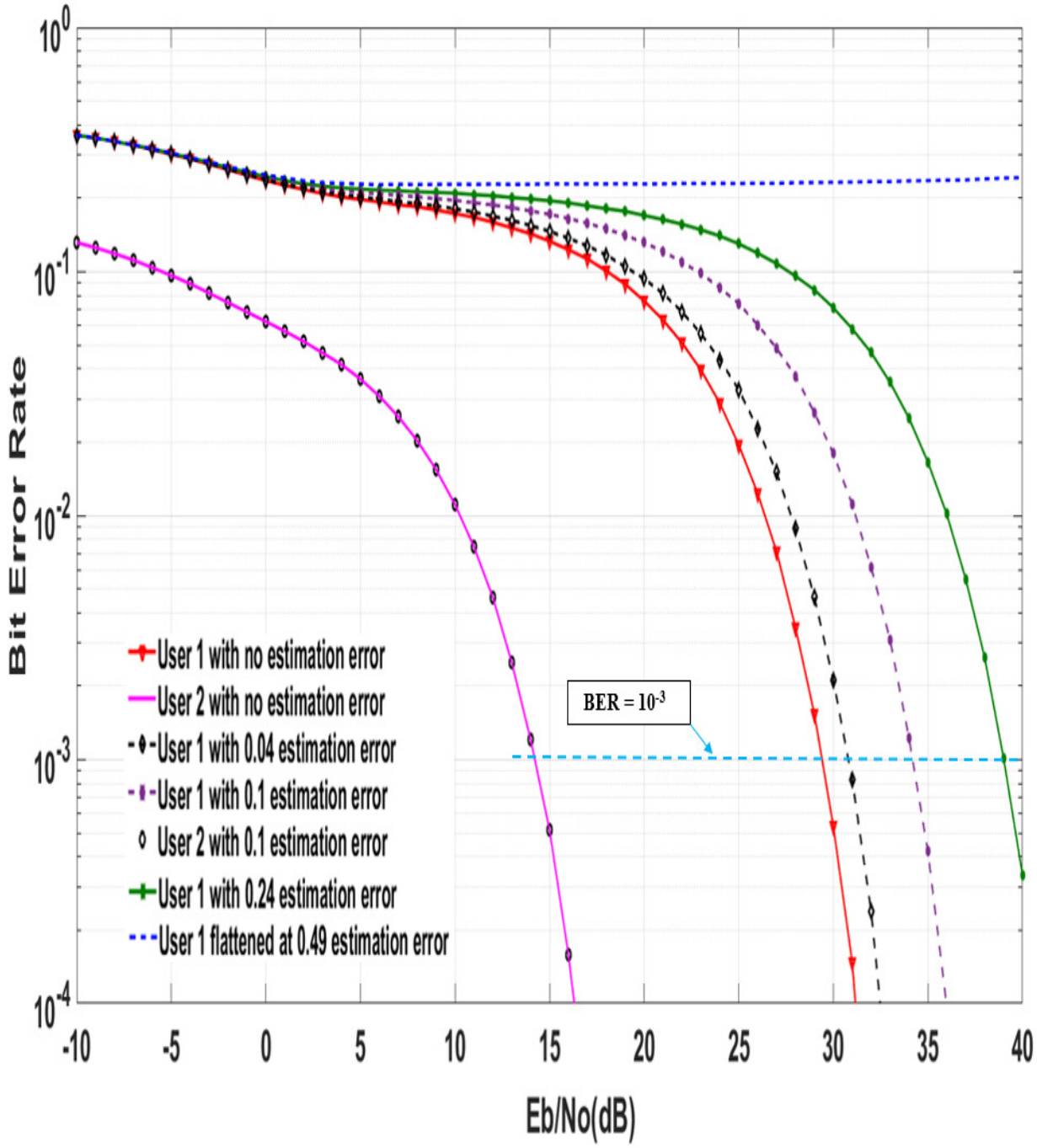

Figure 5.8 SIC degradation vs. channel estimation errors of a 16-QAM BPSK uplink NOMA system for BER = 10^{-3}.

As illustrated in this figure, as the modulation level increases, a higher SIC degradation level occurs for lower estimation error values. For example, for BER = 10^{-3}, a SIC degradation level of 1 dB SNR occurs at an estimation error value of 0.04 compared to 0.1 for BPSK and 0.052 for QPSK with the same degradation level of 1 dB SNR. Also, an estimation error of 0.1 leads to a 4 dB SNR degradation level compared to 0.17 for QPSK and 0.28 for BPSK. Similarly, a SIC degradation of 8 dB occurs at an estimation error of 0.24 compared to 0.34 for QPSK and 0.54 for the BPSK. However, the performance of 16-QAM is flattened at an estimation error of 0.49 compared to a channel estimation error of 0.66, which leads to a flattened performance for QPSK and 0.86 for BPSK, respectively.

According to the results in Figure 5.6, Figure 5.7, and Figure 5.8, more detail for the SIC degradation is shown Figure 5.9. In this figure, a relation between the SIC degradation and the channel estimation error is presented for the three modulation schemes.

The figure shows that, as expected, for the three modulation schemes, increasing of the estimation error increases the SIC degradation. Similarly, increasing of the modulation order, increases the SIC degradation. The BPSK curve shows that, for a BER = 10^{-3}, an estimation error of 0.2 leads to a SIC degradation of 3 dB SNR. Additionally, a SIC degradation of 8 dB SNR results from a 0.52 estimation error. As illustrated, it is observed that there is a linear relation (in dB) between the SIC degradation and the estimation error for small values of estimation error and that the curve deviates from this linearity, for BPSK, at an estimation error value of 0.7. By increasing the estimation error value, the curve starts sloping upward quickly until the performance is flattening, at 0.86 as shown in Figure 5.6, and this means that SIC becomes useless. This means that no matter how much the SNR is increased the BER is not reduced.

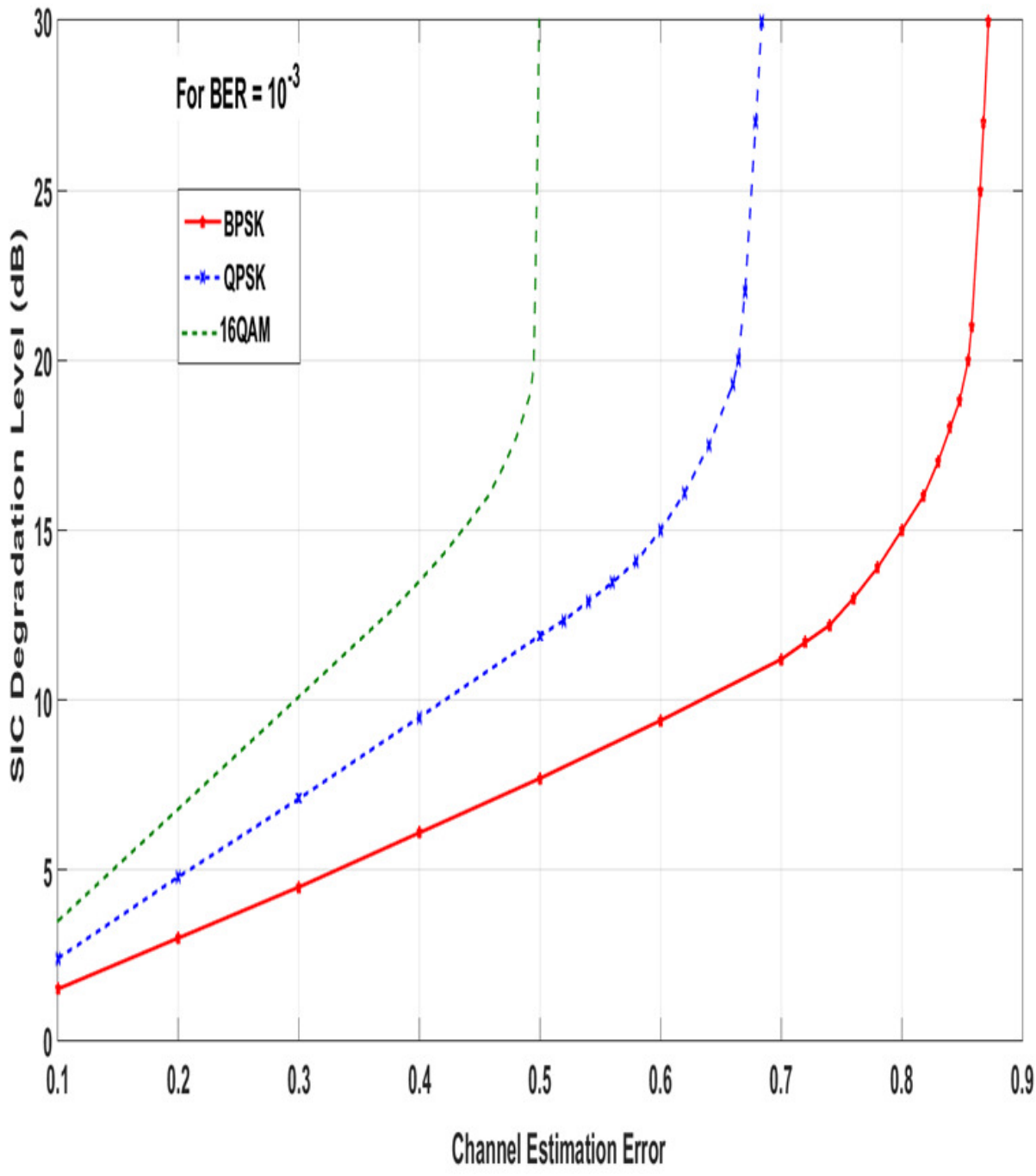

Figure 5.9 SIC degradation vs. channel estimation errors for uplink NOMA system with different modulation schemes for BER = 10^{-3}.

Similarly, for QPSK and BER = 10^{-3}, the relationship between the SIC degradation and the estimation error shows that an estimation error of 0.2 leads to a SIC degradation of 5 dB compared to a 3 dB for the same estimation error value of the BPSK. In addition, a SIC degradation of 10

dB occurs at an estimation error of 0.42 compared to an estimation error of 0.6 for the same degradation level of 10 dB for BPSK.

In the same way, the relationship for QPSK starts as a linear relation for small values of estimation error. After that, the curve deviates from linearity at an estimation error of 0.54. Then, by increasing the estimation error value, the curve starts sloping upward quickly for higher estimation error values and the SIC becomes useless as a result of the flattened performance that occurs at an estimation error of 0.66 compared to an estimation error of 0.86 that leads to a flattened performance for the BPSK.

In summary, for QPSK, the same degradation level of the SIC detector occurs at an estimation error lower than the one of the BPSK. This is expected since a higher modulation level leads to higher BER for lower estimation error values which means that a higher degradation level is observed faster than the case of the lower modulation level.

The 16-QAM curve follows the same logical flow as the BPSK and QPSK curves. The relation starts as a linear relation and then the curve deviates from linearity with increasing estimation error. After that, it starts sloping upward quickly. As a comparison, Figure 5.9 shows that a 5 dB SNR degradation level occurs at an estimation error of 0.15 where the same degradation level is occurred at 0.2 estimation error for the QPSK and at 0.32 estimation error for the BPSK. Furthermore, for 16-QAM, an estimation error of 0.3 leads to a degradation level of 10 dB where this degradation level occurs at an estimation error of 0.42 for QPSK and 0.6 for BPSK. However, the 16-QAM result shows that the curve deviates from linearity at 0.44 that is lower than the values of 0.54 of QPSK and 0.7 of the BPSK. Similarly, for high estimation error values, the 16-QAM curve starts sloping upward quickly and the SIC becomes useless as a result of the flattened

performance that occurs at an estimation error of 0.49 compared to an estimation error of 0.86 for BPSK and 0.66 for QPSK modulation.

5.5 Concluding Remarks

In this chapter, the BER performance of two-user uplink NOMA system using various modulation levels, BPSK, QPSK, and 16-QAM, in the presence of channel estimation errors was investigated. For each modulation level, two scenarios have been considered: perfect channel estimation and a channel with estimation errors. As expected, the simulation results for perfect channel estimation show that the BER of the SIC receiver increases as the modulation order is increased. Similarly, with channel estimation errors, the BER increases as the estimation error is increased for a given noise level. As a result of the degradation in the SIC receiver at a high estimation error value, all the modulation levels results show a very high BER compared to the perfect and lower estimation errors results.

Furthermore, for the same modulation levels, a simulation study of the SIC receiver degradation of uplink NOMA due to different channel estimation errors was presented. As expected, increasing the estimation error and the modulation scheme increases the SIC degradation level. However, for a higher modulation level, the same SIC degradation level is observed at lower estimation errors than the ones of lower modulation level. In addition, for high estimation errors, the performance of the three modulations start sloping upward quickly which leads to a flattened performance (i.e., an error floor condition). Somewhat surprisingly, for the three modulation levels with a small estimation error, a linear relation is shown between the SIC degradation in dB and the estimation error. This result will aid system designers in realizing practical 5G NOMA-based SIC receivers.

Chapter 6: Channel Capacity in a Dynamic Random Waypoint (RWP) Mobility Model[5]

6.1 Introduction

As introduced earlier in Chapter 1, channel capacity represents a key parameter that is used to characterize the capacity of 5G wireless network systems. The studying of such performance parameters is central to enhancing the quality and capacity of wireless networks. Channel capacity is a basic limit on the performance of communication media. In 1948 Claude Shannon defined the channel capacity as the upper bound on the maximum rate at which information can be reliably transmitted over a communication channel [80]. In particular, he derived the channel capacity for Additive White Gaussian Noise (AWGN) channel. Subsequently, the channel capacity for fading environments was introduced and the channel capacity has been used to study the maximum capacity effects of various multipath fading statistical models. To date, static wireless networks have mostly been used to analyze using these models. In this chapter, the capacity of a dynamically fading wireless channel model is analyzed.

The average received power represents a primary parameter that characterize the system behavior and it is used as an indicator in designing power control and determining wireless network capacity. The average received power level, in static models, is generally a function of the transmitter-receiver distance, transmitted power, and path loss exponent. Owing to constant transmitter-receiver distance in these models, the average received power is constant. In contrast, in mobile systems, the transmitter-receiver distance is not fixed and it follows a random pattern.

5 The content of this chapter has been published in [69], and it is included in this dissertation with a permission. Permission is included in Appendix A.

This variation of received signal power depends upon node mobility, distance dependent path loss, and multipath fading which results in time varying received power, which, in general, does not exhibit the same behavior as static wireless networks. The Random waypoint (RWP) mobility model [74], which is one of several mobility models, is a popular model. This model describes how the mobile users (nodes) change their velocity and location over time in addition to their movement pattern.

Recent research [155] and [156], has studied the outage probability in a dynamic model. In [155], an expression of the outage probability using the above dynamic mobility model over a Rayleigh fading channel has been derived. In [156], the distribution probability density (PDF) function and the outage probability with a dynamic mobility model has been derived over an eta-mu (η-μ) fading channel, where η-μ is the distribution that describes the variation of the signal envelope in channels with different powers of in-phase and quadrature components. However, these research studies addressed the outage probability not the channel capacity.

In this chapter, the channel capacity for a RWP mobility model of a Rayleigh fading channel using a maximum ratio combining (MRC) diversity receiver [79], which represents an antenna diversity technique to mitigate the multipath fading effect, is derived. The effect of the number of receiver branches on the channel capacity is determined, and the channel capacity is compared with the classic AWGN Shannon capacity and the static model Rayleigh fading channel capacity.

This chapter is organized as follows. The derivation of the channel capacity for a RWP model is presented in the next section. Then, in Section 6.3, the numerical results and the comparison of the channel capacity of RWP mobility model with the classic AWGN Shannon

capacity and the static model Rayleigh fading channel capacity are introduced and analyzed. Finally, the conclusion of this chapter is presented in the last section.

6.2 Channel Capacity of RWP Mobility Model

As discussed in Section 1, in a mobile wireless network, the nodes are mobile and because of that the distance between these nodes is random. As a result, multipath fading is time varying in nature. So, it is appropriate to investigate the mobility effect and evaluate the performance of mobile wireless network in terms of the channel capacity.

In order to conduct this study, one of the widely available dynamic mobility models is assumed, which is the RWP model [74]. In the RWP model, each mobile user (node) selects one location in the network as a destination. Then, this node travels with random and uniform velocity toward its destination at velocity $[0, V_{max}]$, where V_{max} is the maximum velocity for each mobile node [74]. The direction and the velocity of each mobile node are independently chosen. After reaching its destination, the mobile node stops for a random period of time. After this time period, the mobility node selects a new random destination and start moving towards it in the same scenario in the previous case. More details about RWP model are available in [165].

Since the channel in this study is a fading channel, one of the major factors that affects the modeling of the fading channel is the distributions that are used to characterize the channel. In our model, the channel is assumed to have a Rayleigh distribution. With a receiver that uses an optimum combiner diversity technique, MRC, with *N*-branches, results in the SNR being the sum of the SNR of each individual diversity branch. The receiving node can mitigate the effect of fading channel and improve the channel capacity of the channel model. This improvement is investigated in Section 6.3 and numerical results are presented.

An expression for the channel capacity of a dynamic RWP mobility model of a Rayleigh fading channel using MRC at the receiver will now be derived. The channel capacity C of a fading channel is given as [166]:

$$C = B \int_{\Omega_0}^{\infty} log_2\left(\frac{r}{\Omega_0}\right) P_r(r)\, dr, \qquad (6-1)$$

where B is the channel bandwidth in [Hz]. The parameter r is the random variable that defines the distance distribution between the mobile device (node) and the access point. The parameter $P_r(r)$ is the probability density function (PDF) of received power. And Ω_0 represents the average received signal power. As mentioned above, the averaged received power depends on the transmitter-receiver distance, this means that the distance from the transmitter to the receiver is reflected in the average received power Ω_0 which is the minimum acceptable SNR for communications.

To evaluate (6-1) it is necessary to determine $P_r(r)$ based on the assumed model. The received power PDF of a RWP mobility model with an N-branch MRC is given in [155] as

$$P_r(r) = \frac{6\, {P_t}^{\frac{2}{\alpha}}\, r^{-\left(1+\frac{2}{\alpha}\right)}}{\alpha\, \Gamma(N)} \left[\gamma\left(\left(N+\frac{2}{\alpha}\right), \frac{r}{P_t}\right) - \left(\frac{r}{P_t}\right)^{-\left(\frac{1}{\alpha}\right)} \gamma\left(N+\frac{3}{\alpha}, \frac{r}{P_t}\right)\right], \qquad (6-2)$$

where P_t is the transmitted power. The parameter α is the path loss exponent. The parameter $\Gamma(N)$ is the Gamma function which is defined in [167]. Furthermore, the function $\gamma(:,:)$ is called the lower incomplete gamma function [168].

By substituting the PDF of the RWP dynamic model of (6-2) in (6-1), the resulting channel capacity of the RWP channel is given as

$$C = \int_{\Omega_0}^{\infty} log_2\left(\frac{r}{\Omega_0}\right) \frac{6\, {P_t}^{2/\alpha}\, r^{-(1+2/\alpha)}}{\alpha\, \Gamma(N)} \left[\gamma\left(\left(N+\frac{2}{\alpha}\right), \frac{r}{P_t}\right) - \left(\frac{r}{P_t}\right)^{-\left(\frac{1}{\alpha}\right)} \gamma\left(N+\frac{3}{\alpha}, \frac{r}{P_t}\right)\right] dr. \quad (6-3)$$

Using [169] and Mathematica software [170] to solve the integral in (6-3), the dynamic RWP mobility model channel capacity of Rayleigh fading using *N*-branches of MRC is given as:

$$C = \frac{1}{6\,\Gamma(N)}\, B\, {\Omega_0}^{-3/\alpha}\, {P_t}^{2/\alpha} \left[9\, {\Omega_0}^{\frac{1}{\alpha}}\, \alpha \left(\Gamma\left(\mathrm{N} + \frac{2}{\alpha}\right) - \gamma\left(\left(N + \frac{2}{\alpha}\right), \frac{\Omega_0}{P_t}\right)\right)\right.$$

$$- 4\,\alpha {P_t}^{\frac{1}{\alpha}} \left(\Gamma\left(\mathrm{N}\ \frac{3}{\alpha}\right) - \gamma\left(\left(N + \frac{3}{\alpha}\right), \frac{\Omega_0}{P_t}\right)\right)$$

$$+\ {\Omega_0}^{\frac{3}{\alpha}} \left(\frac{1}{P_t}\right)^{\frac{2}{\alpha}} \left(- \left(-9 + 4 \left(\frac{1}{P_t}\right)^{\frac{1}{\alpha}} {P_t}^{\frac{1}{\alpha}} \right) \alpha\ \gamma\left(N, \frac{\Omega_0}{P_t}\right)\right.$$

$$\left.\left. -\ 6 \left(-3 + 2 \left(\frac{1}{P_t}\right)^{\frac{1}{\alpha}} {P_t}^{\frac{1}{\alpha}} \right) meijerG\left[\{\{\},\{1,1\}\},\{\{0,0,N\},\{\}\}, \frac{\Omega_0}{P_t}\right] \right) \right], (6-4)$$

where the 'Meijer G-function' function [171] is a very general function that reduces to simpler special functions in many common cases.

6.3 Numerical Results

Based on the result in (6-4), Mathematica software [170] has been used to investigate the relation of the channel capacity versus $\overline{\mathrm{SNR}}$, where the thermal noise fixed at unity. The path loss exponent α has been assumed to be 3. The results have been analyzed by normalizing the resulting channel capacity with respect to the channel bandwidth B. In Figure 6.1, the effect of the number of MRC branches, *N*, on the resulting proposed model channel capacity has been depicted.

As expected in Figure 6.1, increasing the number of branches, *N*, leads to improved channel capacity. With these results it is founded that, for example, in the absence of diversity N =1, the proposed channel capacity is equal to approximately 6 bps/Hz for $\overline{\mathrm{SNR}}$ = 20 dB. As N is increased, for example N = 3, the channel capacity is increased to 8.3 bps/Hz for the same value of $\overline{\mathrm{SNR}}$, respectively. Therefore, the channel capacity of a dynamic RWP Rayleigh channel for N = 3 is

increased by 38.3% compared to no diversity. As a result, by combining more diversity branches, the channel capacity is increased since the effect of the fading will be decreased. Furthermore, as expected for a large N, the C_{RWP} saturates since the maximum effective receiver diversity is realized.

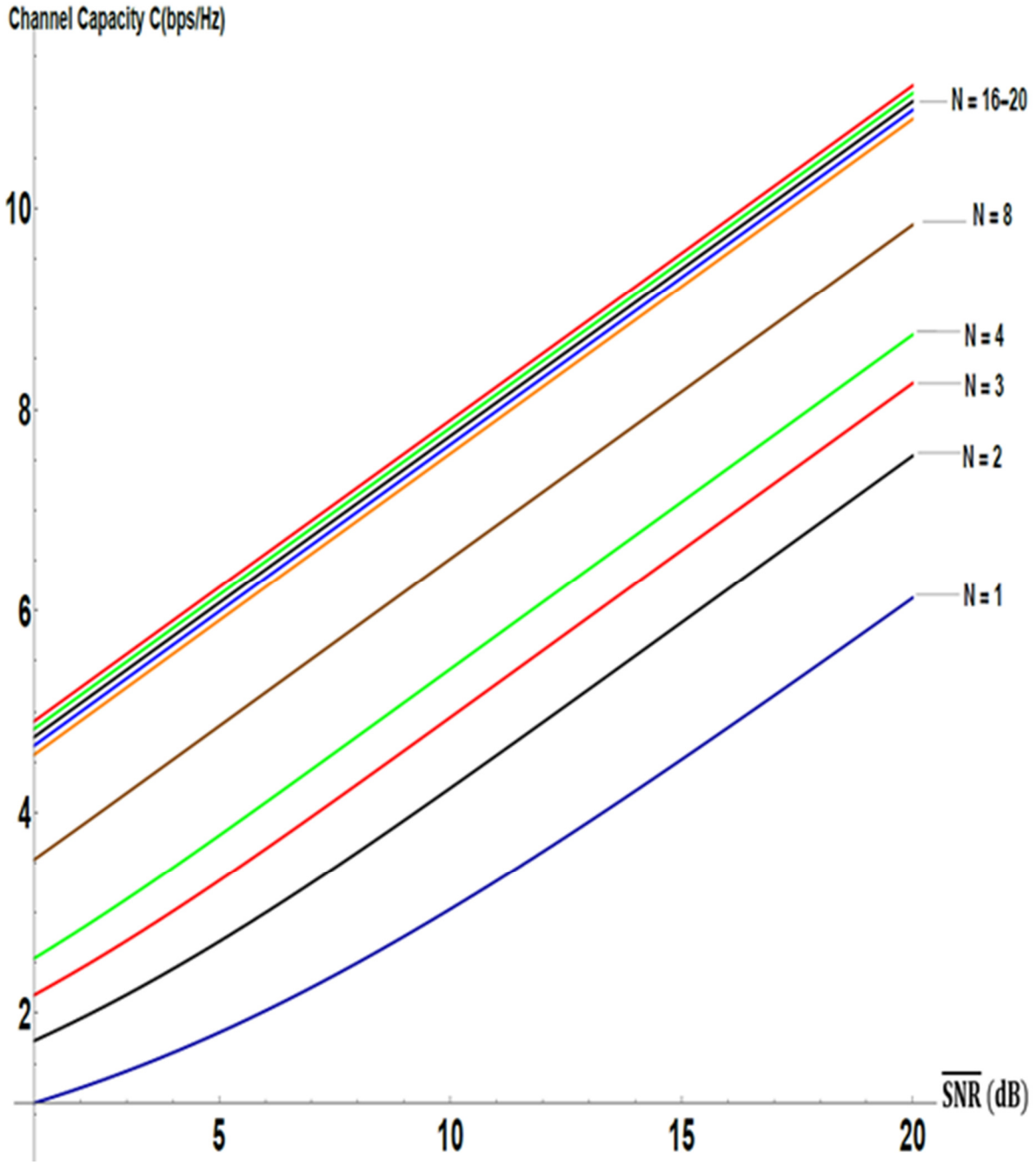

Figure 6.1 The effect of the number of branches, N, on the RWP model channel capacity.

A comparison between the RWP channel capacity (C_{RWP}) with the AWGN channel Shannon capacity (C_{AWGN}) and the static model Rayleigh fading channel capacity ($C_{Rayleigh}$) is shown in Figure 6.2.

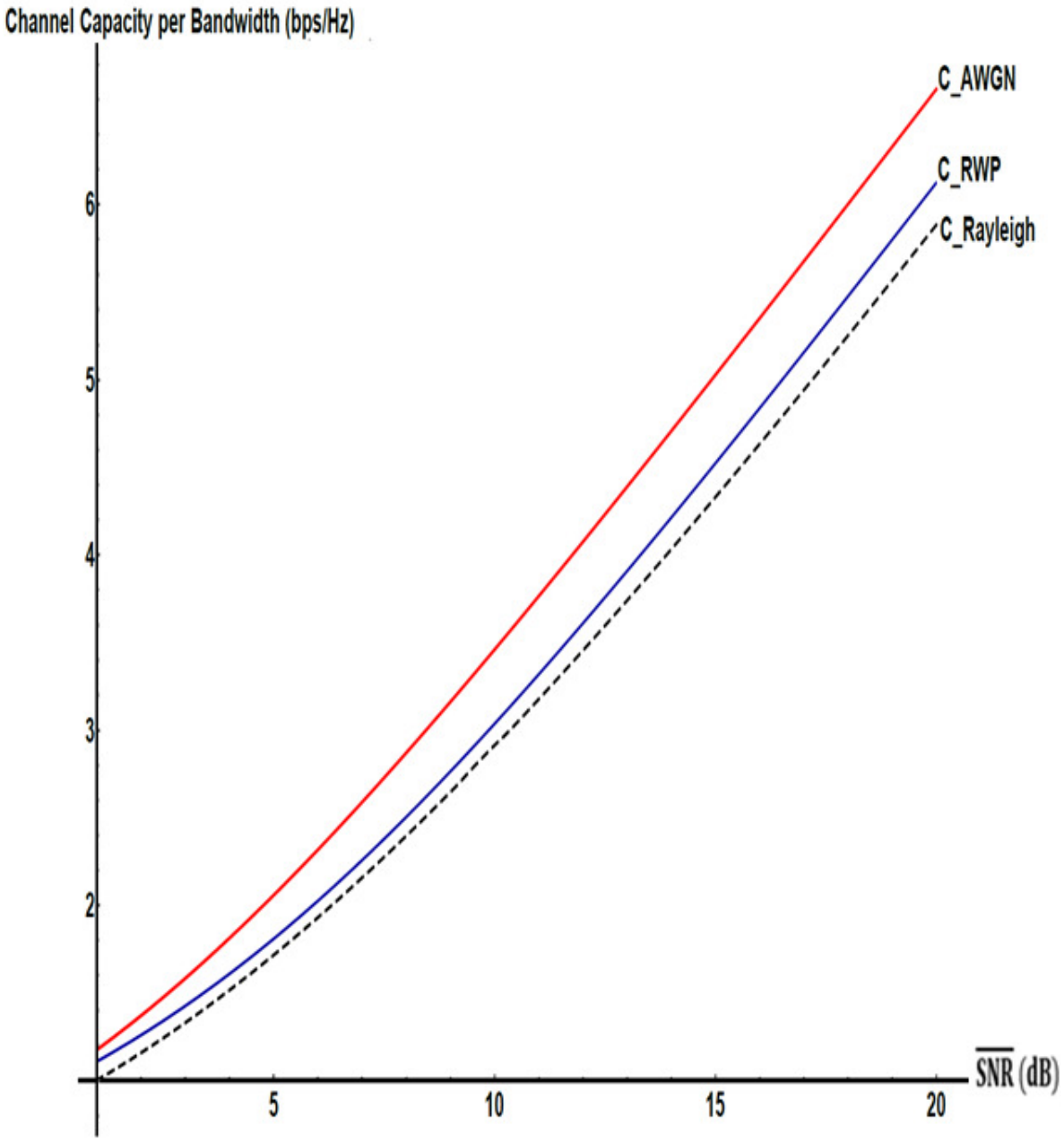

Figure 6.2 The RWP mobility model channel capacity (C_{RWP}) in comparison with the AWGN (C_{AWGN}) and the static model Rayleigh fading channel capacities ($C_{Rayleigh}$).

The figure shows that the AWGN channel capacity is better than the RWP model channel capacity. For example, for $\overline{\text{SNR}}$ = 15 dB, C_{AWGN} = 5.1 bps/Hz, whereas C_{RWP} = 4.48 bps/Hz. For $\overline{\text{SNR}}$ = 20 dB, C_{AWGN} = 6.7 bps/Hz, whereas C_{RWP} = 6.11 bps/Hz. Therefore, the channel capacity of the suggested dynamic RWP model is reduced by 14% for $\overline{\text{SNR}}$ = 15 dB and by 10% for $\overline{\text{SNR}}$ = 20 dB, respectively. The AWGN channel capacity has a larger channel capacity as it is not affected as severely by fading as in the RWP mobility model. However, the comparison of the resulting channel capacity (C_{RWP}) with the static model Rayleigh fading channel capacity ($C_{Rayleigh}$) shows that the C_{RWP} is slightly larger than the $C_{Rayleigh}$ for the same $\overline{\text{SNR}}$. For example, for $\overline{\text{SNR}}$ = 15 dB, $C_{Rayleigh}$ = 4.31 bps/Hz, whereas C_{RWP} = 4.48 bps/Hz. For $\overline{\text{SNR}}$ = 20 dB, $C_{Rayleigh}$ = 5.87 bps/Hz, whereas C_{RWP} = 6.11 bps/Hz. Therefore, the channel capacity of the suggested dynamic RWP model (C_{RWP}) is approximately increased by 4% for $\overline{\text{SNR}}$ = 15 dB and $\overline{\text{SNR}}$ = 20 dB, respectively. The reason is that severe fading will not affect the RWP model for as long a time period as it affects the static Rayleigh model.

6.4 Concluding Remarks

In this chapter, an expression for the channel capacity of a dynamic RWP mobility model based on a Rayleigh fading channel, with a MRC receiver, was derived. The result shows that the channel capacity increases as the number of MRC branches, *N*, is increased, e.g., the resulting channel capacity is increased from 6 bps/Hz at *N* = 1 to 8.3 bps/Hz at *N* = 3 for the same value of $\overline{\text{SNR}}$ = 20 dB. However, the resulting channel capacity for a large *N* saturates since the maximum effective receiver diversity is realized. In addition, the derived channel capacity result was compared with the classic AWGN Shannon capacity and with the static model Rayleigh fading channel capacity. The numerical results show that the dynamic RWP mobility channel capacity (C_{RWP}) is lower than the AWGN channel capacity (C_{AWGN}) as expected. For example, the proposed

model channel capacity (C_{RWP}) is decreased by 10% compared to the AWGN channel capacity (C_{AWGN}) at the same $\overline{\text{SNR}}$ = 20 dB as a result of the AWGN channel capacity is not affected as severely by fading as in the RWP mobility model. However, the comparison of the resulting channel capacity with the static model Rayleigh fading channel capacity $\left(C_{Rayleigh}\right)$ reflects that the derived result shows a slightly better channel capacity for the same $\overline{\text{SNR}}$. For example, for $\overline{\text{SNR}}$= 20 dB, the channel capacity of the RWP model is increased by 4% compared to the well-known result of the static model Rayleigh fading channel capacity. The result is expected since severe fading will not affect the RWP model for as long a time period as it affects the static Rayleigh model.

Chapter 7: Conclusions and Future Directions

7.1 Main Contributions and Conclusions

In this dissertation, an approach for enhancing 5G system performance by using NOMA (Non-Orthogonal Multiple Access) as the multiple access technique was investigated under different scenarios and performance metrics.

In Chapter 3, a relation for the optimum received power level for uplink power-domain NOMA with ideal Successive Interference Cancellation (SIC) reception was derived for any number of transmitters. The results show that the optimum received power level increases linearly (in dB) as the number of transmitters N are increased and the maximum required received SINR increases exponentially (or equivalently, linearly in dB) with the number of users N. Since the requirement of constant SNR, for each signal detection, is similar to that in Pulse Code Modulation (PCM) voice coding, of constant Signal-to-Quantizing Noise for each signal level, it was observed that the optimum power levels are very similar to the output levels of μ-law encoding used in the PCM speech companders.

In Chapter 4, a new MAC protocol (ALOHA-NOMA) for Machine to Machine (M2M) communication was presented. The ALOHA-NOMA protocol is an easy to implement, scalable, energy efficient, and a high throughput MAC protocol. The superior throughput of the ALOHA-NOMA protocol is a result of using NOMA along with the ability to resolve collisions via use of a SIC receiver (when the SIC receiver is operating in a "good" signal-to-noise" environment). As a result, the simplicity of ALOHA with the superior throughput of NOMA makes ALOHA-NOMA a good MAC candidate for low complexity IoT applications. For example, ALOHA-NOMA

significantly improves the throughput performance with respect to the pure ALOHA, e.g., a SIC receiver that separates 5 signals can boost the throughput of classical ALOHA from 0.18 to 1.27.

In Chapter 5, the BER performance of uplink power-domain NOMA and SIC detector, using BPSK, QPSK, and 16-QAM modulations levels, in the presence of channel estimation error was analyzed. For each modulation level, two scenarios have been considered: perfect channel estimation and a channel with estimation errors. For perfect channel estimation, as expected, the simulation results show that the BER of the SIC receiver increases as the modulation order is increased. Similarly, with channel estimation errors, the BER increases as the estimation error is increased for a given noise level and the performance is degraded at high estimation error values.

In addition to the BER performance study, for the same system model, a SIC detector degradation study in the presence of channel estimation errors, for the three modulations schemes, was presented. As expected, the results show that the SIC degradation increases as a result of increasing the estimation errors and/or the modulation level. Somewhat surprisingly, for the three modulation schemes and for a small estimation error values, a linear relation is shown between the SIC degradation and the estimation error. This result will aid system designers in realizing practical 5G NOMA-based SIC receivers.

In Chapter 6, a channel capacity analysis for a random waypoint (RWP) mobility model in a wireless system network was introduced. The expression for the channel capacity for this model was derived for a Rayleigh fading channel and with a maximum ratio combining (MRC) diversity receiver. The effect of the number of receiver branches on the channel capacity was analyzed. The derived channel capacity was compared with the classic AWGN Shannon capacity and the static model Rayleigh fading channel capacity. The results show that, as expected, the derived channel capacity increases as the number of MRC branches is increased. Also, the AWGN channel capacity

is greater than the RWP model channel capacity as it is not affected as severely by fading as the RWP mobility model. On the other hand, the RWP channel capacity is slightly larger than the static model Rayleigh fading channel capacity since severe fading will not affect the RWP model for as long a duration as it affects the static Rayleigh model.

7.2 Future Directions

Beyond what has been presented throughout the contributions in this dissertation, there are some promising directions for future work can be further explored. For example:

- Investigate the ALOHA-NOMA protocol using other performance metrics such as latency and fairness, as well as extending the analysis for a fading channel.
- Investigate the use of the proposed protocol for more demanding IoT applications for a larger number of devices, critical latency requirements, and the need for power control for each device.
- Compare the performance of ALOHA-NOMA with other MAC protocols such as TDMA/CSMA protocol.
- Analyze the channel capacity of RWP model using other fading channel models such as the Rician fading channel.
- Investigate that the performance of 5G wireless system with integrated NOMA and mmWave beamforming.

References

[1] A. Hazareena and B. A. Mustafa, "A Survey: On the Waveforms for 5G," *2018 Second International Conference on Electronics, Communication and Aerospace Technology (ICECA)*, Coimbatore, 2018, pp. 64-67.

[2] S. Zhang, X. Xu, Y. Wu, L. Lu and Y. Chen, "A survey on 5G New Waveform: From Energy Efficiency Aspects," *2014 48th Asilomar Conference on Signals, Systems and Computers, Pacific Grove, CA*, 2014, pp. 1939-1943.

[3] P. Pirinen, "A Brief Overview of 5G Research Activities,"1*st International Conference on 5G for Ubiquitous Connectivity*, Akaslompolo, 2014, pp. 17-22.

[4] R. Zi, X. Ge, J. Thompson, C. Wang, H. Wang and T. Han, "Energy Efficiency Optimization of 5G Radio Frequency Chain Systems," in *IEEE Journal on Selected Areas in Communications*, vol. 34, no. 4, 2016, pp. 758-771.

[5] S. Swetha and D. Raj, "Optimized Video Content Delivery over 5G Networks," *2017 2nd International Conference on Communication and Electronics Systems (ICCES)*, Coimbatore, 2017, pp. 1000-1002.

[6] 3rd Generation Partnership Project (3GPP), "Technical Specifications; LTE (Long Term Evolution)," Tech. Rep. [Online]. Available: https://www.3gpp.org/technologies/keywords-acronyms/98-lte.

[7] International Telecommunication Union (ITU) [Online]. Available: https://www.itu.int/en/ Pages/default.aspx.

[8] N. H. Mahmood, M. Lauridsen, G. Berardinelli, D. Catania, and P. Mogensen, "Radio Resource management techniques for eMBB and mMTC services in 5G dense small cell scenarios," in *Proc. IEEE Veh. Technol. Conf. (VTC)*, 2016, pp. 1–5.

[9] S. Chae, S. Cho, S. Kim and M. Rim, "Coded random access with multiple coverage classes for massive machine type communication," *2016 International Conference on Information and Communication Technology Convergence (ICTC)*, 2016, pp. 882-886.

[10] Z. Wu, F. Zhao, and X. Liu, "Signal Space Diversity Aided Dynamic Multiplexing for eMBB and URLLC Traffics," in *IEEE Int. Conf. Comp. Commun. (ICCC)*, 2017, pp. 1396–1400.

[11] A. Gupta and R. K. Jha, "A Survey of 5G Network: Architecture and Emerging Technologies," in *IEEE Access*, vol. 3, 2015, pp. 1206-1232.

[12] A. A. Esswie and K. I. Pedersen, "Null Space Based Preemptive Scheduling for Joint URLLC and eMBB Traffic in 5G Networks," *2018 IEEE Globecom Workshops (GC Wkshps*), Abu Dhabi, United Arab Emirates, 2018, pp. 1-6.

[13] J. M. Khurpade, D. Rao and P. D. Sanghavi, "A Survey on IOT and 5G Network," *2018 International Conference on Smart City and Emerging Technology (ICSCET)*, Mumbai, 2018, pp. 1-3.

[14] Anwer Al-Dulaimi; Xianbin Wang; Chih-Lin I, "Standardization: The Road to 5G," in *5G Networks: Fundamental Requirements, Enabling Technologies, and Operations Management*, IEEE, 2018, pp.691-708

[15] H. Magsi, A. H. Sodhro, F. A. Chachar, S. A. K. Abro, G. H. Sodhro and S. Pirbhulal, "Evolution of 5G in Internet of Medical Things," *2018 International Conference on Computing, Mathematics and Engineering Technologies (iCoMET)*, Sukkur, 2018, pp. 1-7.

[16] C. Gheorghe, D. A. Stoichescu and R. Dragomir, "Latency Requirement for 5G Mobile Communications," *2018 10th International Conference on Electronics, Computers and Artificial Intelligence (ECAI)*, Iasi, Romania, 2018, pp. 1-4.

[17] X. Ge, "Ultra-Reliable Low-Latency Communications in Autonomous Vehicular Networks," in *IEEE Transactions on Vehicular Technology*, vol. 68, no. 5, 2019, pp. 5005-5016.

[18] Y. Ji, J. Zhang, Y. Xiao and Z. Liu, "5G Flexible Optical Transport Networks with Large-Capacity, Low-Latency, and High-Efficiency," in *China Communications*, vol. 16, no. 5, 2019, pp. 19-32.

[19] G. A. Akpakwu, B. J. Silva, G. P. Hancke and A. M. Abu-Mahfouz, "A Survey on 5G Networks for the Internet of Things: Communication Technologies and Challenges," in *IEEE Access*, vol. 6, 2018, pp. 3619-3647.

[20] Y. Huo, X. Dong, W. Xu and M. Yuen, "Cellular and WiFi Co-design for 5G User Equipment," *2018 IEEE 5G World Forum (5GWF)*, Silicon Valley, CA, 2018, pp. 256-261.

[21] Anritsu, "Understanding 5G," [Online]. Available: http://vertassets.blob.core.windows.net/download/f1a51e7f/f1a51e7f-17ab-4a1f-a4af-21607a0924dd/understanding_5g.pdf.

[22] H. Hejazi, H. Rajab, T. Cinkler and L. Lengyel, "Survey of Platforms for Massive IoT," *2018 IEEE International Conference on Future IoT Technologies (Future IoT)*, Eger, 2018, pp. 1-8.

[23] N. Shahid and S. Aneja, "Internet of Things: Vision, application areas and research challenges," *2017 International Conference on I-SMAC (IoT in Social, Mobile, Analytics and Cloud) (I-SMAC)*, Palladam, 2017, pp. 583-587.

[24] D. Fang, Y. Qian and R. Q. Hu, "Security for 5G Mobile Wireless Networks," in *IEEE Access*, vol. 6, 2018, pp. 4850-4874.

[25] M. M. Alsulami and N. Akkari, "The Role of 5G Wireless Networks in the Internet-of- Things (IoT)," *2018 1st International Conference on Computer Applications & Information Security (ICCAIS),* Riyadh, 2018, pp. 1-8.

[26] G. Thirunavukkarasu and G. Murugesan, "A Comprehensive Survey on Air-Interfaces for 5G and Beyond," *2019 10th International Conference on Computing, Communication and Networking Technologies (ICCCNT)*, Kanpur, India, 2019, pp. 1-7.

[27] N. H. M. Adnan, I. M. Rafiqul and A. H. M. Z. Alam, "Massive MIMO for Fifth Generation (5G): Opportunities and Challenges," *2016 International Conference on Computer and Communication Engineering (ICCCE)*, Kuala Lumpur, 2016, pp. 47-52.

[28] X. Wang et al., "Millimeter Wave Communication: A Comprehensive Survey," in *IEEE Communications Surveys & Tutorials*, vol. 20, no. 3, 2018, pp. 1616-1653.

[29] L. Dai, B. Wang, Z. Ding, Z. Wang, S. Chen and L. Hanzo, "A Survey of Non-Orthogonal Multiple Access for 5G," in *IEEE Communications Surveys & Tutorials*, vol. 20, no. 3, 2018, pp. 2294-2323.

[30] K. Zheng, L. Zhao, J. Mei, B. Shao, W. Xiang and L. Hanzo, "Survey of Large-Scale MIMO Systems," in *IEEE Communications Surveys & Tutorials*, vol. 17, no. 3, 2015, pp. 1738-1760.

[31] S. Sanayei and A. Nosratinia, "Antenna Selection in MIMO systems," IEEE Commun. Mag., vol. 42, no. 10, 2004, pp. 68–73.

[32] K. Nishimori, "Antenna Systems for Next 50 Years," *2016 International Symposium on Antennas and Propagation (ISAP)*, Okinawa, 2016, pp. 554-555.

[33] S. Sun, T. S. Rappaport, R. W. Heath, A. Nix and S. Rangan, "Mimo for Millimeter-Wave Wireless Communications: Beamforming, Spatial Multiplexing, or Both?," in *IEEE Communications Magazine*, vol. 52, no. 12, pp. 110-121, December 2014.

[34] S. Narayanan, M. J. Chaudhry, A. Stavridis, M. Di Renzo, F. Graziosi and H. Haas, "Multi-User Spatial Modulation MIMO," *2014 IEEE Wireless Communications and Networking Conference (WCNC)*, Istanbul, 2014, pp. 671-676.

[35] P. Wongchampa and M. Uthansakul, "Orthogonal Beamforming for Multiuser Wireless Communications: Achieving Higher Received Signal Strength and Throughput Than with Conventional Beamforming.," in *IEEE Antennas and Propagation Magazine*, vol. 59, no. 4, 2017, pp. 38-49.

[36] T. Nakamura, "Research Activities of the Fifth Generation Mobile Communication Promotion Forum Radio Access Technologies Towards the Fifth Generation Mobile Communications System," 2015 21st Asia-Pacific Conference on Communications (APCC), Kyoto, 2015, pp. 169-173.

[37] A. Gupta and R. K. Jha, "A Survey of 5G Network: Architecture and Emerging Technologies," in *IEEE Access*, vol. 3, 2015, pp. 1206-1232.

[38] S. K. Agrawal and K. Sharma, "5G Millimeter Wave (mmWave) Communications," *2016 3rd International Conference on Computing for Sustainable Global Development (INDIACom)*, New Delhi, 2016, pp. 3630-3634.

[39] C. Jeong, J. Park and H. Yu, "Random Access in Millimeter-Wave Beamforming Cellular Networks: Issues and Approaches," in *IEEE Communications Magazine*, vol. 53, 2015, no. 1, pp. 180-185.

[40] Y. Niu, Y. Li, D. Jin, L. Su, and A. V. Vasilakos, "A Survey of Millimeter Wave Communications (mmWave) for 5G: Opportunities and challenges," *Wireless Networks*., vol. 21, no. 8, 2015, pp. 2657–2676.

[41] M. Xiao et al., "Millimeter Wave Communications for Future Mobile Networks," in *IEEE Journal on Selected Areas in Communications*, vol. 35, no. 9, 2017, pp. 1909-1935.

[42] S. M. R. Islam, N. Avazov, O. A. Dobre and K. Kwak, "Power-Domain Non-Orthogonal Multiple Access (NOMA) in 5G Systems: Potentials and Challenges," in *IEEE Communications Surveys & Tutorials*, vol. 19, no. 2, 2017, pp. 721-742.

[43] H. Tabassum, M. S. Ali, E. Hossain, M. J. Hossain and D. I. Kim, "Uplink Vs. Downlink NOMA in Cellular Networks: Challenges and Research Directions," *2017 IEEE 85th Vehicular Technology Conference (VTC Spring)*, Sydney, NSW, 2017, pp. 1-7.

[44] A. Benjebbour, K. Saito, A. Li, Y. Kishiyama and T. Nakamura, "Non-orthogonal multiple access (NOMA): Concept, Performance Evaluation, and Experimental Trials," *2015 International Conference on Wireless Networks and Mobile Communications (WINCOM)*, Marrakech, 2015, pp. 1-6.

[45] Y. Tao, L. Liu, S. Liu and Z. Zhang, "A Survey: Several Technologies of Non-Orthogonal Transmission for 5G," in *China Communications*, vol. 12, no. 10, 2015, pp. 1-15.

[46] Z. Wu, K. Lu, C. Jiang and X. Shao, "Comprehensive Study and Comparison on 5G NOMA Schemes," in *IEEE Access*, vol. 6, 2018, pp. 18511-18519.

[47] N. I. Miridakis and D. D. Vergados, “A Survey on the Successive Interference Cancellation Performance for Single-Antenna and Multiple-Antenna OFDM Systems,” *IEEE Commun. Surveys Tutorials*, vol. 15, no. 1, 2013, pp. 312-335.

[48] Y. Zuo, X. Zhu, Y. Jiang, Z. Wei, H. Zeng and T. Wang, "Energy Efficiency and Spectral Efficiency Tradeoff for Multicarrier NOMA Systems with User Fairness," *2018 IEEE/CIC International Conference on Communications in China (ICCC),* Beijing, China, 2018, pp. 666-670.

[49] A. D. Kucar, "Mobile Radio: An overview," in *IEEE Communications Magazine*, vol. 29, no. 11, 1991, pp. 72-85.

[50] A. Urie, "On the application of TDMA in UMTS," *IEE Colloquium on Advanced TDMA Techniques and Applications*, London, UK, 1996, pp. 1-4.

[51] Lajos L. Hanzo; L-L. Yang; E-L. Kuan; K. Yen, "CDMA Overview," in *Single and Multi-Carrier DS-CDMA: Multi-User Detection, Space-Time Spreading, Synchronization, Networking? And Standards, IEEE*, 2004, pp.

[52] C. Ciochina and H. Sari, "A Review of OFDMA and Single-Carrier FDMA," *2010 European Wireless Conference (EW)*, Lucca, 2010, pp. 706-710.

[53] M. Shafi et al., "5G: A Tutorial Overview of Standards, Trials, Challenges, Deployment, and Practice," in *IEEE Journal on Selected Areas in Communications*, vol. 35, no. 6, 2017, pp. 1201-1221.

[54] A. Benjebbour, A. Li, K. Saito, Y. Saito, Y. Kishiyama and T. Nakamura, "NOMA: From Concept to Standardization," *2015 IEEE Conference on Standards for Communications and Networking (CSCN)*, Tokyo, 2015, pp. 18-23.

[55] H. Sari, A. Maatouk, E. Caliskan, M. Assaad, M. Koca and G. Gui, "On the Foundation of NOMA and its Application to 5G cellular networks," *2018 IEEE Wireless Communications and Networking Conference (WCNC)*, Barcelona, 2018, pp. 1-6.

[56] H. Jiang, Q. Cui, Y. Gu, X. Qin, X. Zhang and X. Tao, "Distributed Layered Grant-Free Non-Orthogonal Multiple Access for Massive MTC," *2018 IEEE 29th Annual International Symposium on Personal, Indoor and Mobile Radio Communications (PIMRC)*, Bologna, 2018, pp. 1-7.

[57] F. T. Al. Rabee, K. Davaslioglu and R. Gitlin, "The Optimum Received Power Levels of Uplink Non-Orthogonal Multiple Access (NOMA) Signals," *2017 IEEE 18th Wireless and Microwave Technology Conference (WAMICON)*, Cocoa Beach, FL, 2017, pp. 1-4.

[58] P. Si, J. Yang, S. Chen and H. Xi, "Adaptive Massive Access Management for QoS Guarantees in M2M Communications," in *IEEE Transactions on Vehicular Technology*, vol. 64, no. 7, 2015, pp. 3152-3166.

[59] R. Nasfi and A. Chorti, "Performance Analysis of the Uplink of a Two User NOMA Network under QoS Delay Constraints," *2019 Eleventh International Conference on Ubiquitous and Future Networks (ICUFN)*, Zagreb, Croatia, 2019, pp. 526-528.

[60] Z. Yang, W. Xu, C. Pan, Y. Pan and M. Chen, "On the Optimality of Power Allocation for NOMA Downlinks With Individual QoS Constraints," in *IEEE Communications Letters*, vol. 21, no. 7, 2017, pp. 1649-1652.

[61] Q. Wang and F. Zhao, "Joint Spectrum and Power Allocation for NOMA Enhanced Relaying Networks," in *IEEE Access*, vol. 7, 2019, pp. 27008-27016.

[62] Y. Fu, Y. Chen and C. W. Sung, "Distributed Power Control for the Downlink of Multi-Cell NOMA Systems," in *IEEE Transactions on Wireless Communications*, vol. 16, no. 9, pp. 6207-6220, Sept. 2017.

[63] R. Gau, H. Chiu, C. Liao and C. Wu, "Optimal Power Control for NOMA Wireless Networks With Relays," in *IEEE Wireless Communications Letters*, vol. 7, no. 1, 2018, pp. 22-25.

[64] E. Balevi, F. T. Al. Rabee and R. D. Gitlin, "ALOHA-NOMA for Massive Machine-to-Machine IoT Communication," *2018 IEEE International Conference on Communications (ICC)*, Kansas City, MO, 2018, pp. 1-5.

[65] A. Rajandekar and B. Sikdar, "A Survey of MAC Layer Issues and Protocols for Machine-to-Machine Communications," in *IEEE Internet of Things Journal*, vol. 2, no. 2, 2015, pp. 175-186.

[66] N. Abramson, “The ALOHA System - Another Alternative for Computer Communications,” FallJoint Comput. *Conf. AFIPS Conf Proc*, vol. 37, 1970, pp. 281-285.

[67] F. Al Rabee and R. D. Gitlin, "Performance of Uplink Non-Orthogonal Multiple Access (NOMA) in the Presence of Channel Estimation Errors," *18th annual Wireless Telecommunications Symposium (WTS 2019)*, New York City, NY, USA, April. 2019. pp. 1-5.

[68] F. Al Rabee and R. D. Gitlin, “Uplink Power-Domain Non-Orthogonal Multiple Access (NOMA): Bit Error Rate Performance with Channel Estimation Errors,” in *International Journal of Interdisciplinary Telecommunications & Networking (IJITN)*, vol. 12, no. 4 , 2020.

[69] F. Al Rabee, Ashraf Al-Rimawi and R. D. Gitlin, "Channel Capacity in a Dynamic Random Waypoint Mobility Model," *9th IEEE Annual Ubiquitous Computing, Electronics & Mobile Communication Conference (UEMCON) 2018*, New York City, NY, USA, Nov. 2018, pp. 1-5.

[70] J. Bae, Y. S. Choi, J. S. Kim and M. Y. Chung, "Architecture and Performance Evaluation of MmWave Based 5G Mobile Communication System," *2014 International Conference on Information and Communication Technology Convergence (ICTC)*, Busan, 2014, pp. 847-851.

[71] W. C. Y. Lee, "Estimate of Channel Capacity in Rayleigh Fading Environment," in *IEEE Transactions on Vehicular Technology*, vol. 39, no. 3, 1990, pp. 187-189.

[72] G. Rafiq and M. Patzold, "Statistical Properties of the Capacity of Multipath Fading Channels," *2009 IEEE 20th International Symposium on Personal, Indoor and Mobile Radio Communications, Tokyo, 2009*, pp. 1103-1107.

[73] T. Huschka, M. Reinhardt and J. Lindner, "Channel Capacities of Fading Radio Channels," *Proceedings of PIMRC '96 - 7th International Symposium on Personal, Indoor, and Mobile Communications*, Taipei, Taiwan, 1996, pp. 467-471.

[74] T. Camp, J. Boleng, and V. Davies. "A Survey of Mobility Models for Ad Hoc Network Research," *Wireless Communications & Mobile Computing (WCMC): Special issue on Mobile Ad Hoc Networking: Research, Trends and Applications*, vol. 2, no. 5, 2002, pp. 483-502.

[75] C. Kaur, "A Comprehensive View of Mobility Models in Wireless Ad Hoc Networks," in *International Journal of Engineering Research and Applications (IJERA)*, vol. 2, no. 3, 2012, pp. 49-54.

[76] Y. Yang, Z. Liu, Z. Fu, T. Peng and W. Wang, "Transmission Capacity of Device-to-Device Communication under Heterogeneous Networks with Cellular Users Assisted," *2013 IEEE Globecom Workshops (GC Wkshps)*, Atlanta, GA, 2013, pp. 635-341.

[77] Z. Liu, T. Peng, H. Chen and W. Wang, "Transmission Capacity of D2D Communication under Heterogeneous Networks with Multi-Bands," *2013 IEEE 77th Vehicular Technology Conference (VTC Spring)*, Dresden, 2013, pp. 1-6.

[78] T. Rappaport, Wireless Communications: Principles and Practice, *Prentice-Hall*, Englewood Cliffs, NJ, 1996.

[79] P. M. Shankar, "Maximal Ratio Combining in Independent Identically Distributed in Nakagami Fading Channels," in *IET Communications*, vol. 5, no. 3, 2011, pp. 320-326.

[80] C. E. Shannon, "A Mathematical Theory of Communication," in *Bell System Technical Journal*, vol. 27, 1948, pp. 623-656.

[81] B. Naeem, R. Ngah and S. Z. Mohd Hashim, "Understanding the Challenges Towards Implementation of the 5G Wireless Networks," *2015 International Symposium on Technology Management and Emerging Technologies (ISTMET)*, Langkawai Island, 2015, pp. 223-226.

[82] Navita and Amandeep, "Performance Analysis of OFDMA, MIMO and SC-FDMA Technology in 4G LTE Networks," *2016 6th International Conference - Cloud System and Big Data Engineering (Confluence)*, Noida, 2016, pp. 554-558.

[83] K. Baybakov, T. Sviridova, M. Lobur and R. Kohut, "Using OFDM for Multiple Access Schemes in 4G Communication Systems," in *The Experience of Designing and Application of CAD Systems in Microelectronics, 2003. CADSM 2003. Proceedings of the 7th International Conference.*, Slavske, Ukraine, 2003, pp. 572-573.

[84] Navita and Amandeep, "Performance Analysis of OFDMA, MIMO and SC-FDMA technology in 4G LTE networks," *2016 6th International Conference - Cloud System and Big Data Engineering (Confluence)*, Noida, 2016, pp. 554-558.

[85] 3rd Generation Partnership Project (3GPP) [Online]. Available: https://www.3gpp.org.

[86] C. Ciochina and H. Sari, "A Review of OFDMA and Single-Carrier FDMA," *2010 European Wireless Conference (EW)*, Lucca, 2010, pp. 706-710.

[87] S. Merchan, A. G. Armada and J. L. Garcia, "OFDM Performance in Amplifier Non-linearity," in *IEEE Transactions on Broadcasting*, vol. 44, no. 1, 19985, pp. 106-114.

[88] T. Jiang and Y. Wu, "An Overview: Peak-to-Average Power Ratio Reduction Techniques for OFDM Signals," in *IEEE Transactions on Broadcasting*, vol. 54, no. 2, 2008, pp. 257-268.

[89] Xu He, Yue Xiao and Shaoqian Li, "PAPR Reduction for Random Interleaved Uplink OFDMA System," *2008 Third International Conference on Communications and Networking*, Hangzhou, China, 2008, pp. 478-481.

[90] K. S. Ramtej and S. Anuradha, "New Error Function Companding Technique to Minimize PAPR in LTE Uplink Communications," *2017 Twenty-third National Conference on Communications (NCC)*, Chennai, 2017, pp. 1-5.

[91] S. Chen and J. Zhao, "The Requirements, Challenges, and Technologies for 5G of Terrestrial Mobile Telecommunication," in *IEEE Communications Magazine*, vol. 52, no. 5, May, pp. 36-43.

[92] Y. Cai, Z. Qin, F. Cui, G. Y. Li and J. A. McCann, "Modulation and Multiple Access for 5G Networks," in *IEEE Communications Surveys & Tutorials*, vol. 20, no. 1, 2018, pp. 629-646.

[93] Z. Ding, X. Lei, G. K. Karagiannidis, R. Schober, J. Yuan and V. K. Bhargava, "A Survey on Non-Orthogonal Multiple Access for 5G Networks: Research Challenges and Future Trends," in *IEEE Journal on Selected Areas in Communications*, vol. 35, no. 10, 2017, pp. 2181-2195.

[94] K. Higuchi and A. Benjebbour, "Non-Orthogonal Multiple Access (NOMA) with Successive Interference Cancellation for Future Radio Access, " *IEICE Trans. Communications*., vol. E98-B, no. 3, 2015, pp. 403–414.

[95] 3GPP TD RP-150496: "Study on Downlink Multiuser Superposition Transmission (MUST) for LTE", 2015.

[96] S. Zhang, X. Xu, L. Lu, Y. Wu, G. He and Y. Chen, "Sparse Code Multiple Access: An Energy Efficient Uplink Approach for 5G Wireless Systems," *2014 IEEE Global Communications Conference*, Austin, TX, 2014, pp. 4782-4787.

[97] B. Wang, K. Wang, Z. Lu, T. Xie and J. Quan, "Comparison Study of Non-Orthogonal Multiple Access Schemes for 5G," *2015 IEEE International Symposium on Broadband Multimedia Systems and Broadcasting*, Ghent, 2015, pp. 1-5.

[98] M. Moltafet, N. Mokari, M. R. Javan, H. Saeedi and H. Pishro-Nik, "A New Multiple Access Technique for 5G: Power Domain Sparse Code Multiple Access (PSMA)," in *IEEE Access*, vol. 6, 2018, pp. 747-759.

[99] J. Dai, K. Niu, C. Dong and J. Lin, "Improved Message Passing Algorithms for Sparse Code Multiple Access," in *IEEE Transactions on Vehicular Technology*, vol. 66, no. 11, 2017, pp. 9986-9999.

[100] J. Zeng et al., "Investigation on Evolving Single-Carrier NOMA Into Multi-Carrier NOMA in 5G," in *IEEE Access*, vol. 6, 2018, pp. 48268-48288.

[101] S. Chen, B. Ren, Q. Gao, S. Kang, S. Sun and K. Niu, "Pattern Division Multiple Access—A Novel Non-Orthogonal Multiple Access for Fifth-Generation Radio Networks," in *IEEE Transactions on Vehicular Technology*, vol. 66, no. 4, 217, pp. 3185-3196.

[102] O. Shental, B. M. Zaidel and S. S. Shitz, "Low-Density Code-Domain NOMA: Better Be Regular," *2017 IEEE International Symposium on Information Theory (ISIT)*, Aachen, 2017, pp. 2628-2632.

[103] J. Zeng, D. Kong, X. Su, L. Rong and X. Xu, "On the Performance of Pattern Division Multiple Access in 5G Systems," *2016 8th International Conference on Wireless Communications & Signal Processing (WCSP)*, Yangzhou, 2016, pp. 1-5.

[104] S. D. Sosnin, G. Xiong, D. Chatterjee and Y. Kwak, "Non-Orthogonal Multiple Access with Low Code Rate Spreading and Short Sequence Based Spreading," *2017 IEEE 86th Vehicular Technology Conference (VTC-Fall)*, Toronto, ON, 2017, pp. 1-5.

[105] Q. Wang et al., "Non-Orthogonal Coded Access for Contention-Based Transmission in 5G," *2017 IEEE 86th Vehicular Technology Conference (VTC-Fall)*, Toronto, ON, 2017, pp. 1-6.

[106] L. Tian, C. Yan, W. Li, Z. Yuan, W. Cao and Y. Yuan, "On Uplink Non-Orthogonal Multiple Access for 5G: Opportunities and Challenges," in *China Communications*, vol. 14, no. 12, 2017, pp. 142-152.

[107] Y. Saito, Y. Kishiyama, A. Benjebbour, T. Nakamura, A. Li and K. Higuchi, "Non-Orthogonal Multiple Access (NOMA) for Cellular Future Radio Access," *2013 IEEE 77th Vehicular Technology Conference (VTC Spring)*, Dresden, 2013, pp. 1-5.

[108] M. R. Usman, A. Khan, M. A. Usman, Y. S. Jang and S. Y. Shin, "On the Performance of Perfect and Imperfect SIC in Downlink Non-Orthogonal Multiple Access (NOMA)," *2016 International Conference on Smart Green Technology in Electrical and Information Systems (ICSGTEIS)*, Bali, 2016, pp. 102-106.

[109] Y. Wu, E. Attang and G. E. Atkin, "A Downlink NOMA System Based on Combinatorial Design," *2018 IEEE 88th Vehicular Technology Conference (VTC-Fall)*, Chicago, IL, USA, 2018, pp. 1-5.

[110] C. Yan, A. Harada, A. Benjebbour, Y. Lan, A. Li and H. Jiang, "Receiver Design for Downlink Non-Orthogonal Multiple Access (NOMA)," *2015 IEEE 81st Vehicular Technology Conference (VTC Spring)*, Glasgow, 2015, pp. 1-6.

[111] H. Zuo and X. Tao, "Power Allocation Optimization for Uplink Non-Orthogonal Multiple Access Systems," *2017 9th International Conference on Wireless Communications and Signal Processing (WCSP)*, Nanjing, 2017, pp. 1-5.

[112] F. Fang, Z. Ding, W. Liang and H. Zhang, "Optimal Energy Efficient Power Allocation with User Fairness for Uplink MC-NOMA Systems," in *IEEE Wireless Communications Letters*, vol. 8, no. 4, 219, pp. 1133-1136.

[113] H. Zheng, S. Hou, H. Li, Z. Song and Y. Hao, "Power Allocation and User Clustering for Uplink MC-NOMA in D2D Underlaid Cellular Networks," in *IEEE Wireless Communications Letters*, vol. 7, no. 6, 2018, pp. 1030-1033.

[114] Y. Zhang, Z. Yang, Y. Feng and S. Yan, "Performance Analysis of a Novel Uplink Cooperative NOMA System with Full-Duplex Relaying," in *IET Communications*, vol. 12, no. 19, 2018, pp. 2408-2417.

[115] C. Guo, A. N. Aljalai, C. Feng, L. Zhao, V. C. M. Leung and R. K. Ward, "Compute-and-Forward for Uplink Non-Orthogonal Multiple Access," in *IEEE Wireless Communications Letters*, vol. 7, no. 6, 218, pp. 986-989.

[116] L. Zhaohua and G. Mingjun, "Survey on Network Lifetime Research for Wireless Sensor Networks," *2009 2nd IEEE International Conference on Broadband Network & Multimedia Technology*, Beijing, 2009, pp. 899-902.

[117] S. R. J. Ramson and D. J. Moni, "Applications of Wireless Sensor Networks — A Survey," *2017 International Conference on Innovations in Electrical, Electronics, Instrumentation and Media Technology (ICEEIMT)*, Coimbatore, 2017, pp. 325-329.

[118] A. S. Altaan, "Effects of Sensor Properties on Power Consumption in Wireless Sensor Network," *2010 Second International Conference on Computer Research and Development, Kuala Lumpur*, 2010, pp. 335-339.

[119] P. Dongarwar and P. Soni, "Design of Failure Aware and Energy Efficient Node Discovery System in Wireless Sensor Network," *2015 International Conference on Innovations in Information, Embedded and Communication Systems (ICIIECS)*, Coimbatore, 2015, pp. 1-5.

[120] V. Accha and S. H. Gupta, "Performance Analysis of Wireless Sensor Network MAC protocols using NS-2," *2018 International Conference on Computing, Power and Communication Technologies (GUCON)*, Greater Noida, Uttar Pradesh, India, 2018, pp. 859-862.

[121] Y. Li, D. Li, W. Cui and R. Zhang, "Research Based on OSI model," *2011 IEEE 3rd International Conference on Communication Software and Networks*, Xi'an, 2011, pp. 554-557.

[122] J. W. Conard, "Services and Protocols of the Data Link Layer," in *Proceedings of the IEEE*, vol. 71, no. 12, 1983, pp. 1378-1383.

[123] "IEEE Standard for Ethernet," in *IEEE Std 802.3-2018 (Revision of IEEE Std 802.3-2015)*, 2018, pp.1-5600.

[124] "IEEE Standard for Local and Metropolitan Area Networks: Overview and Architecture," in *IEEE Std 802-2001 (Revision of IEEE Std 802-1990)*, 2002, pp.1-48.

[125] M. Conti, E. Gregori and L. Lenzini, "Metropolitan Area Networks (MANs): Protocols, Modeling and Performance Evaluation," *2011 IEEE 3rd International Conference on Communication Software and Networks,* Xi'an, 2011, pp. 554-557.

[126] "IEEE Standard for Local Area Networks - Logical Link Control," in *ANSI/IEEE Std 802.2-1985*, 1984, pp.1-116.

[127] T. Chand and A. Kakria, "Comparative Analysis of a Contention Based (RI-MAC) and TDMA Based (ATMA) MAC Protocols for Wireless Sensor Networks," *2015 IEEE Sensors, Busan*, 2015, pp. 1-4.

[128] C. Busch, M. M. Ismail, F. Sivrikaya, and B. Yener, "Contention-Free MAC Protocols for Wireless Sensor Networks." *Distributed Computing*, 2004, pp. 245-259.

[129] T. Hsieh, K. Lin and P. Wang, "A Hybrid MAC Protocol for Wireless Sensor Networks," *2015 IEEE 12th International Conference on Networking, Sensing and Control*, Taipei, 2015, pp. 93-98.

[130] A. A. Mishra, "Enhanced Slotted ALOHA," *2011 3rd International Conference on Electronics Computer Technology*, Kanyakumari, 2011, pp. 278-282.

[131] S. Yun, Y. Yi, J. Shin and D. Y. Eun, "Optimal CSMA: A Survey," *2012 IEEE International Conference on Communication Systems (ICCS)*, Singapore, 2012, pp. 199-204.

[132] F. A. Tobagi and V. B. Hunt, "Performance Analysis of Carrier Sense Multiple Access with Collision Detection," *Comput. Networks*, vol. 4, 1980, pp. 245–259.

[133] S. U. Rehman, S. Berber and A. Swain, "Performance Analysis of CSMA/CA Algorithm for Wireless Sensor Network," *TENCON-2010 IEEE Region 10 Conference*, Fukuoka, 2010, pp. 2012-2017.

[134] T. W. Carley, M. A. Ba, R. Barua and D. B. Stewart, "Contention-Free Periodic Message Scheduler Medium Access Control in Wireless Sensor/Actuator Networks," *RTSS 2003. 24th IEEE Real-Time Systems Symposium,* Cancun, Mexico, 2003, pp. 298-307.

[135] F. Ghavimi and H. Chen, " Machine-to-Machine (M2M) Communications: A survey," in *Journal of Network and Computer Applications*, vol. 66, 2016, pp. 83-105.

[136] T. Taleb and A. Kunz, "Machine Type Communications in 3GPP Networks: Potential, Challenges, and Solutions," in *IEEE Communications Magazine*, vol. 50, no. 3, 2012, pp. 178-184.

[137] D. Tyagi, R. Agrawal and H. M. Singh, "A Survey on MAC Layer Protocols for Machine-to-Machine Communication," *2018 International Conference on Advances in Computing, Communication Control and Networking (ICACCCN)*, Greater Noida (UP), India, 2018, pp. 285-288.

[138] C. M. Ramya, M. Shanmugaraj and R. Prabakaran, "Study on ZigBee Technology," *2011 3rd International Conference on Electronics Computer Technology*, Kanyakumari, 2011, pp. 297-301.

[139] M. Singh, S. Singh, P. Pancholi, N. Saxena and R. K. Mehrotra, "Modelling of Machine-to-Machine Communication Networks," *2013 IEEE Conference on Information & Communication Technologies*, Thuckalay, Tamil Nadu, India, 2013, pp. 258-262.

[140] M. E. Rivero-Angeles, D. Lara-Rodriguez and F. A. Cruz-Perez, "A New EDGE Medium Access Control Mechanism Using Adaptive Traffic Load Slotted ALOHA," *IEEE 54th Vehicular Technology Conference. VTC Fall 2001. Proceedings (Cat. No.01CH37211),* Atlantic City, NJ, USA, 2001, pp. 1358-1362.

[141] In-Seop Park, E. Shitiri and Ho-Shin Cho, "An Orthogonal Coded Hybrid MAC Protocol with Received Power Based Prioritization for M2M Networks," *2016 Eighth International Conference on Ubiquitous and Future Networks (ICUFN)*, Vienna, 2016, pp. 733-735.

[142] Y. Liu, C. Yuen, X. Cao, N. U. Hassan and J. Chen, "Design of a Scalable Hybrid MAC Protocol for Heterogeneous M2M Networks," in *IEEE Internet of Things Journal*, vol. 1, no. 1, 2014, pp. 99-111.

[143] V. Naghshin, M. C. Reed and N. Aboutorab, "On the Performance of Finite Machine-to-Machine Wireless Communications with the ALOHA MAC Protocol," *2017 IEEE 85th Vehicular Technology Conference (VTC Spring)*, Sydney, NSW, 2017, pp. 1-5.

[144] S. Banerji and R. S. Chowdhury, " On IEEE 802.11: Wireless LAN Technology," in *International Journal of Mobile Network Communications & Telematics (IJMNCT)*, vol. 3, no. 4, 2013, pp. 45–64.

[145] F. Ghavimi and H. Chen, " The Challenges of M2M Massive Access in Wireless Cellular Networks," in *Digital Communications and Networks*, vol. 66, 2016, pp. 83-105.

[146] I. Bettesh and S. Shamai, "Outage Analysis for Multiple Access Channel with Rayleigh Fading," *2000 IEEE International Symposium on Information Theory* (Cat. No.00CH37060), Sorrento, Italy, 2000, pp. 303.

[147] W. C. Y. Lee, "Estimate of Channel Capacity in Rayleigh Fading Environment," in *IEEE Transactions on Vehicular Technology*, vol. 39, no. 3, 1990, pp. 187-189.

[148] M. Alouini and A. Goldsmith, "Capacity of Nakagami Multipath Fading Channels," *1997 IEEE 47th Vehicular Technology Conference. Technology in Motion*, Phoenix, AZ, USA, 1997, pp. 358-362.

[149] J. Lee, S. Lim, J. G. Andrews and D. Hong, "Achievable Transmission Capacity of Secondary System in Cognitive Radio Networks," *2010 IEEE International Conference on Communications*, Cape Town, 2010, pp. 1-5.

[150] S. A. Goldsmith, "Wireless Communications," *Cambridge University Press*, New York, NY, 2005.

[151] D. B. Johnson, and D. A. Maltz, "Dynamic Source Routing in Ad Hoc Wireless Networks," *Kluwer Academic Publishers*, 1996.

[152] J. Lee, S. Lim, J. G. Andrews and D. Hong, "Achievable Transmission Capacity of Secondary System in Cognitive Radio Networks," *2010 IEEE International Conference on Communications*, Cape Town, 2010, pp. 1-5.

[153] Z. Liu, T. Peng, Q. Lu and W. Wang, "Transmission Capacity of D2D Communication under Heterogeneous Networks with Dual Bands," *2012 7th International ICST Conference on Cognitive Radio Oriented Wireless Networks and Communications (CROWNCOM)*, Stockholm, 2012, pp. 169-174.

[154] C. Yin, L. Gao, T. Liu and S. Cui, "Transmission Capacities for Overlaid Wireless Ad Hoc Networks with Outage Constraints," *2009 IEEE International Conference on Communications*, Dresden, 2009, pp. 1-5.

[155] M. Das, B. Sahu and U. Bhanja, "Diversity Effect on Outage Probability in Mobile Wireless Network," in *Electronics Letters*, vol. 53, no. 4, 2017, pp. 283-285.

[156] A. Al-Rimawi, J. Siam and A. Abdo, "The Outage Probability of Mobile Wireless Networks over η-μ Fading Channel," *2018 IEEE Middle East and North Africa Communications Conference (MENACOMM)*, Jounieh, 2018, pp. 1-5.

[157] J. G. Proakis and M. Salehi, “Analog-to-Digital Conversion,” in *Fundamentals of communication systems*, *2nd ed. Upper Saddle River, NJ: Pearson Prentice Hall*, 2005, ch. 7, sec. 4, pp. 345-354.

[158] E. Casini, R. De Gaudenzi and O. Del Rio Herrero, "Contention Resolution Diversity Slotted ALOHA (CRDSA): An Enhanced Random Access Scheme for Satellite Access Packet Networks," in *IEEE Transactions on Wireless Communications*, vol. 6, no. 4, 2007, pp. 1408-1419.

[159] G. Liva, "Graph-Based Analysis and Optimization of Contention Resolution Diversity Slotted ALOHA," in *IEEE Transactions on Communications*, vol. 59, no. 2, 2011, pp. 477-487.

[160] F. Ricciato and P. Castiglione, "Pseudo-Random ALOHA for Enhanced Collision-Recovery in RFID," in *IEEE Communications Letters*, vol. 17, no. 3, 2013, pp. 608-611.

[161] J. P. Shaffer, "Multiple hypothesis testing," *Annual Review of Psychology*, 46, 1995, pp.561–584.

[162] P. J. Chung, J. F. Bohme, A. O. Hero and C. F. Mecklenbrauker, "Detection of the Number of Signals Using a Multiple Hypothesis Test," *Processing Workshop Proceedings, 2004 Sensor Array and Multichannel Signal*, Barcelona, Spain, 2004, pp. 221-224.

[163] N. Zhang, J. Wang, G. Kang and Y. Liu, "Uplink Non-Orthogonal Multiple Access in 5G Systems," in *IEEE Communications Letters*, vol. 20, no. 3, 2016, pp. 458-461.

[164] M. Elkourdi, A. Mazin, E. Balevi and R. D. Gitlin, "Enabling Slotted Aloha-NOMA for Massive M2M Communication in IoT Networks," *2018 IEEE 19th Wireless and Microwave Technology Conference (WAMICON),* Sand Key, FL, 2018, pp. 1-4.

[165] C. Bettstetter, G. Resta and P. Santi, "The Node Distribution of the Random Waypoint Mobility Model for Wireless Ad Hoc Networks," in *IEEE Transactions on Mobile Computing*, vol. 2, no. 3, 2003, pp. 257-269.

[166] M. Alouini and A. J. Goldsmith, "Capacity of Rayleigh Fading Channels under Different Adaptive Transmission and Diversity-Combining Techniques," in *IEEE Transactions on Vehicular Technology*, vol. 48, no. 4, July 1999, pp. 1165-1181.

[167] M. Abramowitz and I. A. Stegun, "Handbook of Mathematical Functions with Formulas, Graphs, and Mathematical Tables," *Dover Publications*, New York, USA, 1965.

[168] G. Jameson, "The Incomplete Gamma Functions," *Math. Gazette*, vol. 100, no. 548, 2016, pp. 298–306.

[169] I. Gradshteyn, and I.M. Ryzhik, "Tables of Integrals, Series, and Products," *Academic Press*, New York, 2000.

[170] P. Wellin, R. Gaylord, and S. Kamin, "An Introduction to Programming with Mathematica," 3rd ed, *Cambridge: Cambridge University Press*, 2005.

[171] R. Beals, J. Szmigielski, "Meijer G-Functions: a Gentle Introduction," *Not. Am. Math. Soc.* vol. 60, 2013, pp. 866-872.

Appendix A: Copyright Permissions

The permission below is for the use of Figure 1.2 in Chapter 1.

USF

Faeik Al Rabee <faeiktayseer@mail.usf.edu>

RE: Priority Customer Comment - Other17273 (reply required within 24 hours)

_AM-Call Center-Quote <_AM-CallCenter-Quote@anritsu.com> Fri, Mar 27, 2020 at 7:24 PM
To: "faeiktayseer@mail.usf.edu" <faeiktayseer@mail.usf.edu>
Cc: _AM-Call Center-Quote <_AM-CallCenter-Quote@anritsu.com>

Hello Faeik,

Thank you for your inquiry! I have spoken with our Legal Department, and they have approved your request.

Thank you and best regards,

Sheila Dunwoodie | Customer Operations Representative

Anritsu Americas Sales Company | 490 Jarvis Drive | Morgan Hill | California | 95037

Tel: 800-267-4878 ext. 1153

From: noreply@anritsu.com [mailto:noreply@anritsu.com]
Sent: Friday, March 27, 2020 4:16 PM
To: _AM-Call Center-Quote <_AM-CallCenter-Quote@anritsu.com>
Subject: Priority Customer Comment - Other17273 (reply required within 24 hours)

Anritsu - Service Request

Please find the feedback details received from Faeik Al Rabee for Other with reference no. 17273

Thank You,
Anritsu Administrator
http://www.anritsu.com

Faeik Al Rabee Contact Information

Product of Interest	Figure Permission Request from your Article

Questions or Comments	Dear Madam/Sir, I am a graduate student at the University of South Florida. I am in the process of preparing my dissertation and I am seeking permission to include the following in my dissertation. Title: Understanding 5G. Publisher: Anritsu . Content Requested: Fig 1 - 5G Mobile Broadband Objectives/Page 8. Would you please grant me permission to include above in my dissertation? Regards Faeik T Al Rabee Ph.D. Candidate Department of Electrical Engineering University of South
First/Last Name	Faeik Al Rabee
Phone Number	8132153264
Company	A PhD student at University of South Flordia
Country	US
Email Address	faeiktayseer@mail.usf.edu
Postal Code	33617
I would like to be contacted	

The permission below is for the use of the material in Chapter 3.

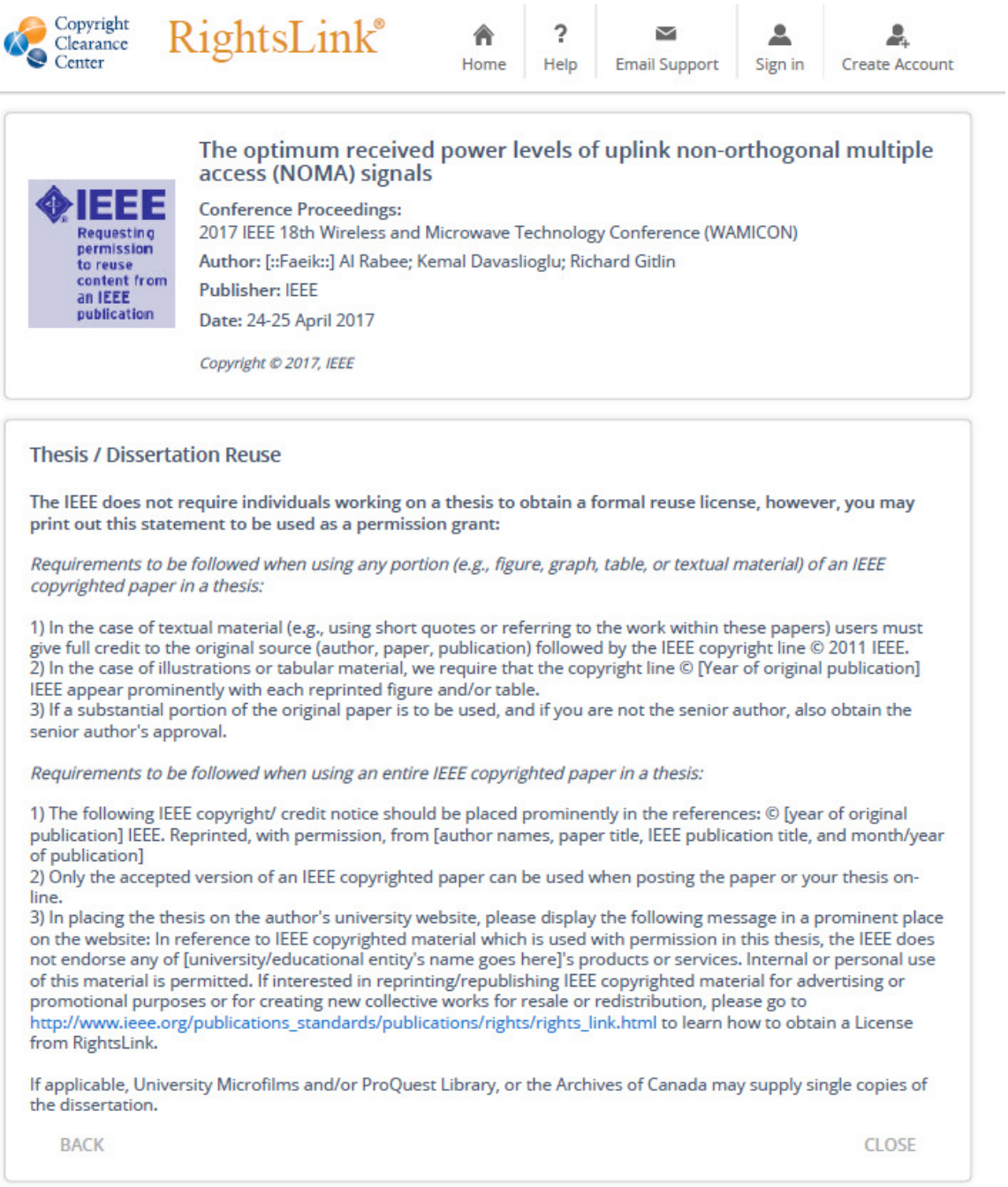

Copyright Clearance Center RightsLink®

Home | Help | Email Support | Sign in | Create Account

IEEE Requesting permission to reuse content from an IEEE publication

The optimum received power levels of uplink non-orthogonal multiple access (NOMA) signals

Conference Proceedings:
2017 IEEE 18th Wireless and Microwave Technology Conference (WAMICON)

Author: [::Faeik::] Al Rabee; Kemal Davaslioglu; Richard Gitlin

Publisher: IEEE

Date: 24-25 April 2017

Copyright © 2017, IEEE

Thesis / Dissertation Reuse

The IEEE does not require individuals working on a thesis to obtain a formal reuse license, however, you may print out this statement to be used as a permission grant:

Requirements to be followed when using any portion (e.g., figure, graph, table, or textual material) of an IEEE copyrighted paper in a thesis:

1) In the case of textual material (e.g., using short quotes or referring to the work within these papers) users must give full credit to the original source (author, paper, publication) followed by the IEEE copyright line © 2011 IEEE.
2) In the case of illustrations or tabular material, we require that the copyright line © [Year of original publication] IEEE appear prominently with each reprinted figure and/or table.
3) If a substantial portion of the original paper is to be used, and if you are not the senior author, also obtain the senior author's approval.

Requirements to be followed when using an entire IEEE copyrighted paper in a thesis:

1) The following IEEE copyright/ credit notice should be placed prominently in the references: © [year of original publication] IEEE. Reprinted, with permission, from [author names, paper title, IEEE publication title, and month/year of publication]
2) Only the accepted version of an IEEE copyrighted paper can be used when posting the paper or your thesis on-line.
3) In placing the thesis on the author's university website, please display the following message in a prominent place on the website: In reference to IEEE copyrighted material which is used with permission in this thesis, the IEEE does not endorse any of [university/educational entity's name goes here]'s products or services. Internal or personal use of this material is permitted. If interested in reprinting/republishing IEEE copyrighted material for advertising or promotional purposes or for creating new collective works for resale or redistribution, please go to http://www.ieee.org/publications_standards/publications/rights/rights_link.html to learn how to obtain a License from RightsLink.

If applicable, University Microfilms and/or ProQuest Library, or the Archives of Canada may supply single copies of the dissertation.

BACK CLOSE

The permission below is for the use of the material in Chapter 4.

Copyright Clearance Center RightsLink®

Home | Help | Email Support | Sign in | Create Account

IEEE Requesting permission to reuse content from an IEEE publication

ALOHA-NOMA for Massive Machine-to-Machine IoT Communication

Conference Proceedings: 2018 IEEE International Conference on Communications (ICC)

Author: Eren Balevi

Publisher: IEEE

Date: May 2018

Copyright © 2018, IEEE

Thesis / Dissertation Reuse

The IEEE does not require individuals working on a thesis to obtain a formal reuse license, however, you may print out this statement to be used as a permission grant:

Requirements to be followed when using any portion (e.g., figure, graph, table, or textual material) of an IEEE copyrighted paper in a thesis:

1) In the case of textual material (e.g., using short quotes or referring to the work within these papers) users must give full credit to the original source (author, paper, publication) followed by the IEEE copyright line © 2011 IEEE.
2) In the case of illustrations or tabular material, we require that the copyright line © [Year of original publication] IEEE appear prominently with each reprinted figure and/or table.
3) If a substantial portion of the original paper is to be used, and if you are not the senior author, also obtain the senior author's approval.

Requirements to be followed when using an entire IEEE copyrighted paper in a thesis:

1) The following IEEE copyright/ credit notice should be placed prominently in the references: © [year of original publication] IEEE. Reprinted, with permission, from [author names, paper title, IEEE publication title, and month/year of publication]
2) Only the accepted version of an IEEE copyrighted paper can be used when posting the paper or your thesis on-line.
3) In placing the thesis on the author's university website, please display the following message in a prominent place on the website: In reference to IEEE copyrighted material which is used with permission in this thesis, the IEEE does not endorse any of [university/educational entity's name goes here]'s products or services. Internal or personal use of this material is permitted. If interested in reprinting/republishing IEEE copyrighted material for advertising or promotional purposes or for creating new collective works for resale or redistribution, please go to http://www.ieee.org/publications_standards/publications/rights/rights_link.html to learn how to obtain a License from RightsLink.

If applicable, University Microfilms and/or ProQuest Library, or the Archives of Canada may supply single copies of the dissertation.

BACK CLOSE

The permissions below are for the use of the material in Chapter 5.

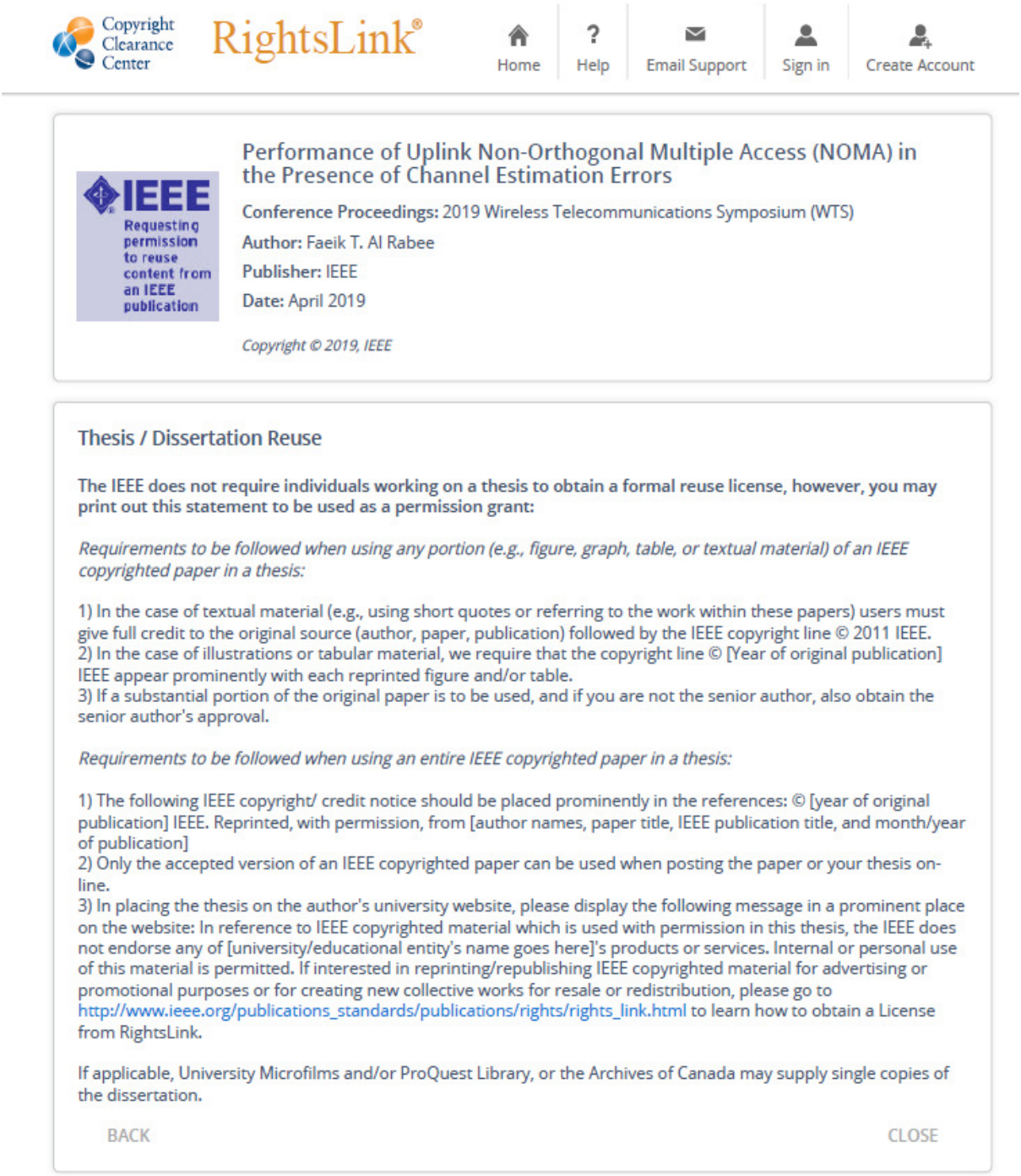

APPROVED
By Jan Travers at 6:14 pm, Mar 30, 2020

Request from Author for Reuse of IGI Global Materials

IGI Global recognizes that some of its authors would benefit professionally from the ability to reuse a portion or all of some manuscripts that the author wrote and submitted to IGI Global for publication. Prior to the use of IGI Global copyrighted materials in any fashion contemplated by the IGI Global Fair Use Guidelines for Authors, the author must submit this form, completed in its entirety, and secure from IGI Global the written permission to use such materials. Further, as a condition of IGI Global providing its consent to the reuse of IGI Global materials, the author agrees to furnish such additional information or documentation that IGI Global, in its sole discretion, may reasonably request in order to evaluate the request for permission and extent of use of such materials.

IGI Global will consider the Reuse request of any author who:

- Completes, signs and returns this form agreeing to the terms; and
- Agrees that unless notified to the contrary, only the final, typeset pdf supplied by IGI Global is authorized to be posted (no pre-prints or author's own file.)

Title of article/chapter you are requesting: Uplink Power-Domain Non-Orthogonal Multiple Access (NOMA): Bit Error Rate Performance with Channel Estimation Errors

Publication Title and editor where this IGI Global material appears:
The International Journal of Interdisciplinary Telecommunications and Networking (IJITN)

Purpose of request (check all that apply):

☐ Posted on a secure university website for your students to access in support of a class. (Posted paper must carry the IGI Global copyright information).

☐ Posted in a university archive. The Website address is: http://_____

☐ Posted on a personal Website: The Website address is: http://_____

☑ Republished in a book of which I am the editor/author. Book title of proposed book:

Publisher of proposed book: _____

Other purpose (please explain): _____
Including it in my dissertation, which is entitled as: " Enhancement of 5G Network Performance Using Non-Orthogonal Multiple Access (NOMA)"

With your signature below, you agree to the terms stated in the IGI Global Fair Use Guidelines. This permission is granted only when IGI Global returns a copy of the signed form for your files and the manuscript pdf.

Your name: Faeik T Al Rabee

Your signature: _____

Organization: University of South Florida

Address: 4202 E. Fowler Avenue, Tampa, Florida, USA

E-mail: faeiktayseer@mail.usf.edu

For IGI Global Use
Request accepted by IGI Global: Jan Travers
Date: _____

Digitally signed by Jan Travers
DN: cn=Jan Travers, o=IGI Global, ou=Director of Intellectual Property and Contracts, email=jtravers@igi-global.com, c=US
Date: 2020.03.30 18:21:15 -04'00'

Please complete and email or fax this request form to:
Jan Travers • IGI Global, 701 E Chocolate Avenue • Hershey PA 17033 • Fax: 717/533-8661 • jtravers@igi-global.com

10/2017

The permission below are for the use of the material in Chapter 6.

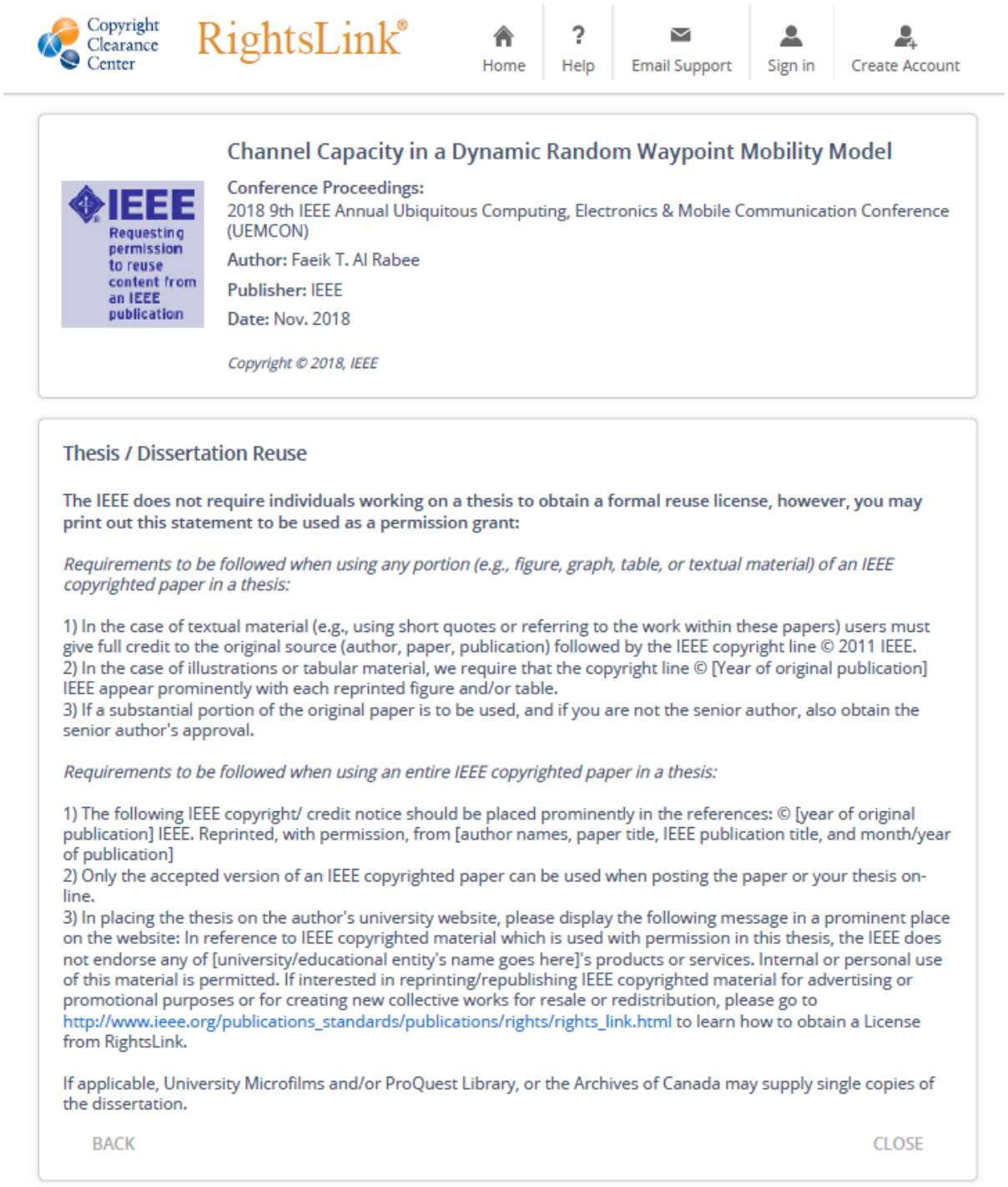

Copyright Clearance Center RightsLink®

Home | Help | Email Support | Sign in | Create Account

IEEE Requesting permission to reuse content from an IEEE publication

Channel Capacity in a Dynamic Random Waypoint Mobility Model

Conference Proceedings:
2018 9th IEEE Annual Ubiquitous Computing, Electronics & Mobile Communication Conference (UEMCON)

Author: Faeik T. Al Rabee

Publisher: IEEE

Date: Nov. 2018

Copyright © 2018, IEEE

Thesis / Dissertation Reuse

The IEEE does not require individuals working on a thesis to obtain a formal reuse license, however, you may print out this statement to be used as a permission grant:

Requirements to be followed when using any portion (e.g., figure, graph, table, or textual material) of an IEEE copyrighted paper in a thesis:

1) In the case of textual material (e.g., using short quotes or referring to the work within these papers) users must give full credit to the original source (author, paper, publication) followed by the IEEE copyright line © 2011 IEEE.
2) In the case of illustrations or tabular material, we require that the copyright line © [Year of original publication] IEEE appear prominently with each reprinted figure and/or table.
3) If a substantial portion of the original paper is to be used, and if you are not the senior author, also obtain the senior author's approval.

Requirements to be followed when using an entire IEEE copyrighted paper in a thesis:

1) The following IEEE copyright/ credit notice should be placed prominently in the references: © [year of original publication] IEEE. Reprinted, with permission, from [author names, paper title, IEEE publication title, and month/year of publication]
2) Only the accepted version of an IEEE copyrighted paper can be used when posting the paper or your thesis on-line.
3) In placing the thesis on the author's university website, please display the following message in a prominent place on the website: In reference to IEEE copyrighted material which is used with permission in this thesis, the IEEE does not endorse any of [university/educational entity's name goes here]'s products or services. Internal or personal use of this material is permitted. If interested in reprinting/republishing IEEE copyrighted material for advertising or promotional purposes or for creating new collective works for resale or redistribution, please go to http://www.ieee.org/publications_standards/publications/rights/rights_link.html to learn how to obtain a License from RightsLink.

If applicable, University Microfilms and/or ProQuest Library, or the Archives of Canada may supply single copies of the dissertation.

BACK CLOSE

About the Author

Faeik T Al Rabee received his B.Sc. degree in Communications and Software Engineering from Al-Balqa' Applied University/ Al-Huson University College, Irbid, Jordan in 2008, with a full scholarship from the Ministry of Higher Education, Jordan. He got 94% percentile rank over Jordan in the University Achievement Test. In 2013, he received the M.Sc. degree in Electrical Engineering majoring in Wireless Communications from Jordan University of Science and Technology (JUST), Irbid, Jordan, under the supervision of Prof. Mansour I. Abbadi. His M.Sc. dissertation was in the Optical Fiber Communications area. He research was directed towards using an optical filter in order to compensate for fiber dispersion. During his graduate studies, he worked as teaching assistant in the Electrical Engineering department at JUST University for three years. Currently, he is pursuing his Ph.D. degree in Electrical Engineering department at the University of South Florida with the Innovations in Wireless Information Networking (*i*WINLAB) group under the supervision of Prof. Richard D. Gitlin. His research interests include 5G wireless systems and networking protocols, multiple access techniques for 5G wireless network (Non-Orthogonal Multiple Access- NOMA), and the Internet of Things (IoT).